

WEDNESDAY POSTER PRESENTATIONS

ICACS-25



We-001 ~ We-077

&

SHIM2012



We-078 ~ We-099

Molecular Dynamic Simulation of KeV Hydrogen Molecular Ions Interaction With Solids

E. Marenkov^{(1)*}, V. Kurnaev⁽¹⁾, A. Lasa⁽²⁾, K. Nordlund⁽²⁾

⁽¹⁾ National Research Nuclear University MEPhI, ⁽²⁾ University of Helsinki, Finland

The study of ion and atomic cluster beams interaction with solid targets has been a topic of interest for many years due to both practical and fundamental reasons [1]. As experimental as theoretical studies show that the effect of the cluster impact on solids is often different from just a sum of single atoms interaction with the solid. Molecular ions consisting of two or three constituents are a limiting case of large clusters. They demonstrate a similar nonlinear behavior comparing to single atom-solid interactions. For example, bombardment of thin (20-70 Å) carbon films by 2-12 keV H^+ , H_2^+ , H_3^+ ions [2] has shown that the larger an amount of ions constituents, the greater the width of energy loss spectra peaks for transmitted particles ("a molecular effect").

We present a molecular dynamic simulation of H^+ , H_2^+ transmission through thin carbon layers. The calculations were carried out using the PARCAS code [3]. The Brenner's potential [4] was used to describe all kinds of elastic C-H interactions while the classical Lindhard's model was employed to account for the electronic stopping of protons in the film [5]. We see that the widths of simulated energy loss spectra for H_2^+ are larger than those for H^+ in correspondence with experimental findings (fig. 1). The origin the broadening of the energy spectra is H_2^+ disintegration due to which the ion fragments get the kinetic energy of order of several eV in the center of mass frame of references. It corresponds to energy straggling of fragments in the laboratory system of reference about of 100 eV, which finally causes the peaks broadening.

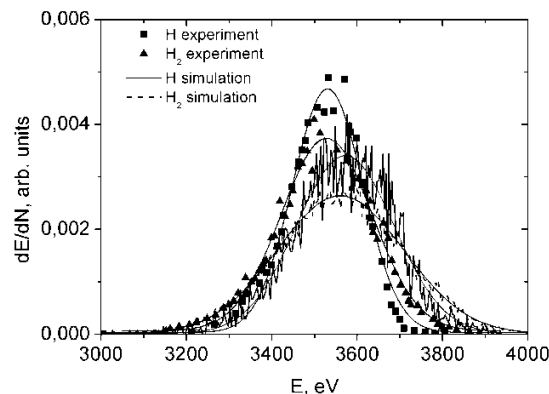


Figure 1. Energy loss spectra for penetration of H_2^+ and H^+ with an initial energy 3860 eV/nucleus through 40 Å carbon film. The markers correspond to experimental results taken from [2].

References

- [1] D. Jacquet and Y. Le Beyec., Nucl. Instr. and Meth. in Physics Research B, 193(1-4):227-239, 2002.
- [2] E.A. Gridneva, et al., JETP letters. 1 (2003).
- [3] K. Nordlund, M. Ghaly, R. S. Averback et al., Phys. Rev. B, 57(13):7556-7570, 1998.

* edmarenkov@gmail.com

Phase diagram for nanostructuring CaF₂ surfaces by slow highly charged ions

A.S. El-Said^{(1),(2)*}, R.A. Wilhelm⁽¹⁾, R. Heller⁽¹⁾, S. Facsko⁽¹⁾, C. Lemell⁽³⁾,

G. Wachter⁽³⁾, J. Burgdörfer⁽³⁾, R. Ritter⁽⁴⁾ and F. Aumayr⁽⁴⁾

⁽¹⁾ Helmholtz-Zentrum Dresden-Rossendorf, Institute of Ion Beam Physics and Materials Research, Germany, EU, ⁽²⁾ Physics Department, Faculty of Science, Mansoura University, Egypt, ⁽³⁾ Institute for Theoretical Physics, Vienna University of Technology, Austria, EU, ⁽⁴⁾ Institute of Applied Physics, Vienna University of Technology, Austria, EU

Slow highly charged ion (HCI) irradiation on insulating surfaces can cause local changes in the surface morphology, commonly known as nanostructures [1,2]. On CaF₂ recent studies [3] showed the creation of nanometer-sized hillocks with a strong dependence on the potential energy of the impinging HCI. Below a Xe charge state of $q=28$ no such hillocks have been found. However, below this threshold for hillock formation defects are created, which become visible by means of scanning force microscopy (SFM) only after chemical etching. These results show that a new regime in the phase diagram of hillock formation exists. For much lower charge states ($q<18$) and small kinetic energies (<10 keV) neither hillocks nor etch-pits could be found. An extended phase diagram for nanostructure formation on CaF₂ due to HCI irradiation is presented and the three obtained phases are discussed in terms of kinetic and potential energy dependence.

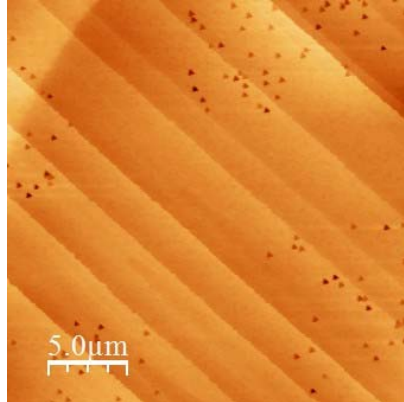


Figure 1. SFM topographic image of a CaF₂ surface showing etch pits after exposure, through a mask, to 1.15 keV/amu Xe³³⁺ and subsequently chemically etched using HNO₃.

References

- [1] S. Facsko et al., *J Phys Condens Matter*, **21** (2009), 224012
- [2] F. Aumayr et al., *J Phys. Condens Matter*, **23** (2011), 393001
- [3] A.S. El-Said et al., *Phys Rev Letters*, **100** (2008), 237601

* a.s.elsaid@fzd.de, elsaid@kfupm.edu.sa

Absolute Detection Efficiencies of keV Energy Atoms Incident on a Microchannel Plate Detector

N. Takahashi, Y. Adachi, M. Saito^{*}, and Y. Haruyama

Laboratory of Applied Physics, Kyoto Prefectural University, Kyoto 606-8522, Japan

A microchannel plate (MCP) detector is widely used to detect keV energy ions and neutrals. The absolute detection efficiency of the MCP detector is known to depend on the incident energy and charge state for individual ionic species. Knowledge about the detection efficiency is therefore essential to determine the absolute counts of the particles incident on the MCP. The absolute detection efficiencies of the MCP detectors for ions are usually obtained by measuring the ion beam current with a Faraday cup and the count rate from the MCP consecutively. However, the detection efficiencies for neutrals are scarce, mainly because of the difficulty in measuring the incident neutral beam current. We developed a new method that enables us to determine the absolute detection efficiencies for neutrals in keV energies [1]. This method uses the single-electron capture process in collisions of ions with gas targets. Using this method, we determined the detection efficiencies for rare gas atoms with energies of 0.5-5 keV [1]. We report here the absolute detection efficiencies for hydrogen, carbon, and tungsten atoms with energies of 0.5-4.5 keV. In addition, we report a scaling relation for our data obtained so far.

The experimental procedure will be described briefly. The charge-changed incident ion and the singly ionized target atom are detected using two identical MCP detectors in coincidence mode. The measured number of coincidences does not coincide with the measured number of target ions because of the detection efficiencies of the MCP detectors. The absolute detection efficiencies (of the MCP for incident ions) are then given as the ratio of the number of coincidences to the number of target ions.

The results for H^0 , C^0 , and W^0 showed similar energy and mass dependencies as for the rare gas atoms. The detection efficiencies increased with increasing impact energy and converged to the open area ratio (~50%) of the MCP used. The efficiencies at fixed energies decreased as the mass of the atom increased.

The detection efficiency of a MCP depends on the yield of an average secondary electron emission from a surface by incoming particles [2]. The ion-induced secondary electron yield is expected to depend largely on the electronic energy loss of the incoming particles on MCP materials. It is shown that our data can scale with the electronic energy loss estimated using the formulas for electronic and nuclear stopping power by Lindhard et al [3, 4].

References

- [1] S. Hosokawa, N. Takahashi, M. Saito, Y. Haruyama, Rev. Sci. Instr. 81, (2010) 063301.
- [2] B. Brehm, J. Grosser, T. Ruscheinski, M. Zimmer, Meas. Sci. Technol. 6 (1995) 953.
- [3] J. Lindhard, Msharff, H. E. Shiøtt, K. Dan. Vidensk. Selsk. Mat. -Fys. Medd. 33 (1963) No. 14.
- [4] J. Lindhard, V. Nielsen, M. Scahrff, K. Dan. Vidensk. Selsk. Mat. -Fys. Medd. 36 (1968) No. 10.

^{*} m_saito@kpu.ac.jp

**Radiolysis of H₂O : H₂CO : CH₃OH ice mixture
by 220 MeV ¹⁶O⁷⁺ bombardment**

A. L. F. de Barros⁽¹⁾, E. F. da Silveira⁽²⁾, P. Boduch⁽³⁾,

A. Domaracka⁽³⁾, H. Rothard⁽³⁾

⁽¹⁾ CEFET-RJ, Av. Maracanã 229, 20271-110 Rio de Janeiro, RJ, Brazil,

⁽²⁾ PUC-Rio, Rua Marquês de São Vicente 225, 22451-900, Rio de Janeiro, RJ, Brazil,

⁽³⁾ CIMAP-CIRIL- Ganil, Boulevard Henri Becquerel, BP 5133, F-14070 Caen Cedex 05, France.

220 MeV ¹⁶O⁷⁺ ion induced radiolysis of H₂O:H₂CO:CH₃OH (10:9:1 mixture) ice is studied in laboratory by infrared spectroscopy (FTIR). The molecular species CH₃OH, H₂CO₃, CO₂, H₂O₂, CO, HCO, CH₃COOH and HCOOH are formed with rates shown in Figure 1. The formation and dissociation cross sections of all observed daughter molecules in the mixture are determined using the procedure described in [1]. The radiation chemical effects led to a general observation that the destruction cross sections by fast ions depend on the electronic stopping power as $\sigma_d = S_e^n$. Moreover, it seems that this power law can be extended to formation cross sections since this rule is followed at least by H₂O₂, one abundant daughter species. As astrophysical implication, the abundance ratios of H₂CO and CO, relative to CH₃OH and obtained with oxygen beam, are compared with hydrogenation data of literature. This result helps the understanding of the ratios observed in interstellar ices, comets, and the Orion hot core.

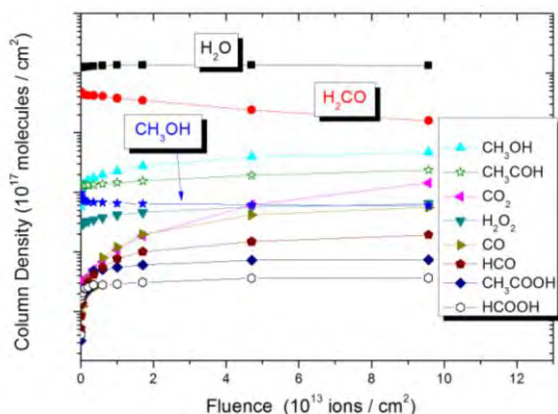


Figure 1. Column density dependence on beam fluence for some species detected on H₂O:H₂CO:CH₃OH ice by infrared bands.

References:

[1] de Barros, A. L. F., Bordalo, V., Seperuelo Duarte, E., F da Silveira, E., Domaracka, A., Rothard, H., Boduch, P., *Astronomy & Astrophysics*, 2011, Volume 531,123.

(*) abarros@if.ufrj.br

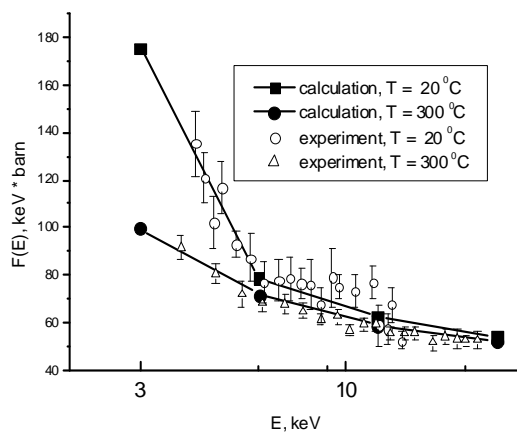
The Increase in Thermonuclear Reaction Yield Due to Ion Channeling in Microcrystals

A.N.Zinoviev

A.F. Ioffe Physical-Technical Institute, 194021, Saint Petersburg, Russia

Cross section of the thermonuclear reaction is $\sigma = F(E)/E \exp\{-\eta(E)\}$, where E is the collision energy, $F(E)$ is the so called astrophysical factor weakly depending on E , and η is the probability of transmission through the Coulomb barrier. In the case of atomic collisions, electron screening of nuclei interaction must be taken into account. According to [1], in this case we need to substitute variable E in the formula considered with effective energy $E' = E + U$, where $U = e^2/R = 20-30$ eV (R is the atom radius). The reaction cross sections were measured at small collision energies $E < 20$ keV [2] to study cold thermonuclear synthesis. In bombarding a number of metals (Zr, Pd, Pt, Co) saturated with deuterium by deuterium ions, authors of [2] observed an increase in factors $F(E)$ with the decrease in collision energy. To fit the experimental data, the authors were forced to assume that $U = 200-600$ eV; they explained such high values by a strong increase in deuterium nuclei screening due to high electron density in a metal. In our opinion, such explanation is doubtful. To compress an electron cloud to such extent, a strong potential field is required (of about U), which breaks molecular bounds in metal.

It is well known that hydrogen atoms occupy free positions along the metal crystal axes. We suggest that the increase in thermonuclear yield is caused by ion focusing in crystal channeling. This focusing increases the effective beam density near crystal axes and, therefore, the corresponding cross section. We have performed a numerical simulation of ion trajectories in Pt crystal saturated by deuterium at collision energies of 3 to 24 keV and confirmed our suggestion. Fig. 1 shows that the proposed model fits satisfactory the experimental data. The fact that channeling particles undulate between the channel potential walls, contributes to the increase in



the beam density near the crystal axis. We took into account also a thermal motion of ions in crystals. When temperature increases, the channel effective size becomes smaller, and a smaller part of particles participate in focusing. Since at small energies mean free paths are only 30 to 300 monolayers, focusing effect can be observed even in quite small metal microcrystals. Our model predicts the existence of the orientation effect in monocrystals.

Fig. 1. Factors $F(E)$ as a function of collision energy E and target temperature T .

References

- [1] H.J.Assenbaum, K.Langanke, C.Rolfs. Z.Phys.A 327, 461 (1987).
- [2] F. Raiola, B.Buchard, Z.Fulop, et al Eur. Phys. J. A27, 79 (2006).

zinoviev@inprof.ioffe.rssi.ru

SHI Irradiation Induced Amorphization of Nanocrystalline Tin Oxide at Low Temperature

R. S. Chauhan^{(1)*}, Vijay Kumar⁽¹⁾, Anshul Jain⁽¹⁾, Deepti Pratap⁽¹⁾,

D. C. Agarwal⁽²⁾, R. J. Chaudhary⁽³⁾, Ambuj Tripathi⁽²⁾

⁽¹⁾*Department of Physics, R. B. S. College, Agra, UP, India-282002*

⁽²⁾*Inter-University Accelerator Centre, Aruna Asaf Ali Marg, New Delhi, India-110067*

⁽³⁾*UGC-DAE CSR Khandwa Road, Indore, M.P., India-452017*

Nanocrystalline tin oxide (SnO₂) thin films were fabricated using pulsed laser deposition (PLD) technique. The as-deposited films were irradiated at liquid nitrogen (LN₂) temperature using 100 MeV Ag ions at different fluences ranging from 3×10^{13} to 3×10^{14} ions/cm² and at 75° with respect to surface normal. Pristine and irradiated samples were characterized using XRD, AFM, Raman and I-V (current-voltage characteristics) for the study of modifications in structural, surface morphological, bond angle and resistivity respectively. XRD patterns show that the pristine film is highly polycrystalline and irradiation amorphizes the film systematically with increasing the irradiation fluence. The surface of the pristine film contains nanograins of tin oxide with roughness 5.14 nm. Irradiation at lower fluences (3×10^{13} and 1×10^{14} ions/cm²) makes the surface featureless and roughness increased to 10.76 nm. Highest fluence (3×10^{14} ions/cm²) irradiation again develops nanograins with roughness 7.412 nm. Raman spectra and I-V characteristics also confirms the irradiation induced amorphization. The observed results are explained in the frame work of thermal spike model [1,2].

References

- [1] A. Benyagoub et al., NIM B 175-177 (2001) 417.
[2] P. K. Kuiry and J. Ghatak, Vacuum 85 (2010) 135

*Corresponding Author: rvschauhan@yahoo.com

Surface Reaction between Water Cluster Ion and Silicon Substrate

H. Ryuto*, G. Ichihashi, M. Takeuchi, and G. H. Takaoka

Photonics and Electronics Science and Engineering Center, Kyoto University

The ion beam technique has been extensively applied to the surface processing and treatment of silicon substrates in the semiconductor industry. Recently, the variety of ion beams used in the semiconductor industry is being extended from atomic ion beams to cluster ion beams. A water cluster ion beam is one of the cluster ion beams that have a high possibility of being applied in the semiconductor industry. The water cluster ion beam is effective in forming oxidized layer on silicon surface [1], or in etching polymer surfaces [2]. The incident angle dependence of the irradiation effects of water cluster ion beams on silicon surfaces was investigated to examine the possibility of further applications.

Water clusters were produced by the supersonic jet method without using a helium support gas. The water clusters were ionized by the electron impact method, and accelerated with the acceleration voltage typically from 3 to 9 kV. The monomers and water clusters with small cluster-sizes were removed by the retarding voltage method. The incident angle dependence of the contact angle of silicon surface was measured by irradiating the water cluster ion beam onto the silicon surface and measuring the contact angle by the $\theta/2$ method.

Figure 1 shows the incident angle dependence of the contact angle of the silicon substrate irradiated with a water cluster ion beam. The contact angle decreased when the water cluster ion beam was irradiated from the vertical direction. On the other hand, the contact angles at the incident angles at 30° and 50° increased by the irradiation of the water cluster ion beam. This variation of the contact angles may be attributable to the competitive processes of the oxidation and sputtering of silicon surfaces.

References

- [1] H. Ryuto, K. Sugiyama, R. Ozaki, G. H. Takaoka, *Applied Physics Express* 2, 016504 (2009).
 [2] H. Ryuto, K. Tada, G. H. Takaoka, *Vacuum* 84, 501 (2010).

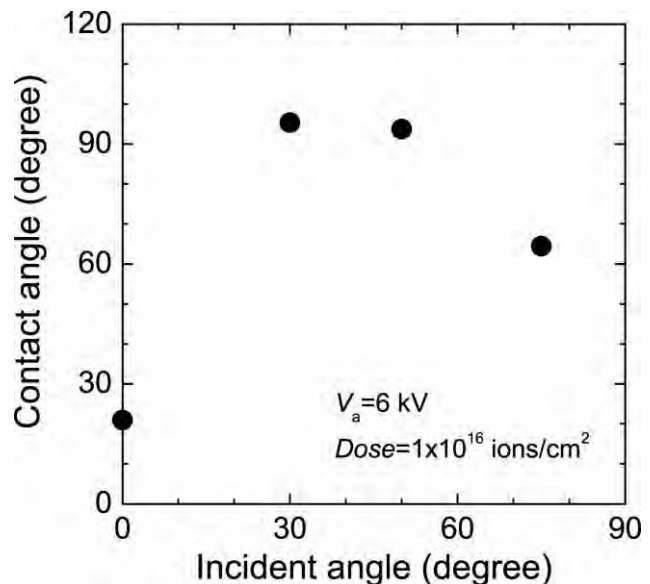


Figure 1. Incident angle dependence of contact angle of silicon surface irradiated with water cluster ion beam.

* ryuto@kuee.kyoto-u.ac.jp

Dynamic ERD Measurements of Depth Profile of H and Li in All Solid State Li-Battery Systems

B. Tsuchiya^{(1)*}, K. Morita⁽²⁾, S. Nagata⁽³⁾, H. Tsuchida⁽⁴⁾, T. Majima⁽⁴⁾, Y. Iriyama⁽⁵⁾

⁽¹⁾ Meijo University, ⁽²⁾ Nagoya Industrial Science Research Institute, ⁽³⁾ Tohoku University,

⁽⁴⁾ Kyoto University, ⁽⁵⁾ Nagoya University

A variety of technologies has been developing for energy production and storage without CO₂ emission at safer, higher energy-efficient and lower cost way to protect the global environment. The catalyst for production and storage of hydrogen from water and the all solid state Li-battery are expected to be newly developed. For their realization, the information on transport behavior of H and Li in the systems of hydrogen storage and solid state Li-battery is of essential importance. So far, we have been developing Pt-covered Li₂ZrO₃ (or Li₄SiO₄) ceramics hydrogen storage materials by means of the ERD technique with 2.8MeV He ion beam [1, 2]. The aim of this work is to demonstrate the possibility of dynamic measurements of depth profile of H and Li at the surface, interface and in the bulk of solid state Li-battery systems of Pt/LiCoO₂/Li_{1+X+Y}Al_YTi_{2-Y}Si_XP_{3-X}O₁₂ (separator) (or Li_{1+X+Y}Al_YTi_{2-Y}Ge_XP_{3-X}O₁₂) under charging and discharging conditions by means of ERD and RBS using 4~9 MeV O ion beams from the Tandem Accelerators.

In experiments, since the ERD technique with O ion beams could detect H and Li atoms simultaneously and the specimens of Li-battery system including some compositions common to those of the hydrogen storage materials might absorb hydrogen from air vapor, the ERD spectra with He ion beams were also obtained to separate overlapped signals of Li and H in the ERD spectra obtained with O ion beam.

From the ERD spectra for Li-battery systems obtained with He ion beams, it has been found that the system with Si-doped separator absorbs a large amount of hydrogen comparable to the hydrogen storage oxide ceramics [1, 2], while that with Ge-doped separator hardly does. The ERD spectra obtained with O ion beams have showed the clear peaks from H and Li atoms at the surface and interface of the specimen as well as in the LiCoO₂ layer (anode electrode) because of its higher depth resolution, although some peaks from H and Li are overlapped. The results on ERD spectra dynamically measured with O ion beams and the other details will be presented at conference.

This work was performed under the valuable co-operations of Tandem Accelerators both at the Quantum Science and Engineering Center, Kyoto University and at the Advanced Research Center of Metallic Glasses, Institute for Materials Research, Tohoku University.

References

- [1] B. Tsuchiya, S. Nagata and K. Morita: Solid State Ionics 192 (2011) 30.
- [2] B. Tsuchiya, K. Morita and S. Nagata: Surf. and Interf. Analysis 44 (2012) 717.

* btsuchiya@meijo-u.ac.jp

High Fluence Ion Erosion of Carbon Composite Fibers

N.N.Andrianova⁽¹⁾, L.B. Begrambekov⁽²⁾, A.M.Borisov⁽¹⁾, E.S.Mashkova⁽¹⁾,
Yu.S.Virgiliev⁽³⁾

⁽¹⁾ Skobeltsyn Institute of Nuclear Physics, Lomonosov Moscow State University, Moscow, Russia,

⁽²⁾ National Research Nuclear University, Moscow, Russia, ⁽³⁾ NII graphite, Moscow, Russia

The structure and morphology of carbon fibers imbedded into uni-directional composite KUP-VM (1D) have been studied under high-fluence ($10^{18} - 10^{19}$ ion/cm²), different irradiation geometry with 10 - 30 keV Ne⁺, Ar⁺ and N₂⁺ ions. The target temperature has been varied during continuous irradiation from room temperature to ~ 400 °C. As for other carbon-based materials, monitoring of the crystal structure change of the carbon fiber composite surface layer has been performed using the temperature dependences of the ion-induced electron emission yield $\gamma(T)$ [1]. Analysis of the surface was performed by the RHEED, SEM and laser goniophotometry (LGP) [2, 3]. It has been found that at sufficiently high energy the ion irradiation results in a loss of an anisotropy of the fiber shell structure because of amorphization at room temperature or recrystallization at temperatures more than the radiation damage annealing temperature T_a . At $T > T_a$ crimping of the carbon fiber is observed. The reason of the modification is the increase of

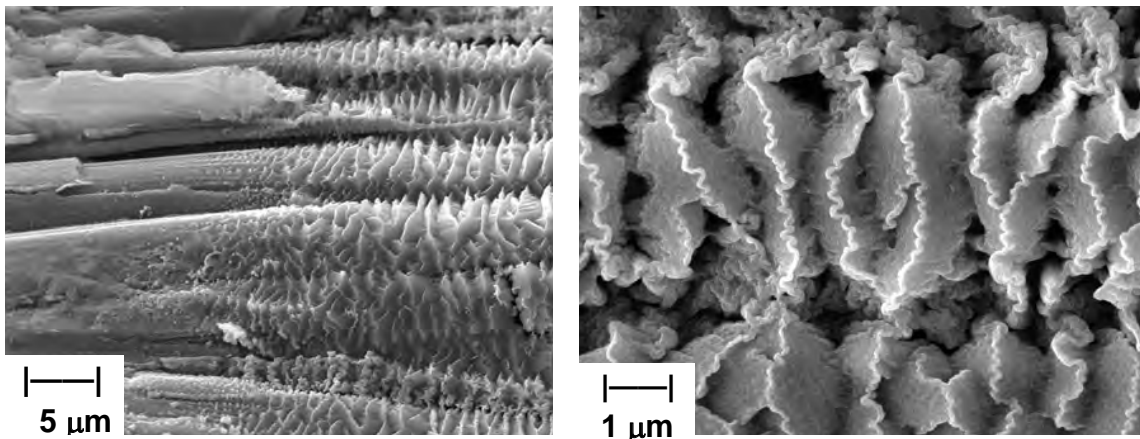


Figure 1. Carbon fiber crimping under 30 keV Ne⁺ irradiation with and without mask

the carbon fiber shell disordering with ion energy as a consequence of increasing stationary level of radiation damage ν (*dpa*). Using an error function of the amorphous fraction on the level ν of radiation damage the threshold values ν_d has been found when the lattice of carbon fiber shell is virtually not disordered under ion irradiation at room temperature. For argon ions the threshold value $\nu_d \approx 40$ *dpa*. For carbon fiber recrystallisation at $T = 400$ °C the cut-off Ar⁺ ion energy ~ 20 keV that corresponds to $\nu \sim 55$ *dpa*. The azimuthal target rotation and irradiation at ion oblique incidence show that the quasiperiodic relief ribs direction is connected not with fiber axis but with ion beam direction. The obtained regularities are discussed in frame of current theories of ion beam erosion.

References

- [1] A.M. Borisov, E.S. Mashkova. Nucl.Instr. and Meth. B. 2007. V. 258. P. 109-115.
- [2] N.N. Andrianova, A.M. Borisov, E.S. Mashkova, Yu.S.Virgiliev. Nucl.Instr. and Meth. B. 2009. V. 267. P. 2778-2781.
- [3] N.N. Andrianova, A.M. Borisov, E.S. Mashkova, Yu.S.Virgiliev. J. Spacecraft and Rockets. 2011. V. 48. P. 45-52.

Energy loss distributions of proton beams interacting with multi-walled carbon nanotubes

J. E. Valdés^(1,2), C. E. Celedón^(1,5), R. Segura⁽⁴⁾, I. Abril⁽²⁾,
C. D. Denton⁽²⁾, P. Vargas⁽¹⁾, R. Garcia-Molina⁽⁴⁾ and N. R. Arista⁽⁵⁾

⁽¹⁾*Departamento de Física, Universidad Técnica Federico Santa María (UTFSM), Valparaíso, Chile*

⁽²⁾*Departament de Física Aplicada, Universitat d'Alacant, Alacant, Spain*

⁽³⁾*Departamento de Química y Bioquímica, Universidad de Valparaíso, Valparaíso, Chile*

⁽⁴⁾*Centro de Investigación en Óptica y Nanofísica, Universidad de Murcia, Murcia, Spain*

⁽⁵⁾*Centro Atómico Bariloche and Instituto Balseiro, S.C. Bariloche, Argentina*

We study experimentally and theoretically the energy loss spectra of energetic proton beams, with energies in the 2-10 keV range, impinging normally to the axis of a multi-walled carbon nanotube (MWCNT). In the experimental setup the MWCNTs are dispersed on top of a holey amorphous carbon (a-C) thin foil. Measurements of the proton energy loss distributions are performed after MWCNT irradiation with energetic proton beams using the transmission technique. The resulting energy loss spectra observed in the forward direction show two well differentiated peaks, whose origin is elucidated by using a semi-classical simulation of the proton trajectory through the nanotube, together with a model for the electronic energy loss based on Density Functional Theory, and with a local electronic density determined by the LMTO-DFT method. We find that the observed low-energy-loss peak corresponds to quasi-planar channelling of protons passing between the outer walls of the MWCNT and exploring lower electronic densities, whereas the high-energy-loss peak is mainly due to protons with intermediate trajectories, moving across the nanotube walls and exploring regions of higher electronic densities.

* email: arista@cab.cnea.gov.ar

A comparative study of the effect of Li^{3+} and C^{5+} ion beam on optical and chemical properties of PADC polymer

Rajesh Kumar*⁽¹⁾, Paramjit Singh⁽¹⁾ and Rajendra Prasad⁽²⁾

⁽¹⁾ *University School of Basic & Applied Sciences,*

Guru Gobind Singh Indraprastha University, New Delhi-110075, India.

⁽²⁾ *Vivekananda College of Technology & Management, Aligarh-202002, India.*

PADC polymers which is also known by the name of CR-39 is homopolymers and high grade optical plastic. Its intrinsic property of ion track detection makes it widely useful for track recording properties in radiation dosimetry. It has been seen that track formation is accompanied by changes in chemical, structural, geometrical, optical and electrical parameters. Ion beam irradiation modifies the optical and chemical properties of the polymers. PADC polymer films were irradiated by 50 MeV Li^{3+} and 70 MeV C^{5+} ion beams at different fluences varying from 10^{10} to 10^{14} ions/cm² from 15 UD Pelletron accelerator at Inter University Accelerator Centre (IUAC), New Delhi, India. The optical and chemical properties were studied by UV-Visible spectroscopy and Fourier Transform Infrared Spectroscopy (FTIR) respectively. The band gap was calculated using Tauc's relation [1]. The band gap decreases with increase in fluence in case of both fluences. There is 24% decrease in band gap by irradiation of C^{5+} ion as compared to 19% decrease in case of Li^{3+} ion at the fluence of 1×10^{13} ions/cm². The FTIR spectrum shows reduction in intensity of typical modes, indicating the degradation of polymer after irradiation in case of both the fluences.

References

[1] R. Kumar et. al Nucl. Instrum. Methods Phys. Res., Sect. B 248 (2006) 279- 28

*rajeshkumaripu@gmail.com

MCs_n⁺ Cluster Formation From Organic Materials During ToF-SIMS Depth Profiling With Cesium

N. Mine^{(1)*}, N. Wehbe and L. Houssiau⁽¹⁾.

⁽¹⁾ *University of Namur (FUNDP), Research centre in Physics of Matter and Radiation (PMR)
61 rue de Bruxelles, B-5000 Namur, Belgium*

Depth-profiling of organic materials has become a major topic in the SIMS community. The advent of large Ar_n⁺ clusters source opens unprecedented possibilities for this task[1]. Our group has also demonstrated the possibility to depth profile organic materials (polymers and amino acids) by using low energy cesium as primary ions [1,2]. The lower sputtering yields compared to cluster sources implies slower profiles, but this drawback is sometimes compensated by a lower difference in the sputtering yields between organic and inorganic layers. The later benefits the depth resolution through a lower induced rugosity. In low energy cesium depth profiling, characteristic fragments are usually followed in the negative polarity. However, in the positive polarity, MCs_n⁺ clusters are formed, where M is a characteristic fragment of the analyzed molecules and n varies from 1 to at least 4. These clusters appear to be a fingerprint of the organic material [4]. For instance, C₆H₅OCs₂⁺ can be used for depth-profiling polycarbonate. The MCs_n⁺ clusters are widely used in dynamic SIMS on inorganics for their lower sensitivity to matrix effects.

In this communication, organic layers of polystyrene and phenylalanine are prepared and studied in ToF-SIMS. Positive polarity depth profiles were acquired using a mixed cesium/xenon sputtering beam (Cs/Xe co-sputtering). The most relevant MCs_n⁺ clusters were monitored as a function of the Cs concentration in the beam, up to a pure Cs beam. Finally, the effect of a pause after the cesium sputtering cycle will be discussed to evaluate their effect on the MCs_n⁺ signals.

References

- [1] S. Ninomiya *et al*, *Nuclear Instruments and Methods in Physics Research Section B: Beam Interactions with Materials and Atoms* **2007**, 256, 493-496
- [2] N. Wehbe, L. Houssiau, *Analytical Chemistry*. **2010**, 82(24), 10052-9
- [3] L. Houssiau, N. Mine, *Surface Interface Analysis*. **2011**, 43, 146-150
- [4] N. Mine, B. Douhard and L. Houssiau, *Applied Surface Science*, **2008**, 255, 973-976

* Nicolas.mine@fundp.ac.be

Interaction between Defects and Deuterium in Tungsten

K. Sato^{(1)*}, R. Tamiya⁽¹⁾, Q. Xu⁽¹⁾, H. Tsuchida⁽²⁾, and T. Yoshiie⁽¹⁾

⁽¹⁾ *Research Reactor Institute, Kyoto University,*

⁽²⁾ *Quantum Science and Engineering Center, Kyoto University*

In a fusion reactor, plasma-facing materials (PFMs) must withstand the damage produced by hydrogen and helium with energy up to 10 keV and heat loads from the plasma, in addition, the neutrons with high energy, high flux and high fluence similar to the structural components. Hydrogen isotopes retain in vacancy-type defects in PFMs, and this is a critical problem for fusion reactors. To know the interaction between vacancy-type defects and hydrogen isotopes is very important. In this study, the size and density of vacancy-type defects in tungsten was obtained by positron annihilation lifetime (PAL) measurements. Next, thermal desorption spectra of deuterium was obtained after deuterium charging. From these results, trapping site and dissociation energy of deuterium were identified.

The samples were 99.95% pure tungsten (A.L.M.T. Corp.). The 0.2-mm-thick sheet was cut to 10×10 mm for ion irradiation and 5mm in diameter for other experiments. These samples were annealed at 1773 K for 1 h in a vacuum of less than 10^{-4} Pa. Electron, deuterium ion and iron ion irradiations were carried out to introduce defects. 8 MeV electrons were irradiated up to 9.4×10^{17} /cm² (1.3×10^{-4} dpa). A displacement threshold energy used for irradiation dose calculation was 42 eV [1]. 5 keV D₂⁺ ions were irradiated up to 1.0×10^{18} /cm² (20 dpa at defect peak) at room temperature (R.T.) and 673 K. 6 MeV Fe³⁺ ions were irradiated up to 2.3×10^{19} /cm² (8.4 dpa at defect peak) at 573 K at 2.0-MV tandem accelerator of Quantum Science and Engineering Center, Kyoto University. After that, 1 keV D₂⁺ ions, which do not form irradiation defects, were implanted. Thermal desorption spectroscopy (TDS) was carried out from R.T. to 1523 K.

From PAL measurement, single vacancies are detected in electron-irradiated sample. Therefore, a peak around 550 K of TDS spectra denotes the elimination of deuterium from single vacancies. Peak separation analysis was performed to spectra of 5 keV D₂⁺ ion- and 6 MeV Fe³⁺ ion irradiation. Spectra of 5 keV D₂⁺ ion irradiation at R.T. and 673 K were resolved into three gauss functions. The peak of them was around 450 K, 560 K and 640 K. Spectra of 6 MeV Fe³⁺ ion irradiation at 573 K were also resolved into three gauss functions. The Peak of them was around 460 K, 630 K and 840 K. 450 K peak denotes the elimination of deuterium from surface. It is concluded that 560 K peak denotes the elimination of deuterium from single vacancies from result of electron-irradiated sample. 640 K peak and 840 K peak denote the elimination of deuterium from dislocations and from voids, respectively.

References

[1] F. Maury, M. Biget, P. Vajda, A. Lucasson and P. Lucasson, Radiat. Eff. 38 (1978) 53.

* ksato@rri.kyoto-u.ac.jp

Embedded ZnO Nanoparticles Irradiated with Swift Heavy Ions: Irradiation-Induced Formation of Metal Phase and Elongation

H. Amekura^{(1)*}, N. Okubo⁽²⁾, N. Ishikawa⁽²⁾,
D. Tsuya⁽¹⁾, Y. Nakayama⁽¹⁾, K. Mitsuishi⁽¹⁾

⁽¹⁾ National Institute for Materials Science, Japan, ⁽²⁾ Japan Atomic Energy Agency, Japan,

Swift heavy ion (SHI) irradiation induces deformation of spherical nanoparticles (NPs) to spheroids of oblate or prolate shapes. The deformation modes are divided into following four categories: (i) Free-standing amorphous or amorphizable NPs, e.g., amorphous silica (a-SiO₂), on a substrate surface show the *oblate* deformation under SHI irradiation, i.e., ion hammering, while (ii) free-standing non-amorphizable crystalline NPs such as Au show almost *no deformation*. However, (iii) spherical metal NPs embedded in a-SiO₂ show *prolate* deformation. While the categories already mentioned have been extensively studied, (iv) the last case, i.e., non-metal NPs embedded in a-SiO₂, has been less studied. An exception is Ge NPs embedded in a-SiO₂. Schmidt et al. [1] observed a bimodal deformation which depends on the sizes of NPs. While larger Ge NPs show the oblate deformation, smaller ones show the prolate deformation.

In this paper, SHI irradiation effects on another example of non-metal NPs, i.e., ZnO NPs, are discussed. This is because ZnO is strong against amorphization, which is in contrast with Ge NPs. Two sets of samples of ZnO NPs were prepared. Free-standing ZnO NPs were formed mainly on a silica substrate surface by ion implantation and thermal oxidation [2]. A set of the free-standing ZnO NPs was irradiated with Xe ions of 200 MeV up to a fluence of 5×10^{13} ions/cm² with an incident angle of 45 deg. The elongation of ZnO NPs was detected by optical absorption spectroscopy using linearly polarized light [3]. No optical anisotropy, i.e., no elongation of NPs, was observed.

The other set of ZnO NPs were covered with an a-SiO₂ layer of 300 nm by chemical vapor deposition (CVD). The same irradiation and measurements were carried out. In contrast with the free-standing ZnO NPs on the surface, the embedded ZnO NPs showed the optical anisotropy, i.e., an indication of the elongation of NPs. Cross-sectional TEM observation combined with the electron energy loss spectroscopy (EELS) confirmed the formation of elongated *metallic Zn* NPs in addition to almost non-deformed ZnO NPs. It seems that the SHI irradiation induced a series of following processes; partial decomposition of ZnO NPs, nucleation and growth of metallic Zn NPs, and the elongation of the metallic Zn NPs.

References

- [1] B. Schmidt, K.H. Heinig, A. Mueklich, and C. Akhmadaliev, Nucl. Instrum. Methods Phys. Res. B **267**, 1345 (2009).
- [2] H. Amekura and N. Kishimoto, in "Lecture Notes in Nanoscale Science and Technology" Vol. 5, edited by Z. Wang (Springer, New York, 2009) pp. 1~75.
- [3] H. Amekura, N. Ishikawa, N. Okubo, M.C. Ridgway, R. Giulian, K. Mitsuishi, Y. Nakayama, Ch. Buchal, S. Mantl, and N. Kishimoto, Phys. Rev. B **83**, 205401 (2011).

* amekura.hiroshi@nims.go.jp

Raman and X-ray Absorption Spectroscopic Study on Defects in Vertically Aligned Multi-walled Carbon Nanotubes irradiated with Ar ions

S. Honda^{(1),(6)*}, Y. Nosho^{(1),(6)}, A. Tsukagoshi^{(1),(6)}, R. Mukouda⁽¹⁾, M. Niibe⁽¹⁾,
M. Terasawa^{(1),(6)}, R. Hirase⁽²⁾, H. Yoshioka⁽²⁾, H. Izumi⁽²⁾, K. Niwase⁽³⁾,
E. Taguchi⁽⁴⁾, K.-Y. Lee⁽⁵⁾, and M. Oura⁽⁶⁾

⁽¹⁾University of Hyogo, ⁽²⁾Hyogo Prefectural Institute of Technology, ⁽³⁾Hyogo University of Teacher Education, ⁽⁴⁾Osaka Univ., ⁽⁵⁾National Taiwan University of Science and Technology, ⁽⁶⁾RIKEN SPring-8 Center

In order to realize the potential nanodevice applications, nanostructured carbon materials, such as carbon nanotube (CNT)[1] and graphene[2], have been extensively studied in the last two decades. Control of morphology of the CNTs is required depending on the nanodevice applications. For example, vertically aligned multi-walled CNT (MWCNT) is available for various nanodevices, such as LSI interconnects, sensors, supercapacitor electrodes, electron field emitters, and heat sink materials. On the other hand, defects in MWCNTs are essential to determine the device performance. Recently, it was reported that there existed the different stages in damaging process of the ion-irradiated MWCNTs by Raman spectroscopy, indicating that the different types of defects were introduced by the ion irradiation[3]. Similar stages were observed in the ion-irradiated graphite[4]. Soft X-ray absorption spectroscopy (XAS) also characterizes defects in MWCNTs introduced by the ion irradiation. Since XAS can provide information on the density of states, it has been powerful tool to characterize the local electronic states of target materials. However, there were a limited number of XAS studies on defects in vertically aligned MWCNTs into which defects are introduced by ions.

In this study, in order to introduce artificial defects into vertically aligned MWCNTs, low energy Ar ions were irradiated to the MWCNT films grown on SiO₂/Si substrates by catalytic CVD, and their structural properties and local bonding configurations were characterized by Raman spectroscopy and XAS. In addition, SEM and TEM were utilized to characterize structural properties of the irradiated MWCNT films. Angle resolved XAS spectra of as-prepared MWCNTs showed that intensity of π^* peak was not strongly dependent on the incident angle of soft X-ray. The MWCNTs may have a wavy form with an averaged orientation perpendicular to the substrate surface. Analysis of Raman spectra showed that there exist the different types of defects in the irradiated MWCNT films as reported in the previous study on the ion-irradiated MWCNT and graphite[3,4]. Analysis of XAS spectra showed that intensity of π^* peak decreased after the irradiation, indicating decrease of sp²-hybridized carbon region and increase of disordered region in the MWCNT films. More detailed results of spectroscopic characterization by Raman spectroscopy and XAS will be presented.

References

- [1] S. Iijima: Nature **354** (1991) 56.
- [2] K. S. Novoselov *et al.*: Science **306** (2004) 666.
- [3] A. Aitkaliyeva *et al.*: Nucl. Instrum. Meth. B **272** (2012) 249.
- [4] K. Niwase and T. Tanabe: Mater. Trans., JIM **34** (1993) 1111.

*s-honda@eng.u-hyogo.ac.jp

We-016

WITHDRAWN

Complex Dielectric Function Formalism for Description of the Electron Kinetics in Swift Heavy Ion Tracks in SiO₂, LiF, Y₂O₃, KBr and Si

N.A. Medvedev^{(1)*}, R.A. Rymzhanov⁽²⁾, A.A. Anikeev⁽³⁾ and A.E. Volkov^(2,3)

⁽¹⁾ *CFEL at DESY, Notkestr. 85, 22607 Hamburg, Germany,* ⁽²⁾ *Flerov Laboratory of Nuclear Reactions, JINR, 141980 Dubna, Russia,* ⁽³⁾ *NRC Kurchatov Institute, Kurchatov Sq. 1, 123182 Moscow, Russia*

Swift heavy ions (SHI, $M > 20$ amu., $E > 1$ MeV/nucl) spend the largest part of their energy for electronic excitations in a target (up to 95%, 1-30 keV/nm). The cross sections of elastic and inelastic channels of scattering of a projectile and appearing fast electrons are the key parameters describing the electronic kinetics in a track.

The Dynamic Structure Factor (DSF) formalism is well appropriate for calculations of these cross sections. It takes into account spatial and temporal correlations in dynamics of target electrons during ionization/excitation of the valence band. The Fluctuation-Dissipation Theorem links the DSF of the electron subsystem with the Complex Dielectric Function (CDF) [1,2] which can be reconstructed from the experimentally accessible optical data. All the collective effects, such as excitation of the collective modes (e.g. plasmons) and dynamical screening of the interaction potential, are taken into account within this approach. The CDF formalism allows obtaining the inelastic mean free path of a charged particle (electron and ion) in solids with high accuracy. For electrons, it can also be used to obtain elastic scattering cross section [3].

A detailed description of the method of calculation of elastic (e.g. on phonon) and inelastic (electron ionization from the valence band or deep atomic shells) scattering cross-section, mean free paths and energy losses of electrons in SiO₂, LiF, Y₂O₃, KBr and Si is presented. Based on the CDF cross sections, a Monte-Carlo (MC) model of event-by-event simulations of the electronic kinetics in a SHI track is developed. Application of this MC model allows us to obtain the spectra and the radial distributions of the valence and conduction band electronic excitations in tracks of different ions (from C to U) in these materials.

The analysis of the mechanism governing creation of the internal (within ~10 nm radius) and external (> 10 nm) segments of the radial distributions of valence holes, electrons and the density of the excess energy of the electron subsystem are presented. A substantial difference in the parameters of the outer segment of these distributions obtained from CDF vs binary collision approximation (BCA) approaches is demonstrated.

References

- [1] A. Akkerman *et al.*, Phys. Stat. Sol. (b) **198**, 769 (1996)
- [2] R. H. Ritchie, A. Howie, Phil.Mag. 36, 463-481 (1977)
- [3] J.-Ch. Kuhr, H.-J. Fitting, J. of Elec. Spectr. Rel. Phen. 105, 257-273 (1999)

* nikita.medvedev@desy.de

Sputtering of frozen oxygen by ion impact: Comparison of experiment and atomistic simulation

Christian Anders⁽¹⁾, Magdalena Skalska⁽²⁾, Roman Pedrys⁽²⁾ and Herbert M. Urbassek^{(1)*}

⁽¹⁾ *Fachbereich Physik und Forschungszentrum OPTIMAS, University Kaiserslautern, Erwin-Schroedinger-Straße, D-67663 Kaiserslautern, Germany*

⁽²⁾ *Marian Smoluchowski Institute of Physics, Jagiellonian University, Reymonta 4, 30-059 Krakow, Poland*

Translational energy distributions of particles sputtered by 750 eV Ne⁺ ion impact into a cryogenic O₂ target are studied both experimentally and using molecular-dynamics simulation. Excellent agreement between experiment and simulation is found for the low-energy spike contribution of sputtered molecules, while at higher energies (≥ 0.5 eV), experiment shows a deficiency in sputtered molecules. These differences are traced back to two sources: (i) inelastic electronic excitation, which is not taken into account in the molecular-dynamics simulation (ii) high rovibrational excitation of sputtered molecules. Due to the increasing probability of molecule dissociation in the high-energy part of the collision cascade, the translational energy spectrum of emitted molecules deviates systematically from a Thompson distribution. Around 2 % of the sputtered particles consist of radicals (atomic O). These originate from direct projectile-molecule collisions; they are emitted early in the collision cascade and feature a strong high-energy contribution.

* urbassek@rhrk.uni-kl.de

Energy distribution of C^+ ion sputtered from graphite surface

I.K. Gainullin⁽¹⁾, V.A. Khodyrev⁽²⁾, V.V. Khvostov⁽¹⁾ and E.Yu. Zykova⁽¹⁾¹

⁽¹⁾ *Physics Faculty, Moscow State University,* ⁽²⁾ *Institute of Nuclear Physics, Moscow State University*

The energy distributions of carbon ions sputtered from the graphite (0001) surface under 1 keV Ar^+ bombardment have been studied both experimentally and involving computer simulation. In our experiments the angle between incident ion direction and the axis of energy analyzer has been fixed to be 90° . The energy spectra obtained in experiments show oscillating behavior and a shift to high energy region. In case of specular geometry (incident ion angle is 45°) we observe the energy distribution (fig.1a) with the absolute maximum at the energy of 55 eV. In addition the apparent maxima are at the energies of 30, 70, 82 and 103 eV. These results cannot be adequately explained within the framework of the theory of elastic interactions of ions with a surface. It has been supposed that the oscillating behavior of energy spectra can be related to resonance charge exchange between positive ion and the surface [1].

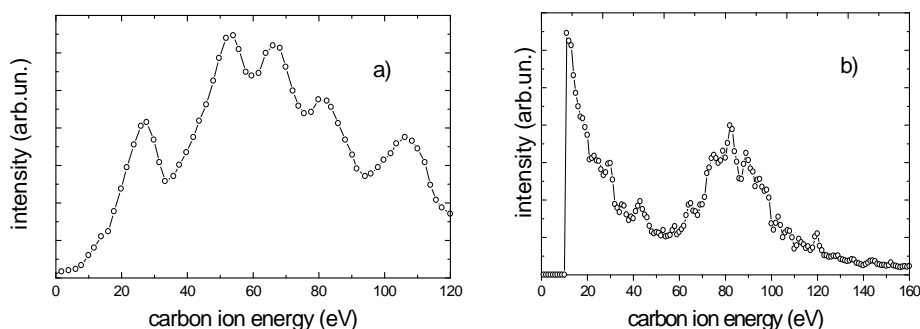


Figure 1. Experimental (a) and calculated (b) energy distributions of C^+ ions sputtered from graphite surface by 1 keV Ar^+ , impinging at angle $\alpha = 45^\circ$.

We have carried out a computer simulation of the carbon ions energy distribution using the binary collision model taking into account the thermal displacements of crystal atoms [2]. The curve obtained (fig.1b) also demonstrates the similar non-monotonic character and a shift to high energy region. These results allow us to conclude the surface structure effects are important in the process of the destruction of the graphite.

This work was supported by the RFFI (10-02-00162-a, 11-02-01500-a) and (GK-14.740.11.1004).

References

- [1] E.R. Amanbaev, I.K. Gainullin, E.K. Zykova, I.F. Urazgildin . *Thin Solid Films* **519**, 4737 (2011).
 [2] V.A. Khodyrev, R. Andrzejewski, A. Rivera, D.O. Boerma, J. E. Prieto, *Phys. Rev. E* **83**, 056707 (2011).

¹ zykova@phys.msu.ru

Mechanisms of improvement of the silicon layer crystal structure

A.A Shemukhin^{(1)*}, Y.V. Balakshin⁽²⁾, V.S. Chernysh⁽²⁾

⁽¹⁾*Moscow Radiotechnical Institute of Russian Academy of Science, Moscow, Russia*, ⁽²⁾*Faculty of Physics, Moscow State University, Moscow, Russia*

The silicon-on-sapphire (SOS) structures are considered to be a promising material for fabrication of radiation-resistant integrated circuits. To create modern devices the active Si layer should be about 100 nm thick. However, due to the growth mechanisms Si on Al₂O₃ substrate such layers contain a lot of defects. The crystalline quality of the mentioned layer can be significantly improved with ion implantation and subsequent annealing. However, mechanisms of this phenomenon are not studied well enough up till now.

Experimental study of an influence of the ion implantation parameters (energy and fluence, as well as, temperature of implanted structure) on characteristics of the active Si layer will be presented in this report.

In these experiments, SOS-structures were irradiated by Si⁺ ion beam at the accelerator HVEE-500. The analysis of the active Si layer was carried out by using RBS, SIMS and HRTEM. Results of this research allowed to make a conclusion about mechanisms of improvement of the silicon layer crystal structure due to implantation of Si⁺ ion and a further temperature treatment.

* shemuhin@gmail.com

Study of Ge amorfization by using MEIS

Y.V. Balakshin^{(1)*}, A.A Shemukhin⁽²⁾, P.N. Chernykh⁽³⁾, V.S. Chernysh^{(1),(3)}

⁽¹⁾Faculty of Physics, Moscow State University, Moscow, Russia, ⁽²⁾ Moscow Radiotechnical Institute of Russian Academy of Science, Moscow, Russia, ⁽³⁾ Scobeltsin Institute of Nuclear Physic, Moscow State University, Moscow, Russia

Thin film structures are usually used to demonstrate the high depth resolution of MEIS. However, some uncertainties can appear due to island growth of the films.

It is possible to evaluate the MEIS resolution by analyzing heterogeneity created at initially smooth single-crystal sample. To fabricate such systems an amorphous layer with a controlled thickness can be created by heavy ion bombardment of semiconductor single crystal surface.

In our experiments, surface roughness of Ge samples was controlled by using AFM before and after Ar ion bombardment. Energy of bombarding Ar ion was 500 eV. Irradiation fluence was about 10^{17} ions/cm² that is enough to amorphization of thin surface layer. Samples were analyzed by using MEIS. He⁺ ions with energy 180 keV were used as analyzing beam.

A description of apparatuses for researching patterns with the help of medium energy ion scattering and the results of the first experiments demonstrating possibilities of the technique will be presented.

* balakshiny@gmail.com

Swift Heavy Ion induced modification in Morphological and Optical Properties of Tin Oxide Nanocomposites

Manoj Kumar Jaiswal^{(1),*}, D. Kanjilal⁽²⁾ and Rajesh Kumar⁽¹⁾

⁽¹⁾University School of Basic and Applied Sciences,

Guru Gobind Singh Indraprastha University, New Delhi, India –110075

⁽²⁾Inter University Accelerator Centre, Aruna Asaf Ali Marg, New Delhi, India –110 067

Abstract

Nanocomposite thin films of tin oxide (SnO₂)/titanium oxide (TiO₂) were grown on silicon <100> substrates by electron beam evaporation deposition technique using sintered nanocomposite pellet of SnO₂/TiO₂ in the percentage ratio of 95:5. Sintering of the nanocomposite pellet was done at 1300⁰C for 24 hours. The thickness of these films were measured to be 100 nm during deposition using piezo-sensor attached with the deposition chamber. Swift heavy ion beam irradiation was done by SHI beams of 100 MeV Au using 16 MV Pelletron Accelerator at IUAC, New Delhi. Irradiation ion fluencies varies between 1×10¹¹ ions.cm⁻² and 5×10¹³ ions.cm⁻². Optical properties of these as deposited and ion irradiation modified thin films were carried out by UV/Vis. Spectroscopy and Fourier Transform Infrared Spectroscopy (FTIR). FTIR peak at 610 cm⁻¹ confirms the presence of O-Sn-O bridge of tin (IV) oxide signifying the composite nature of the as-deposited and irradiated thin films. Atomic force microscopy (AFM) technique in tapping mode was used to study the surface morphology and grain growth due to swift heavy ion irradiation. Grain size calculations were compared with results obtained from glancing angle X-ray diffraction (GAXRD) measurements using Scherrer's formulae. Phase transformation due to irradiation was observed from glancing angle X-ray diffraction (GAXRD) results. The prominent 2θ peaks observed in GAXRD spectrum are at 30.67⁰, 32.08⁰, 43.91⁰, 44.91⁰ and 52.35⁰ in irradiate films. Detailed experimental results and their analyses will be presented.

Key words: SHI, AFM, GAXRD, UV/Visible, FTIR.

*E-mail Address for correspondence : m.k.jaiswal7979@gmail.com, rajeshkumaripu@gmail.com

Coincidence Measurement of Secondary Electrons with Scattered Ions under Irradiation of Fast Carbon-Cluster Ions

Y. Shiina^{(1)*}, S. Tamura⁽¹⁾, I. Harayama⁽¹⁾, K. Yamazaki⁽¹⁾, K. Sasa⁽²⁾, S. Ishii⁽²⁾, and S. Tomita⁽¹⁾

⁽¹⁾ *Institute of Applied Physics, University of Tsukuba, Tsukuba, Ibaraki 305-8573, Japan*

⁽²⁾ *Tandem Accelerator Complex, University of Tsukuba, Tsukuba, Ibaraki 305-8577, Japan*

The secondary electron yield of a fast atomic ion is proportional to stopping power over a broad energy range [1], while that of a cluster ion does not follow the same trend [2]. This is an example of phenomenon called as cluster effects. It is already known that the cluster effect on energy losses is so weak compared with that on secondary electron yields [3]. Therefore, it seems that the cluster effect on secondary electron yields stems mainly from the transport or transmission process, rather than the production process. However, the detailed mechanism is not yet explained.

We investigated correlation of secondary electron emission with scattering of ions in solids. The schematic setup is shown in fig. 1. The SSD is located in forward angle. The ions emitted in small angle (smaller than 3 degrees) are detected by SSD. The secondary electron yield in backward angle is measured with MCP, in coincidence with the number of detected ions by SSD. We studied the correlation between the secondary electron yield and the number of detected ions by SSD.

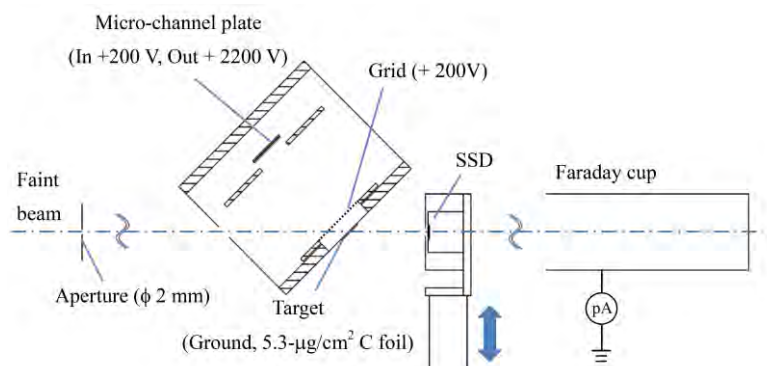


Figure 1. A schematic of the experimental setup

References

- [1] H. Rothard, K. Kroneberger, A. Clouvas, E. Veje, P. Lorenzen, N. Keller, J. Kemmler, W. Meckbach and K. O. Groeneveld, *Phys. Rev. A* 41, 2521 (1990).
- [2] H. Arai, H. Kudo, S. Tomita and S. Ishii, *J. Phys. Soc. Jpn.* 78, 104301 (2009).
- [3] S. Tomita, M. Murakami, N. Sakamoto, S. Ishii, K. Sasa, T. Kaneko and H. Kudo, *Phys. Rev. A* 82, 044901 (2010).

* shiina@ilab.bk.tsukuba.ac.jp

Micro-PIXE Analysis for Light Elements Using He Beam

S.Uomori⁽¹⁾, K. Takahashi⁽¹⁾, K. Yasuda⁽²⁾, H. Yamashita⁽¹⁾,

M. Saito⁽¹⁾, Y. Haruyama⁽¹⁾

⁽¹⁾ *Department of Informatics and Environmental Science, Kyoto Prefectural University*

⁽²⁾ *The Wakasa Wan Energy Research Center*

A nuclear microprobe is widely adopted to investigate near surface structure and elemental distributions. Proton micro-beam PIXE became a popular tool above all. In the PIXE measurement, a thin foil is located just before an x-ray detector to prevent scattered protons entering the detector. This foil causes rapid decrease of characteristic x-rays from light elements. We changed the incident beam from proton to alpha particle to reduce the thickness of the foil and improved the overall detection efficiency for the light elements. We tried to measure the distributions of light elements in plant using this setup.

It is well known that aluminum have high toxicity for almost all plants. However, there are some strange plants that hyperaccumulate aluminum, such as hydrangea, tea and buckwheat. We adopted tea leaf as a specimen and tried to measure elemental distributions in it.

We used 5MV tandem-accelerator of the Wakasa Wan Energy Research Center. A combination of 2.5 MeV He micro beam and 8.5 μm thick mylar foil was used. The foil thickness was reduced to 1/10 compared with that for the same energy proton beam. The transmission of aluminum K-X ray increased by the order of 4. This improvement makes us easier to measure the elemental distribution of aluminum in the tea leaf.

The beam spot size was $10 \times 10 \mu\text{m}^2$. The beam current was about 200 pA. The scan area was $400 \times 400 \mu\text{m}^2$. Almost specimens were irradiated for about 45 min. The following elements were detected, such as Al, Si, P, S, Cl, K, Ca and Mn. We found that aluminum and silicon spatial distributions in tea leaf changed according to the growing period. In a young leaf, aluminum and silicon were found all over the mesophyll cell, however, they localized in the upper epidermis in a matured leaf.

We-025

WITHDRAWN

The Absorption Spectra of LiYF₄ Crystals Irradiated at 15K

Y. Bikhert⁽¹⁾, V. Lisitsyn⁽²⁾, A. Akilbekov⁽¹⁾, V. Reiterov⁽³⁾, M. Zdorovets⁽⁴⁾ and

A. Dauletbekova^{(1)*}

⁽¹⁾L.N. Gumilyov Eurasian National University, ⁽²⁾ National Research Tomsk Polytechnic University
, ⁽³⁾INCROM, ⁽⁴⁾Astana Branch of INP RK

Spectra of the induced optical absorption in nominally "pure" and doped with Nd in LiYF₄ crystals under irradiation with electrons flows at 15 K were studied.

Samples were irradiated with electrons, the source of radiation - high-current pulsed accelerator generating flow with 0.2 MeV average energy of electrons, the pulse duration - 10 ns, energy per pulse 10²Gy absorbed by the crystal. Irradiation and measurement of the induced absorption were performed on the pulsed optical spectrometer. Additional absorption of the crystal during irradiation was measured with respect to non-irradiated crystal.

Figure 1 shows the spectra of the induced and measured at 15 K an additional absorption in crystals of pure LiYF₄ and Nd-containing with concentrations of 0.7 and 4 mol%. All crystals were irradiated with electron beam pulses, the dose of 8×10³ Gy. In the spectrum of induced absorption in the pure crystal LiYF₄ bands at 2.1, 2.9 and 3.6 eV can be clearly distinguished.

In Nd-doped crystals induced absorption in the region of 2.5 ...6 eV is similar to the induced in pure crystals. There is only a band shift towards the shorter wavelengths. Additional absorption can also be observed for doped crystals in the region of 1.5 ...2.5 eV but with a pronounced split into two bands at 2 and 2.3 eV. Stability of the induced color centers was studied. The crystal was irradiated with a series of pulses of electrons with a dose of 10⁴Gy, induced absorption spectrum was measured at this temperature. Then the crystal is heated to a temperature $T_i > 15K$, cooled to 15 K and spectrum of induced absorption was measured again. It was found that up to 45K induced absorption remains practically unchanged. At temperatures above 45K there is a sharp decline in the absorption indicating the beginning centers destruction. Maximum rate of destruction of the centers is at 60K. At 80K points and corresponding induced absorption completely disappears.

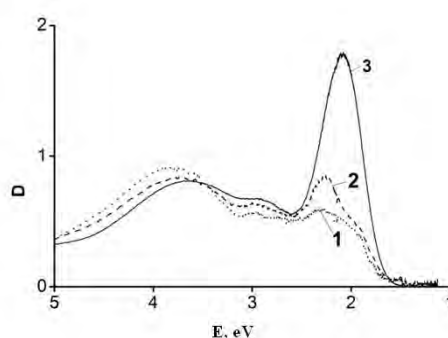


Figure 1 Spectra of the induced and measured at 15 K an additional absorption in crystals of pure LiYF₄ (3) and Nd-containing with concentrations of 0.7 (2) and 4 (1) mol%.

* alma_dauletbek@mail.ru

ELECTRON EMISSION STATISTICS OF SLOW HIGHLY CHARGED IONS DURING INTERACTION WITH INSULATING SURFACES

W. Meissl ⁽¹⁾, D. Schrempf ⁽¹⁾, R.A. Wilhelm ⁽²⁾, D. Winklehner ⁽³⁾, S. Facsko ⁽²⁾, F. Aumayr ⁽¹⁾ and R. Heller ^{(2)*}

⁽¹⁾ *Institute of Applied Physics, TU Wien, 1040 Vienna, Austria,* ⁽²⁾ *Helmholtz-Zentrum Dresden-Rossendorf, Institute of Ion Beam Physics and Materials Research, Bautzner Landstraße 400, 01328 Dresden, Germany,* ⁽³⁾ *National Superconducting Cyclotron Laboratory, Michigan State University, 640 S Shaw Lane, East Lansing, Michigan 48824, USA*

The important role of highly charged ions (HCI) as a promising candidate for creation of nanometer-sized surface structures has been demonstrated in several experiments in recent years. The underlying physical processes of nano structure creation strongly differ for different kind of target materials. Nevertheless, the majority of proposed models have one point in common: They underline the major role of the electrons emitted by the projectile during HCI neutralization above and below the surface.

Hence, a detailed understanding of the electron emission characteristics becomes more and more necessary. Experiments observing the electron emission statistics of very slow highly charged ions have been carried out so far only for metal surfaces [1,2]. For surfaces of insulators measurements of the total electron emission statistic exist only for moderate ion velocities between 1 and 5 keV/amu [3].

In this contribution we will present first results of electron emission statistic measurements for highly charged Xenon ions ($q \leq 44+$) impinging on insulating surfaces of CaF₂, KBr as well as LiF at kinetic energies as low as $10 \cdot eVq$. This is well within a regime where kinetic electron emission is not contributing to the total electron emission yield giving us the opportunity to compare our results with predictions from the classical-over-the-barrier model. Our results reveal an unexpectedly high electron emission yield on insulators even for lowest velocities. The effect of projectile energy gain due to image charge acceleration can be derived from the velocity dependence of the electron yield.

References

- [1] A. Arnau et al., *Surf. Sci. Rep.* **27** (1997) 113
- [2] F. Aumayr, HP. Winter, *NIMB* **233** (2005) 111
- [3] W. Meissl et al., *e-J. Surf. Sci. Nanotech.* **6** (2008) 54-59

* r.heller@hzdr.de

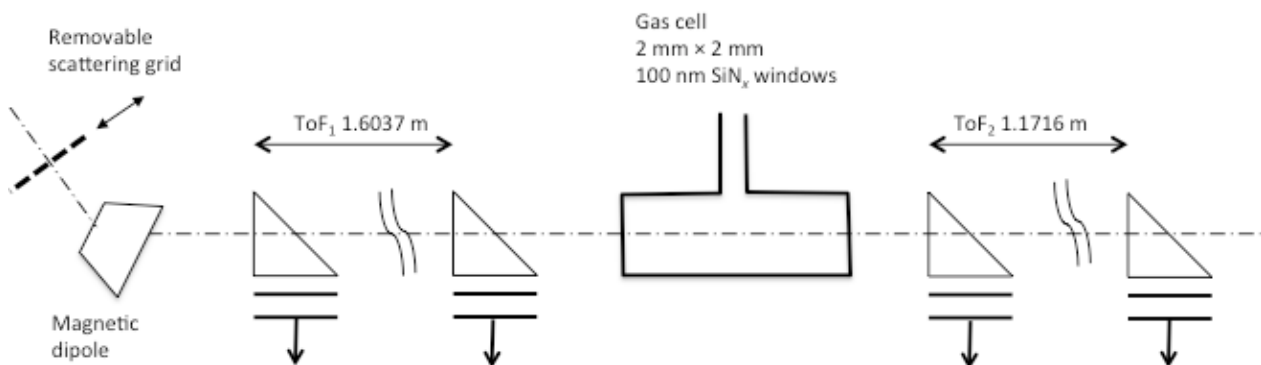
Straggling of MeV Kr Ions in Gases

J. Jensen⁽¹⁾, J. Julin⁽²⁾, H. Kettunen⁽²⁾, M. Laitinen⁽²⁾, O. Osmani⁽³⁾, M. Rossi⁽²⁾, T. Sajavaara⁽²⁾, A. Schinner⁽⁴⁾, P. Sigmund⁽⁵⁾, C. Vockenhuber⁽⁶⁾, H.J. Whitlow^{(2,7)1}

⁽¹⁾Linköping University, Sweden, ⁽²⁾Department of Physics, University of Jyväskylä, Finland, ⁽³⁾Donostia International Physics Center, San Sebastian, Spain, ⁽⁴⁾J. Kepler University Linz, Austria, ⁽⁵⁾University of Southern Denmark, Odense, Denmark, ⁽⁶⁾ETH Zürich, Switzerland, ⁽⁷⁾Haute Ecole Arc Ingénierie, Switzerland.

It is well established that energy-loss straggling of swift heavy ions may considerably exceed the Bohr value [1]. While both experiment and theory predict a pronounced maximum in the dependence of straggling on beam energy, there is considerable uncertainty on position and value of that maximum. Since straggling is expected to be greater in gases than in otherwise equivalent solids [2,3], we have built an apparatus to study straggling in gases at the Jyväskylä K130 cyclotron by the time-of-flight technique (Fig. 1). Entrance and exit to the gas cell goes through thin SiN foils which are characterized by high uniformity. To create ion beams with a range of well defined lower energies and charge state than the primary beam, it is scattered from a removable grid and momentum-charge state separated using a magnetic dipole.

Measurements are reported for krypton ions in noble gases and nitrogen. Straggling has been determined from measured time-of-flight spectra in front of and behind the gas cell with and without gas, taking into account straggling in the entrance and exit foils.



References

- [1] Q. Yang, D. J. O'Connor, Z. Wang, NIMB 61, 149 (1991)
- [2] P. Sigmund, A. Schinner, EPJD 58, 105 (2010)
- [3] P. Sigmund, O. Osmani, A. Schinner, NIMB 269, 804 (2011)

1 harry.whitlow@he-arc.ch

Study of Mechanisms of MeV Light Ion-beams Focusing by Tapered Glass Capillaries

Sha Yan^{(1)*}, Zhiyu Gong⁽¹⁾, Yizhou Zhu⁽¹⁾, Hongji Ma⁽²⁾, Rui Nie⁽²⁾, Jianming Xue⁽¹⁾,
and Yugang Wang⁽¹⁾

⁽¹⁾ *State Key laboratory of Nuclear Physics and Technology, Institute of Heavy Ion Physics, Peking University, Beijing, 100871, China*

⁽²⁾ *State Key laboratory of Nuclear Physics and Technology, Department of Technical Physics, Peking University, Beijing, 100871, China*

Many experimental results from different labs show that the tapered glass capillary not only can focus low energy (usually in magnitude of keV) highly charged ions (HCIs), but also can focus single charged light ion beams with MeV energy. It is in wide agreement that the focusing mechanism of glass capillary to HCIs is elastic scattering by Coulomb potential of self-organized state charges on the wall of the capillary. This theory is also used to explain the guiding function of nano-pores in insulator membrane to HCIs. However, the focusing mechanism for single charged light ions with MeV energy is still in discussion. Scattering by Coulomb potential of self-organized static charges, by continuous surface potential, and Rutherford scattering, are candidates.

Our experiments took 2 MeV He⁺ ions as incident beams. The fluence rates were quite weak, about 10⁻²~10⁻³ pA. We analyzed the energy spectra of output ions and the density distributions on ejected beam cross sections, and found that are in accord with the results of last two kind of scattering, rather than the case of self-organized electric field. We deduced the reason is that the fluence rates is too weak to form an effect self-organized electric field. We estimated the necessary fluence rate for producing an enough strong self-organized electric field. Further experiments are needed to prove it.

* syan@pku.edu.cn

Sputtering yields of Au/Si films under the impact of 20 - 160 keV Ar⁺ ions

S. Mammeri⁽¹⁾, H. Ammi⁽¹⁾, S. Ouichaoui^{(2)*}, A. Dib⁽¹⁾

⁽¹⁾ CRNA, B.P. 399, 02 Bd. Frantz Fanon, Alger-Gare, Algiers, Algeria

⁽²⁾ USTHB, Faculté de Physique, B.P. 32, El-Alia, 16111 Bab Ezzouar, Algiers, Algeri.

The sputtering yields induced in Au thin films deposited onto Si substrates under the impact of swift Ar⁺ ions have been measured over the (20 - 160) keV energy range. Then, the irradiated films have been analyzed by Rutherford backscattering (RBS) spectroscopy using a 2 MeV beam of ⁴He⁺ ions. The obtained results were found to be consistent with previously measured data that are extended to higher bombarding energies. The whole set of experimental data is compared to numerical sputtering yields predicted by Sigmund's theory [1] and other models or derived by Monte Carlo simulation using the SRIM-2008 computer code [2], and shows to be best consistent with Yamamura et al. revised semi-empirical formula [3]. In addition, the morphology and surface state evolution of the Au films under Ar⁺ ion irradiation have been investigated by means of the scanning electron microscopy (SEM) and X-ray diffraction (XRD) techniques. It was found that the irradiated Au film surfaces were drastically altered with increasing ion energy, with formation of increasingly sized grains of preferred (111) crystalline orientations. Finally, the relevance of the performed different sputtering yield calculations to account for the measured sputter yields is discussed by invoking the observed Ar⁺ ion-induced surface effects.

Keys words: Sputtering yields, Rutherford backscattering spectrometry, Scanning electron microscopy, X-ray diffraction spectroscopy.

References

- [1] P. Sigmund, Phys. Rev. **184** (1969) 38.
- [2] J.F. Ziegler, J.P. Biersack and U. Littmark, The stopping and range of ions in solids, Pergamon, New York, 1985; SRIM computer code, available at <http://www.srim.org>.
- [3] Y. Yamamura, Y. Mizuno, H. Kimura, Nucl. Instr. and Meth. in Phys. Res. B **13** (1986) 393..

* souichaoui@gmail.com

NRA for hydrogen analysis in atmospheric condition

D. Sekiba^{(1)*}, Y. Narita⁽¹⁾, S. Harada⁽¹⁾, S. Ogura⁽²⁾, and K. Fukutani⁽²⁾

⁽¹⁾*Institute of Applied Physics, University of Tsukuba, Tennodai 1-1-1, Tsukuba, Ibaraki 305-8577, Japan.*

⁽²⁾*Institute of Industrial Science, University of Tokyo, Komaba 4-6-1, Meguroku 153-8505, Tokyo, Japan.*

Mg-based nano-superlattices has attracted much attention as novel hydrogen storage materials. A. Baldi *et al.* reported that hydrogen absorption process in Mg-based superlattices is strongly affected by the strain at the interfaces [1]. In order to investigate such a hydrogen absorption process in subsurface region of materials with nano-meter scale directly, we developed nuclear reaction analysis (NRA) of $^1\text{H}(^{15}\text{N}, \alpha\gamma)^{12}\text{C}$ for hydrogen analysis in atmospheric condition with using SiN membrane with 100 nm thickness [2]. Then we estimated the depth resolution of this system. Considering the energy straggling of ~ 6 MeV ^{15}N beam in the SiN membrane with Au coating and Doppler effect, the energy spread of the beam at the target surface was estimated as ~ 45 keV. This corresponds to the depth resolution of hydrogen analysis of ~ 30 nm in Mg and Ti film. From this estimation we prepared a following Mg-based nano-superlattice; Pd (20 nm) / Mg₁ (20 nm) / Ti (30 nm) / Mg₂ (20 nm) / Ti (30 nm) / substrate. According to the model by Baldi *et al.*, the Mg₂ layer is hydrogenated at lower hydrogen gas pressure ~ 50 Pa, and then the Mg₁ layer is hydrogenated at much higher pressure ~ 300 Pa [1]. Figure 1 shows the obtained NRA profiles on the Mg-based nano-superlattice taken with changing the hydrogen gas pressure from high vacuum up to 500 Pa. As results, we observed the hydrogenation of the Ti layers at 10 \sim 50 Pa, that of the Mg₂ layer at 100 Pa, then finally the Mg₁ layer was hydrogenated at ~ 500 Pa. Thus we successfully observed the strain effect in the hydrogen absorption process in nano-scale materials.

References

[1] A. Baldi, M. Gonzalez-Silveria, V. Palmisano, B. Dam, R. Griessen, Phys. Rev. Lett., 102 (2009) 226102..

[2] H. Yonemura, Y. Kitaoka, D. Sekiba, H. Matsuzaki, S. Ogura, M. Matsumoto, Y.

Iwamura, T. Ito, T. Narusawa, K. Fukutani, Nucl. Instr. Meth. B 269 (2011) 632.

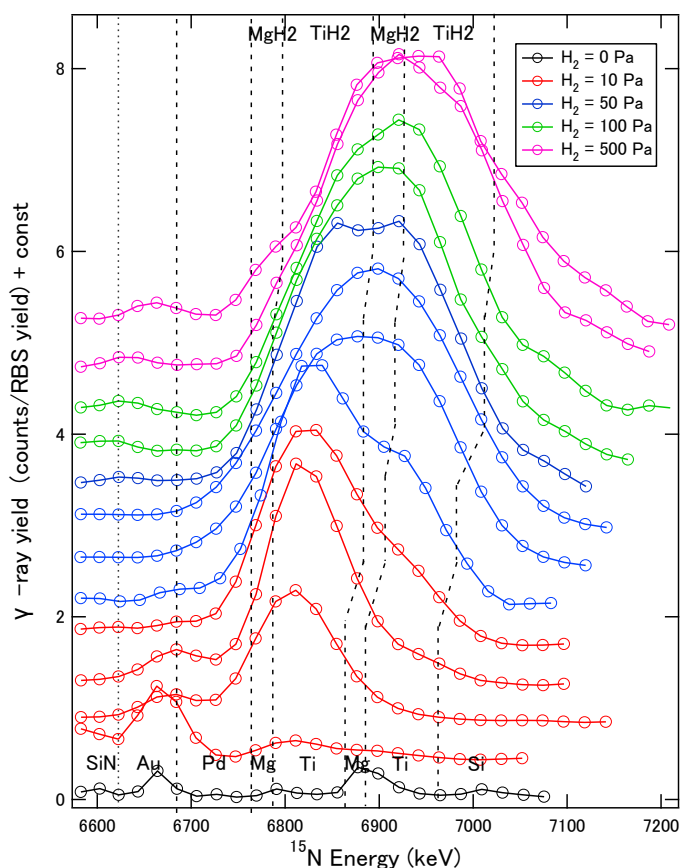


Figure 1. NRA profiles on Mg-based nano super-lattice taken with changing the hydrogen gas pressure

The Quantum Trajectory Approach in Description of Ion-atom Collisions

V A Khodyrev*

Institute of nuclear physics, Moscow state university, 119991 Moscow, Russia

As for classical systems, where the Monte Carlo simulation is sometimes the only applicable method of calculation, analogous approach can be used in treatment of quantum atom dynamics. The possibility follows from the de Broglie-Bohm formulation of quantum theory, the quantum state of an individual system is supplemented by a deterministic trajectory in configuration space. Such interpretation of quantum theory was inspired by the fact that, with the uni-polar amplitude-phase ansatz for the wave function $\Psi(\mathbf{r}, t) = R(\mathbf{r}, t)e^{iS(\mathbf{r}, t)/\hbar}$, the Schrödinger equation can be transformed to the classical-like continuity and Hamilton-Jacobi equations. The only specifics in the latter equation

$$\frac{\partial S}{\partial t} = -\frac{(\nabla S)^2}{2m} - (U + Q)$$

is the additional "quantum potential" term $Q(\mathbf{r}, t)$ which is determined by the curvature of the amplitude $Q = -(\hbar^2/2)(\Delta R/R)$. The motion along quantum trajectories is guided by the wave function according to the velocity field $\mathbf{v} = \nabla S/m$.

When the wave function is known the quantum trajectories can be used as an effective interpretation tool. Like in the classical description this shows origin of interesting effects not easily accessible from solution of the time-dependent Schrödinger equation, TDSE. Additionally, as it was recognized in the last decade [1], the quantum trajectory method, QTM, can be used also as a method of solution of TDSE (exact in the limits of numerical accuracy). In calculation the wave function can be generated simultaneously, on the fly, the time-dependent amplitude R and the phase S of the wave function can be synthesized by the density $\rho = R^2$ and velocities \mathbf{v} of the Bohmian particles. Compared to the straightforward numerical solution of TDSE this method is dramatically more efficient.

Up to now QTM was used mainly in the Chemical Physics domain. We explore its possibilities in description of evolution of electron state in fast ion-atom collisions. Specific problems in usage of QTM here are the following. First is due to the singular Coulomb potentials of nuclei which could result in necessity of high resolution of motion nearby. Analysis show, however, that in close electron-nucleus collisions where their interaction is dominating the singularity of the potential U is exactly compensated by equivalent singularity of the quantum potential (the Kato cusp condition). The second is the "node problem": the quantum potential Q diverges at surfaces where R is zero. Near these surfaces the trajectories closes and it is hard in numerical calculations to satisfy the condition that they never cross. As a result the numerical calculation can simply crash. Notice, however, that the quantum current $\mathbf{j} = \rho \nabla S$ is a smooth function of coordinates, also near the node surfaces. Therefore, it is reasonable to replace the Hamilton-Jacobi equation by equivalent equation for $\mathbf{j}(\mathbf{r}, t)$.

References

- [1] Wyatt R E 2005 *Quantum Dynamics with Trajectories: Introduction to Quantum Hydrodynamics* (New York: Springer)

*khodyrev@gmail.com

A compact biological cell irradiation system with Van de Graaff accelerator

I.C. Cho^(a), H. Niu^{b*}, C.H. Chen^{cd}

^a Department of Biomedical Engineering and Environmental Sciences, National Tsing Hua University, Taiwan

^b Nuclear Science and Technology Development Center, National Tsing Hua University, Taiwan

^c Center for Nano Science and Technology, National Chiao Tung University, Hsinchu, Taiwan

^d Microelectronics and Information systems Research Center, National Chiao Tung University, Taiwan

A compact irradiation system for biological cells was set up with the 3MV KN Van de Graaff accelerator situated in the NTHU accelerator Laboratory. Figure 1 depicts the end station. The energetic ions produced from the accelerator are sent into the scattering chamber to bombard a 100 nm gold foil. Some of the vertically scattered incident particles would pass through a window to the cell target. The irradiating flux and area could be adjusted by altering the incident particle current and the exit window. The test results show that the system is suitable for biological cell irradiating experiments.

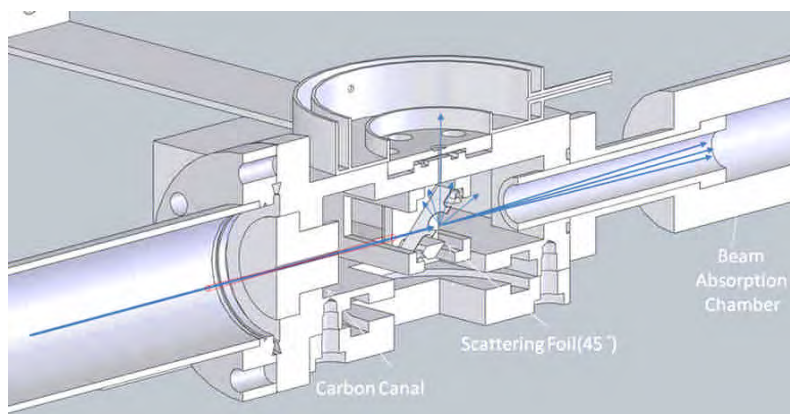


Figure 1. The end station of biological cell irradiation

References

- [1] I. C. Cho, M. F. Weng, J. M. Wu, S. Y. Chiang, W. T. Chou, H. Niu and C. H. Hsu, A Novel Cell Irradiation System Using 90°-scattering Technique. *Nuclear Science, IEEE Transactions on* **58**, 95-98 (2011).
- [2] I. C. Cho, H. Niu, C. H. Chen, Y. C. Yu and C. H. Hsu, DNA double-strand breaks induced along the trajectory of particles. *Nuclear Instruments and Methods in Physics Research Section B: Beam Interactions with Materials and Atoms* **269**, 3129-3131 (2011).

* hniu@mx.nthu.edu.tw

Absorption of radiation damage by interface investigated by molecular dynamics simulations

Ning Gao and Zhiguang Wang

Laboratory of Advanced Nuclear Materials, Institute of Modern Physics,
Lanzhou 730000, China.

Abstract: The properties of nano-scale interface of Fe/Cu bilayer films with and without displacement cascades initiated by energetic Fe or Cu particles have been investigated at atomic scale by molecular dynamics simulations. The high binding energies (up to 3 eV) of Fe or Cu interstitials with such interfaces demonstrate the strong absorption of interfaces to these interstitial defects. The emission of interstitial from interface to annihilate the nearby vacancy has been found as another way to reduce the possible radiation damage. The tensile stress response of such bilayer is also found to be affected by the intermixing at interface caused by the displacement cascade. All these results indicate the nano-scale Fe/Cu interfaces can act as sinks for radiation-induced point defects.

We-035

WITHDRAWN

S adsorption on Au(111) and Ag(111): a comparative study of Ion Scattering and Electron Spectroscopies

G. Ruano, E. Tosi, S. Bengi , L. Salazar Alarc n, E. A. S nchez, M. Khalid, O. Grizzi*, M.L. Martiarena, H. Ascolani and G. Zampieri

Centro At mico Bariloche, Instituto Balseiro, Comisi n Nacional de Energ a At mica, Bariloche, Argentina

The adsorption of S on Au and Ag surfaces is a subject of interest due to several reasons; among the most important are the poisoning effect in catalysis, the degradation of electronic contacts under S containing atmospheres, and the growth of Self Assembled Monolayers (SAMs) of thiol based molecules. The S/Au system has been studied with different electron and photon spectroscopies, with electron diffraction and by means of electrochemical techniques [1, 2], however a number of controversies still remains unsolved precluding a full understanding of the system behavior. In this work we present an ion scattering study performed in the forward direction in order to detect recoils (DRS) and forward scattered projectiles. Low energy electron diffraction patterns taken at specific exposures were used to identify the S phases. We measured the S and substrate recoiling intensities versus S dose in UHV conditions for both Au(111) and Ag(111), and compared these intensities with Auger (AES) and photoemission (XPS) Au4f and S2p signals. At low incident angles and specific doses we observed strong changes in both spectrum shape and intensity which allow determination of the critical coverages for phase transitions. The difference in the sticking coefficient in Ag and Au is discussed. A detailed study of TOF-DRS versus sample temperature for Au helped us to link previous measurements in UHV and in solution.

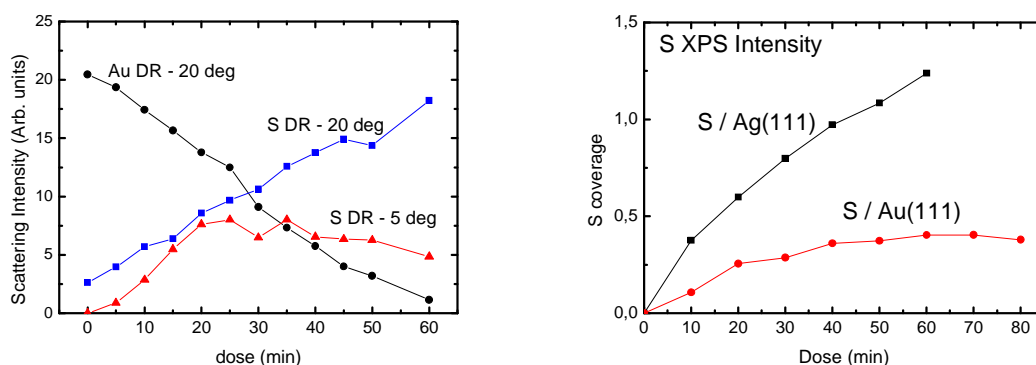


Figure 1: a) S and Au Recoiling intensity measured versus S dose at 20° incidence and S recoiling intensity measured at 5° incidence, b) S XPS intensity versus dose for Ag and Au substrates.

[1] J. A. Rodr guez et al, J. Am. Chem. Soc. **2003**, *125* (1), pp 276–285

[2] Miao Yu, H. Ascolani, G. Zampieri, D. P. Woodruff, C. J. Satterley, Robert G. Jones and Dhanak, J. of Phys. Chem. C *111*, 10904 (2007).

Charge-State Distributions of Fast Diatomic Carbon Ions Passing through A Single Microcapillary

J. Yokoe, S. Mori, R. Murakoshi

H. Tsuchida^{*}, T. Majima, M. Imai, H. Shibata and A. Itoh

Department of Nuclear Engineering, Kyoto University, Kyoto 606-8501, Japan

By using a tapered glass capillary with micrometer-sized outlet diameters, we investigated capillary-transmission properties of fast diatomic carbon ions in an energy range 0.48-1.92 MeV. The outlet diameter of the capillary used was about 13 μm . In this work, charge state distributions of transmitted particles of C_2 and dissociated fragments of C_1 were measured by electrostatic deflection analysis.

Figure 1 shows results of charge fractions of dissociated fragments (C_1) for different projectile energies and outlet diameters of capillary. The fraction of higher charge states is found to increase with increasing the projectile velocity. On the other hand, a very weak dependence was observed for the outlet diameter of capillary. The results obtained are compared to data of equilibrium charge distribution of single carbon projectile at the same velocity [1], showing that they are almost the same. This indicates that molecular dissociation occurs via collision in bulk of the capillary wall. We also found that majority of the incident C_2 ions are transported keeping their initial charge state and their angular distributions are almost the same as a divergence of incident beam.

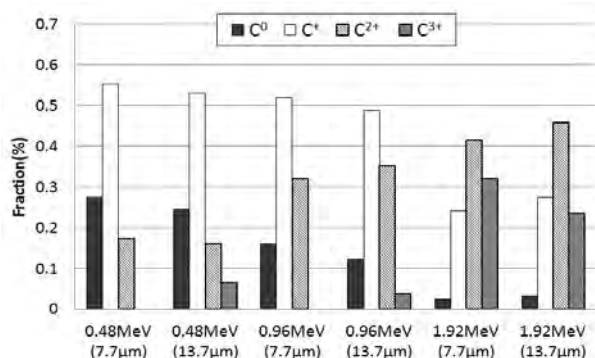


Figure 1. Charge fraction of C_1 fragments after transmitting through a capillary

References

- [1] J. B. Marion and F. C. Young, *Nuclear Reaction Analysis: Graphs and tables*, North-Holland Publishing Company-Amsterdam, (1968)

^{*} tsuchida@nucleng.kyoto-u.ac.jp

In-situ Deuterium Observation in Deuterium-implanted Tungsten

Y. Furuta, I. Takagi*, K. Yamamichi, S. Kawamura, M. Akiyoshi, T. Sasaki, and T. Kobayashi

Graduate School of Engineering, Kyoto University, Kyoto 606-8501, Japan

Tritium is a radioisotope and used as the fuel of a DT fusion reactor. For safe operation, the amount of tritium in reactor components, especially a tungsten divertor, should be reduced. It is important to know interactions between tungsten and energetic tritium from fusion plasma. In the present work, a substitute isotope of deuterium has been in-situ observed in tungsten, continuously implanted with deuterium ions. Temperature dependence of deuterium retention and desorption will be discussed.

Samples were high-pure tungsten disks with thickness of 1 mm. After annealed at 1173 K for 0.5 hr and mechanically polished, the samples were recrystallized at 1573 K for 1 hr. Under continuous implantation of 3-keV deuterium ions, deuterium depth profiles were observed by using a nuclear reaction analysis. Temperatures of the samples were 384, 473, 573 and 673 K. The surface density and the bulk concentration of deuterium were derived from the depth profile.

It is considered that there exists an intrinsic trap site for hydrogen isotopes in tungsten. Since deuterium detrapping from the trap site and desorption from the sample became active at high temperatures, the bulk concentration decreased with increasing the sample temperature. There was an exception at 384 K where the concentration was very low, probably due to a small amount of the trap sites at a very low temperature [1].

From the surface density of deuterium, a rate constant for desorption of a deuterium molecule was directly determined. It agreed well with that in the case of plasma exposure [2], where deuterium was absorbed on the surface. The agreement can be explained that all deuterium atoms in the sample are not directly desorbed from the bulk but from the surface. It is suggested that desorption behavior of tritium from tungsten would not depend on incident ion energy, in other words, plasma temperature.

Reference

- [1] I. Takagi et al., Fusio Sci. Tech. 60 (2011) 1451-1454.
- [2] I. Takagi et al., J. Nucl. Mater. 417 (2011) 564-567.

* Takagi@nucleng.kyoto-u.ac.jp

Growth direction change observation by the temperature change in Au/Ni(111) by LEEM

M.Hashimoto^{(1)*}, K.Umezawa⁽²⁾, T.Yasue⁽¹⁾, and T.Koshikawa⁽¹⁾

¹Fundamental Electronics Research Institute, Osaka Electro-Communication University,

²Department of Physical Science, Osaka Prefecture University

It is known that Au/Ni(111) exhibits two kinds of epitaxial orientation relationships and their ratio alternatively oscillates with growth temperature, which has been shown by the low energy ion scattering [1, 2]. However, the detailed growth process has not been observed so far, and hence how areas with different orientations develop in the growth process is still open question. In the present study, dynamic observation of the growth process of Au/Ni(111) was carried out with low energy electron microscopy (LEEM).

Ni(111) substrate was cleaned by repeated Ar⁺ ion sputtering and heating up to about 650°C, and the clean surface was checked by AES and LEED. Au was evaporated at several substrate temperature. The dynamic observation of the growth process was performed by LEEM, and the structure of the formed thin film was observed by LEED. Areas with different orientation were distinguished using the dark-field LEEM image.

Fig. 1 shows an example of experimental results, which was observed at the substrate temperature of about 400 °C. (a) is a bright field LEEM image taken at about 4.4 ML of Au. There are several areas with different gray levels. However, the LEED pattern shows Au(111) 1×1 structure as shown in (b) in all areas. Therefore, it is considered that the different gray levels seen in the bright field LEEM image is not due to the different surface structure but by a difference in film thickness. That is, the growth mode of Au/Ni(111) is not ideal layer-by-layer mode. Because Au/Ni(111) shows three-fold symmetry in the LEED pattern, adjacent LEED spots indicated by circles in (b) produce the dark field LEEM images of two different areas with opposite orientation as shown in (c) and (d). The contrast in these dark field LEEM images is reversed with each other, so that one can distinguish two opposite epitaxial orientations using the dark field images. In the dark field image of (d), the bright area is much more dominant than the dark area. At the other substrate temperature, the ratio between the bright and dark areas was different.

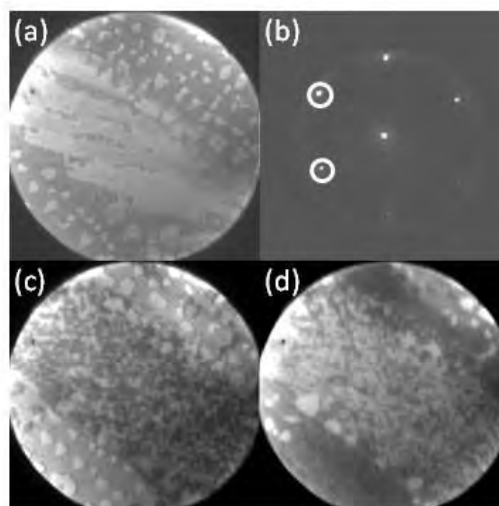


Fig. 1 (a) Bright field LEEM image, (b) LEED pattern, (c) and (d) dark field LEEM images. The coverage of Au is about 4.4 ML. The field-of-view is 10 μ m.

References

- [1] K.Umezawa, S.Nakanishi and W.M.Gibson, Phys.Rev. B57 (1998) 8842.
 [2] K. Umezawa, S. Nakanishi and W.M. Gibson, Surf. Sci. 426 (1999) 225.

*Email: h-michi@isc.osakac.ac.jp

Irradiation-induced Recovery of Plasmonic Property in Tarnished Ag Nanoparticles

K. Takahiro^{(1)*}, M. Wada⁽¹⁾, N. Terazawa⁽¹⁾, F. Nishiyama⁽²⁾, and M. Sasase⁽³⁾

⁽¹⁾ *Kyoto Institute of Technology*, ⁽²⁾ *Hiroshima University*, ⁽³⁾ *The Wakasa Wan Energy Research Center*

Silver nanoparticles (Ag NPs), which possess useful surface-plasmon resonance (SPR) properties for many potential applications, are rapidly tarnished even in ambient laboratory air due to adsorption of extrinsic impurities (e.g. C, N, S, Cl detected in our measurements). In our previous work [1], we demonstrated that a plasma treatment could control the SPR property for Ag NPs prepared by sputter deposition. During the treatment, Ar plasma and/or energetic Ar ions cleans up impurity contamination on the Ag surfaces, resulting in the blue shift and sharpening of an SPR band in UV-Vis optical absorption. Low energy ion irradiation can be an alternative tool to remove contaminated layer on Ag surfaces. In the present work, Ag NPs on SiO₂ are irradiated with 0.4 keV-Ar ions to purify them. As can be seen in Figure 1, an SPR band appeared in the wavelength range of 350–600 nm is found to recover significantly by Ar⁺ irradiation, indicative of the reduction of impurity content. The recovery behavior of the SPR band will be discussed in terms of impurity elimination as well as morphological change in Ag NPs.

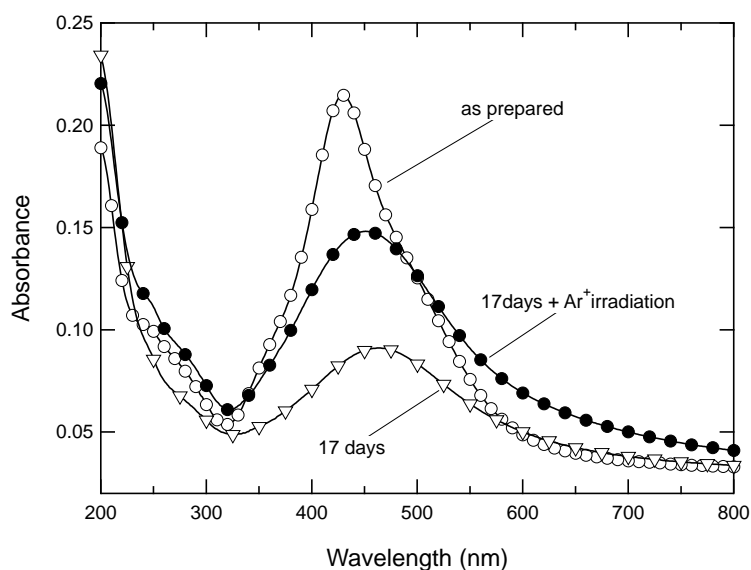


Figure 1. Optical absorption spectra of Ag NPs/SiO₂ for as prepared (open circles), stored in ambient air for 17 days (open triangles) and irradiated for 2 s (filled circles) samples.

References

- [1] K. Kawaguchi, M. Saito, K. Takahiro, S. Yamamoto, M. Yoshikawa, *Plasmonics* 6, 535 (2011).

* takahiro@kit.ac.jp

Anisotropy of Ly- α_1 and Ly- α_2 from H-like heavy ions aligned by resonant coherent excitation

Y. Nakano^{(1)*}, Y. Nakai⁽²⁾, A. Hatakeyama⁽³⁾, K. Komaki^(4,5), and E. Takada⁽⁶⁾,
T. Murakami⁽⁶⁾, T. Azuma^(1,7)

⁽¹⁾ *Atomic, Molecular and Optical Physics Laboratory, RIKEN*
⁽²⁾ *Nishina Center, RIKEN*

⁽³⁾ *Department of Applied Physics, Tokyo University of Agriculture and Technology*

⁽⁴⁾ *Atomic Physics Laboratory, RIKEN,*

⁽⁵⁾ *Graduate School of Arts and Sciences, University of Tokyo*

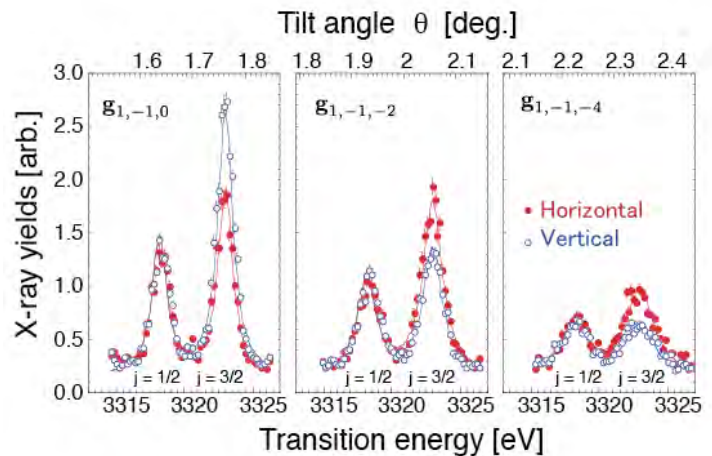
⁽⁶⁾ *National Institute of Radiological Sciences*

⁽⁷⁾ *Department of Physics, Tokyo Metropolitan University*

When high-energy ions are passing through a crystalline target, they experience a rapid oscillation of electric field created by regularly ordered atoms in the crystal. In a same manner as laser excitation, this oscillating field can induce the electronic excitation of the ions. This process is called resonant coherent excitation (RCE). Using polarization control technique in three-dimensional resonant coherent excitation (3D-RCE) [1,2] we can excite the heavy ions into a specific magnetic substate of certain excited states. We controlled the alignment direction of the 2p state, and observed the Ly- α_1 and Ly- α_2 by Si(Li) x-ray detectors installed at horizontal and vertical directions. As shown in Fig. 1, the x-rays from the 2p_{3/2} state showed large anisotropies depending on the polarization direction of the excitation field. On the other hand, the x-ray from the 2p_{1/2} state showed no anisotropy due to the depolarization by the spin-orbit (LS) interaction. We studied the ratios of the x-ray intensities in horizontal and vertical directions with theoretical calculations taking the depolarization effect into account.

References

- [1] C. Kondo et al., Phys. Rev. Lett. 97, 135503 (2006).
[2] Y. Nakano et al., Phys. Rev. Lett. 102, 085502 (2009).



* nakano-y@riken.jp

Measurement of the number spectrum of secondary electrons by using an avalanche photodiode detector

T. Nishio⁽¹⁾, T. Kishimoto⁽¹⁾, T. Majima^{(1), (2)*}, M. Imai⁽¹⁾,

H. Shibata⁽¹⁾, H. Tsuchida^{(1), (2)} and A. Itoh^{(1), (2)}

⁽¹⁾ *Department of Nuclear Engineering, Kyoto University, Kyoto 606-8501, Japan,*

⁽²⁾ *Quantum Science and Engineering center, Kyoto University, Kyoto 606-8501, Japan*

Secondary electron emission from solid surfaces induced by energetic ion collisions has been studied extensively for several decades. As one of the experimental studies, the measurement of number distributions of secondary electrons (called “number spectra” hereafter) with solid-state semiconductor detectors (SSD) was well-established for studying emission statistics of electrons [1]. This technique was extended to gas-phase molecular targets too [2,3]. The measurement principle depends on the characteristic of SSD which provides output signals with pulse heights proportional to the total energy of detected particles. The energy spectra, i.e., pulse height distributions of the SSD signals, provide information of the number of secondary electrons emitted in each collision event. Thus, detectors with a higher energy resolution are desired for improving the analysis of the number spectra. In this work, we have applied an avalanche photodiode (APD) detector for a measurement of the number spectra of secondary electrons emitted from a gold target induced by 2-MeV C⁺ ions. The APD has internal charge amplification mechanism in itself. This feature makes the output signals higher and relative contributions of the electronic noise in the peaks might become smaller. As a result, improvement of the energy resolution is expected.

A beam of 2-MeV C⁺ ions was injected to a gold plate target to which a high voltage of -20 kV was applied. An APD or a SSD was located in front of the Au target and at the ground potential. A number spectrum of secondary electrons was successfully obtained with the APD. The spectrum with the APD shows narrower peaks in a lower number range than those with the SSD. For example, the FWHMs of the second peaks are 6.4 and 3.0 keV for the SSD and APD, respectively. Meanwhile the peak widths become broader in a higher number range. To reproduce the whole structure of the number spectra obtained with the APD, a model function used for the SSD spectra was modified. It was found that the APD spectrum is well reproduced by adding an additional broadening factor due to the charge amplification in the APD detector itself.

References

- [1] A. Itoh, T. Majima, F. Obata, Y. Hamamoto and A. Yogo, Nucl. Instr. and Meth. B 193 (2002) 626.
- [2] S. Martin, L. Chen, A. Denis, and J. Désesquelles, Phys. Rev. A 57 (1998) 4518.
- [3] T. Majima, Y. Nakai, H. Tsuchida, and A. Itoh, Phys. Rev. A 69 (2004) 031202(R).

* majima@nucleng.kyoto-u.ac.jp

Magnetization Behavior during Growth of Co/Ni Multilayer —Study with High Brightness and Highly Spin-Polarized LEEM—

M. Suzuki^{(1)*}, T. Yasue⁽¹⁾, T. Koshikawa⁽¹⁾, and E. Bauer⁽²⁾

⁽¹⁾ Osaka Electro-Communication University, ⁽²⁾ Arizona State University

Current induced domain wall motion [1] is a key phenomenon to realize novel spintronic devices such as a race-track memory [2] and a domain wall motion magneto-resistive random access memory [3]. It has been indicated that domain walls in nanowires with perpendicular magnetic anisotropy can move with lower current density than those with in-plane magnetic anisotropy [4, 5]. Co/Ni multilayer is known to exhibit perpendicular magnetic anisotropy and is expected as a material for the devices with low operation current [6, 7]. In the present study, we investigated magnetization behavior during growth of the Co/Ni multilayer with high brightness and highly spin-polarized LEEM [8– 10].

Figure 1 shows magnetic domain images of a multilayer consisting of pairs of 2 ML of Ni and 1 ML of Co on W(110). Magnetization of one Co/Ni pair was in-plane (Fig. 1 a). The magnetization became perpendicular upon Ni deposition (Fig. 1 b). The in-plane magnetic component appeared again upon the following Co deposition (Fig. 1 c). It is indicated that the Ni and Co deposition enhance perpendicular and in-plane magnetic anisotropy, respectively. In the following growth, the in-plane magnetic contrast after Co depositions became weaker with number of Co/Ni pairs and only the perpendicular magnetic domains were observable above four Co/Ni pairs (Figs. 1 d– i). It is shown very clearly that the perpendicular magnetization is stabilized with number of Co/Ni pairs as the perpendicular magnetic anisotropy prevails against the in-plane one.

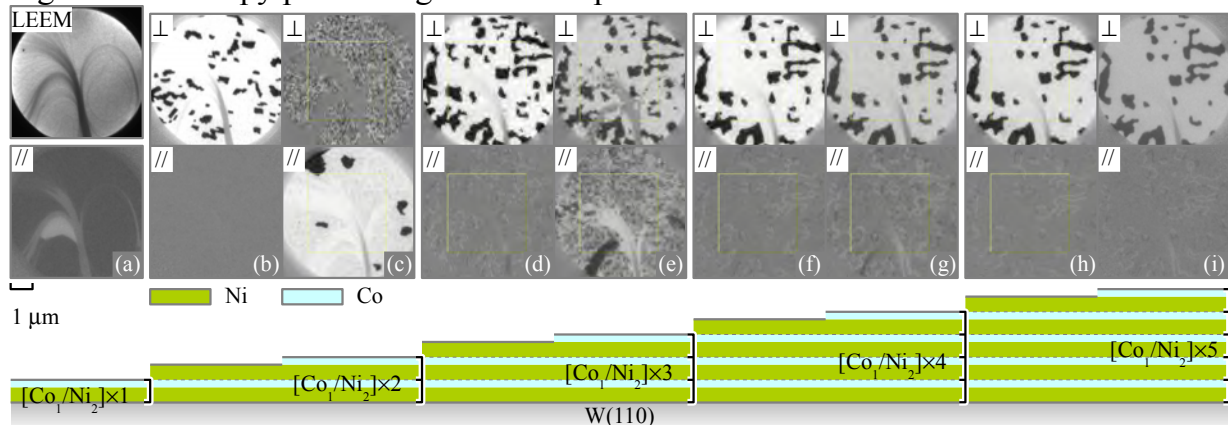


Figure 1. SPLEEM images with perpendicular (\perp) and in-plane [$1 -1 0$] (\parallel) magnetization of a multilayer consisting of pairs of 2 ML of Ni and 1 ML of Co on W(110). Field of view = $6 \mu\text{m} \phi$.

References. [1] L. Berger, *J. Appl. Phys.* 55, 1954 (1984). [2] S.S.P. Parkin, M. Hayashi, and L. Thomas, *Science* 320, 190 (2008). [3] N. Ohshima *et al.*, *J. Appl. Phys.* 107, 103912 (2010). [4] S. W. Jung *et al.*, *Appl. Phys. Lett.* 92, 202508 (2008). [5] S. Fukami *et al.*, *J. Appl. Phys.* 103, 07E718 (2008). [6] T. Koyama *et al.*, *Appl. Phys. Express* 1, 101303 (2008). [7] H. Tanigawa *et al.*, *Appl. Phys. Express* 2, 053002 (2009). [8] N. Yamamoto *et al.*, *J. Appl. Phys.* 103, 064905 (2008). [9] X.G. Jin *et al.*, *Appl. Phys. Express* 1, 045602 (2008). [10] M. Suzuki *et al.*, *Appl. Phys. Express* 3, 026601 (2010).

* m-suzuki@isc.osakac.ac.jp.

Microstructural and dielectric properties of PET polymer irradiated with 100 MeV Si⁸⁺ ions

S. Asad Ali^{1*}, Wasi Khan¹, Rajesh Kumar², F. Singh³ S. A. H. Naqvi¹ and Rajendra Prasad⁴

¹Centre of Excellence in Materials Science (Nanomaterials), Department of Applied Physics, Z. H. College of Engineering & Technology, Aligarh Muslim University, Aligarh-202 002, India

²University School of Basic & Applied Sciences, G. G. S. I.P. University, Delhi-110403

³Inter-University Accelerator Center, Aruna Asaf Ali Marg, New Delhi -110067.

⁴Vivekananda College of Technology and Management Aligarh-202002

Abstract

Polyethylene terephthalate (PET) belongs to the polyester family of polymers and attracted due to its excellent physical and mechanical properties. In the present study we have investigated structural and dielectric properties of pristine and irradiated PET polymer using XRD, FTIR and LCR meter. PET polymer of thickness 50 μm was procured from Good fellow, Cambridge Ltd. England (UK), and irradiated with various fluences of Si⁸⁺ ions of 100 MeV energy using pelletron accelerator at Inter University Accelerator Center (IUAC), New Delhi. XRD analysis clear shows decrease in crystallite size with increase in fluence and no other impurity phase was observed. FTIR spectra indicate overall decrease in the intensity of typical band at higher fluence. On irradiation dielectric constant (ϵ') decreases with frequency whereas it increases with the ion fluence. Variation of loss factor ($\tan \delta$) with frequency for pristine and irradiated with Si ions reveals that $\tan \delta$ increases as the frequency increases. Loss factor also increases with fluence. Due to irradiation the increase in conductivity with fluence at a given frequency may be attributed to scissoring of polymer chains, resulting in an increase of free radicals, unsaturation, etc.

Corresponding author;

***E-mail: asadsyyed@gmail.com (Dr. S. Asad Ali)**

Tel. No.; +91-9412537464,

Etching Damage Analysis of TiO₂ Thin Film with Soft X-ray Absorption Spectroscopy

M. Niibe^{(1)*}, T. Kotaka⁽¹⁾, K. Sano⁽¹⁾, R. Kawakami⁽²⁾, K. Tominaga⁽²⁾, Y. Nakano⁽³⁾

⁽¹⁾ University of Hyogo, ⁽²⁾ The University of Tokushima, ⁽³⁾ Chubu University

TiO₂ thin film is expected to apply not only as photocatalyst but also as gate insulator films for MOS devices. Because of these backgrounds, it is desired to develop a damage-less etching technique. We report an etching damage analysis of TiO₂ thin films etched by N₂ and He plasmas with the use of X-ray absorption spectroscopy (XAS) technique.

The TiO₂ thin films (anatase) were prepared on glass substrates by an RF magnetron sputtering system [1]. The TiO₂ films were etched by capacitively coupled RF N₂ and He plasmas [2] at gas pressure ranging from 10 to 100 mTorr and with etching time ranging from 5 to 200 min. The surface of the etched samples was characterized with SEM, AFM, XPS etc. Here we report mainly about the results of XAS analysis. Soft X-ray absorption spectra at O-K and Ti-L edges of the etched samples were measured at the NewSUBARU SR facility at the University of Hyogo [3] with the use of total electron yield (TEY, surface sensitive) and total fluorescence yield (TFY, bulk sensitive) methods.

Figure 1 shows the XAS spectra of Ti-L_{2,3} edge of the TiO₂ thin films etched by N₂ plasma. The spectra of the samples obtained by TFY method changed with increasing gas pressure. However, change in spectral shape of the same samples obtained by the TEY method was almost not observed. The fact that the spectral change did not observed in the surface sensitive TEY method could be an anomalous result comparing to the spectral change for n-GaN crystals etched with the same system [4]. According to the particle collision model (PIS) calculation, N₂ plasma etches preferentially to Ti atoms, while, He plasma etches preferentially to O atoms in TiO₂ films [5]. For the samples etched by N₂ plasma, the damaged configuration around Ti atoms near the surface might be recovered by structural relaxation to the stable crystalline configuration when the samples were exposed to the atmosphere.

References

- [1] K. Tominaga et al.: e-J. Surf. Sci. Nanotechnol. **7**, 290 (2009).
- [2] R. Kawakami et al.: Thin Solid Films, **516**, 3478 (2008).
- [3] M. Niibe et al.: AIP Conf. Proc. **705**, 576 (2004).
- [4] M. Niibe et al.: Jpn. J. Appl. Phys. **51**, 01AB02 (2012).
- [5] R. Kawakami et al. submitted to 11th APCPST Conf. (2012).

*niibe@lasti.u-hyogo.ac.jp

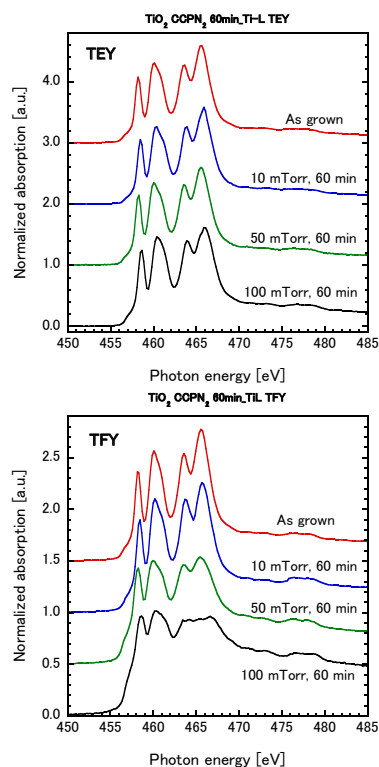


Fig. 1. Ti-L edge XAS Spectra (TEY and TFY) of TiO₂ thin film etched by N₂ plasma.

Alanine Dosimeter Response Characteristics for Charged Particles in BNCT

T. Kawamura⁽¹⁾, R. Uchida⁽¹⁾, H. Tsuchida^{(1)*}, H. Tanaka⁽²⁾
Y. Sakurai^{(2)†} and A. Itoh⁽¹⁾

⁽¹⁾ *Department of Nuclear Engineering, Kyoto University, Kyoto, 606-8501, Japan*

⁽²⁾ *Research Reactor Institute, Kyoto University, Osaka, 590-0494, Japan*

In radiation cancer therapy, it is of practical importance to achieve an accurate determination of absorbed dose distribution and localization of the radiation dosage around tissues. We are studying on dose evaluation in the radiation fields for boron neutron capture therapy (BNCT), in which a variety of secondary radiation (charged particles, neutrons, and γ -rays) are generated. The purpose of this work is to develop direct method of dose evaluation related to free radical production using alanine dosimeter. The use of alanine dosimeter allows quantitative measurements of free radicals produced by irradiation using electron spin resonance (ESR) spectroscopy. Response characteristics of the dosimeter for charged particles of H, He and Li ions generated in BNCT was investigated.

The sample used was commercially available alanine dosimeters (Kodak BioMax, USA). A sensitive layer of the sample is composed of polycrystalline L- α alanine and binder. The sample was irradiated with various projectile ions of 0.3-1.0 MeV H⁺ ions, 1.47 MeV He⁺ ions, and 0.84 MeV Li⁺ ions. The irradiated samples were analyzed by ESR spectroscopy. From the analysis, we obtained ESR signal amplitude per unit mass of irradiated alanine (ESR/g). Figure 1 shows results of the amount of ESR/g as a function of LET for projectiles with different atomic number Z at the same dose of 1 kGy. One can see that in the low LET region (up to about 1000 MeVcm²/g) the amount of ESR/g decreases with increasing the LET. Furthermore, it becomes constant in the high LET region (above 5000 MeVcm²/g), suggesting that recombination of the generated radicals occurs because of high ionization density within an ion track. We will discuss the LET dependence for different dose.

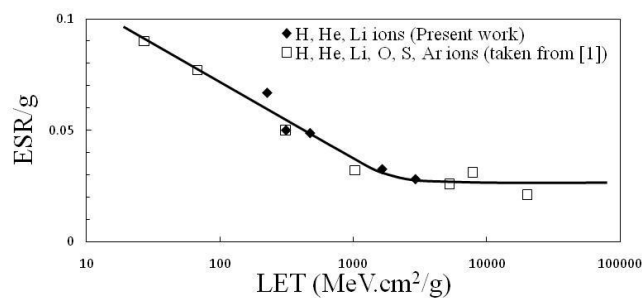


Figure 1.
LET dependence
of the response of
alanine dosimeter

References

[1] J. W. Hansen, et al., Radiat. Prot. Dosimetry 19, 43-47 (1987)

* tsuchida@nucleng.kyoto-u.ac.jp, † yosakura@rri.kyoto-u.ac.jp

Energy Dependence of Non-Rutherford Proton Elastic Scattering in Hafnium Nitride Thin Film

Y. Gotoh⁽¹⁾, W. Ohue⁽¹⁾, and H. Tsuji⁽¹⁾

⁽¹⁾ *Kyoto University*

Hafnium nitride (HfN) is expected to be used in various kinds of applications [1]. One of the important parameters of such films is the nitrogen composition. Rutherford backscattering spectrometry is a powerful tool to make a quantitative analysis of the elements in the film, but the sensitivity becomes worse for light elements. Non-Rutherford proton elastic scattering is one of the methods that can improve the sensitivities of light elements. One of the problems of this technique is such that the scattering cross section may not vary gradually with a decrease in the proton energy. For example, the scattering cross section for nitrogen (N) changes rapidly between 1.5 and 1.6 MeV [2]. This is inconvenient for the compositional analysis, and therefore, we investigated the energy dependence of the backscattering spectrum of proton elastic scattering.

A HfN thin film deposited on a silicon substrate was used as a sample. Helium RBS revealed that the areal atomic density was 5.5×10^{17} atoms cm^{-2} and the ratio of N/Hf was 0.74. Backscattering spectra were acquired at the scattering angle of 170° . The energy of the proton beam was varied between 1.54 and 1.62 MeV. The backscattering yield from N together with those of C and Hf was acquired.

Figure 1 shows the energy dependence of the N/Hf ratio obtained in the above experiments. Although the changes of the relative cross sections for C and Hf were not large, that for N changed suddenly at around 1.57 MeV.

This critical energy varies when the thickness and composition of the HfN film varies. Careful determination of N composition is necessary.

References

- [1] K. Ikeda, W. Ohue, K. Endo, Y. Gotoh, H. Tsuji, *J. Vac. Sci. Technol. B* 29 (2011) 02B116.
 [2] A. Gurbich, *Nucl. Instrum. Meth. B* 266 (2008) 1193.

e-mail: ygotoh@kuee.kyoto-u.ac.jp

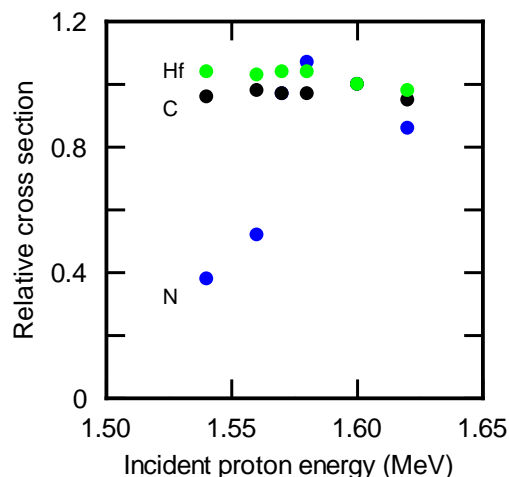


Figure 1. The ratio of the cross section to that of 1.60 MeV as a function of the incident proton energy

Surface Modification using Highly Charged Ions

M. Sakurai^{(1)*}, S. Liu⁽¹⁾, S. Sakai⁽¹⁾, S. Ohtani⁽²⁾, T. Terui⁽³⁾, and H.A. Sakaue⁽⁴⁾

⁽¹⁾ Kobe University, ⁽²⁾ University of Electro-communications, ⁽³⁾ National Institute of Information and Communications Technology, ⁽⁴⁾ National Institute for Fusion Science

The interaction of slow highly charged ions (HCIs) with solid surfaces is useful for 'nanoprocess'; the modification, activation, machining and analysis in nanometer scale. The atomic scale modification of surfaces irradiated with HCIs have been observed by using STM, and the structure of irradiation traces have been investigated. The advantages of HCIs over singly charged ions (SCIs) as a tool of surface modification reside in their potential energy which is transferred to topmost surface layers of the sample. This feature appear in the high sensitivity for SEM contrast; fluence of HCI necessary for giving good SEM contrast ($10^{13-14}/\text{cm}^2$) is much smaller than that of SCIs ($10^{15-16}/\text{cm}^2$). The HCI beam produced by an electron beam ion source has low emittance which is suitable for the application of nanoprocess where the incident ion beam must be focused or limited in nanometer size. Figure 3 shows SEM image of Si wafer irradiated with HCIs (Ar^{11+}) with the fluence of $10^{14}/\text{cm}^2$ through a cantilever with a window of $10\mu\text{m}$ square. The distance between the window and Si wafer is $\sim 0.3\text{mm}$. We have proved that HCIs modify the magnetic property of graphite with the fluence of $10^{14}/\text{cm}^2$ for the first time. At the conference, we will present various results on the surface modification using HCIs and discuss about the strategies toward nanoprocess using HCIs.

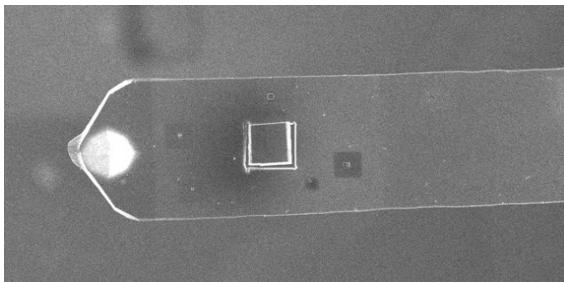


Figure 1. SEM image of cantilever with window.

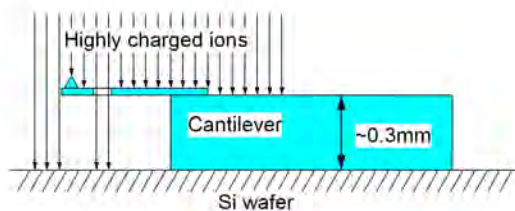


Figure 2. Schematics of irradiation condition.

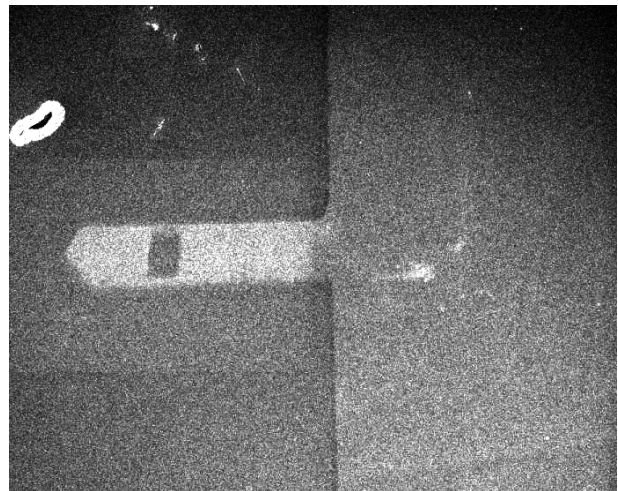


Figure 3. SEM image of Si wafer irradiated with highly charged ions through the cantilever.

Spin Reorientation in Au/CoNi₂/W(110) Observed Using Spin Polarized Low Energy Electrons

M. Suzuki⁽¹⁾, T. Yasue^{(1)*}, E. Bauer⁽²⁾, and T. Koshikawa⁽¹⁾

⁽¹⁾Osaka Electro-Communication University, ⁽²⁾Arizona State University

Magnetic thin films have been extensively studied because of their application to the spintronic devices. Understanding of the magnetic properties of the magnetic thin film is basically of importance, and also it is required to control them in order to achieve the highly sophisticated function. It is known that non-magnetic overlayer can modify the magnetic anisotropy of the magnetic thin films [1]. In the present study, we have observed the spin reorientation process during the deposition of Au overlayer on CoNi₂/W(110) with high brightness and highly spin polarized low energy electron microscopy (SPLEEM) [2].

Figure 1(a) shows out-of-plane (upper row) and in-plane (lower row) components of the magnetic domain structure of CoNi₂ on W(110). The CoNi₂ film exhibits the uniaxial in-plane anisotropy along [1 -1 0] direction. As Au deposition, the in-plane magnetic anisotropy becomes weak and almost vanishes at around a half ML of Au (fig. 1(c)). Then the out-of-plane component starts to develop after 0.5 ML, and the strong perpendicular magnetic anisotropy is established at 1 ML of Au. The domain structure observed here is completely different from that before Au deposition. We can obtain LEEM images simultaneously with the magnetic images. The intensity of LEEM image decreases with Au coverage up to around 0.5 ML and recovers after that. It would be suggested that the spin reorientation process seen in fig. 1 is relevant to the growth process of Au layer on top of CoNi₂ film.

References

- [1] T. Duden and E. Bauer, Phys Rev. B59 (1999) 468.
 [2] M. Suzuki *et al.*, Appl. Phys. Express 3 (2010) 026601.

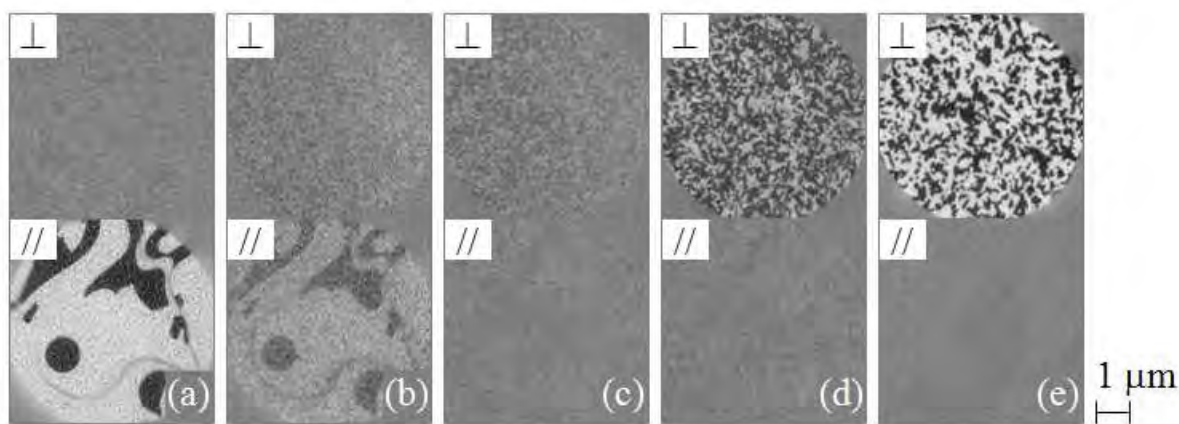


Figure 1. SPLEEM images during Au deposition on CoNi₂/W(110). Upper : out-of-plane, lower : in-plane component. The Au coverage is (a) 0 ML, (b) 0.25 ML, (c) 0.5 ML, (d) 0.75 ML and (e) 1 ML.

* E-mail: yasue@isc.osakac.ac.jp

Ionoluminescence of a thin rear-earth oxide film by slow highly-charged ions

D. Kato^{(1)*}, H.A. Sakaue⁽¹⁾, M. Sakurai⁽²⁾, Y. Hishinuma⁽¹⁾, and S. Ohtani⁽³⁾

⁽¹⁾ National Institute for Fusion Science, ⁽²⁾ Kobe University, ⁽³⁾ Inst. Laser Sci., Univ. Electro-Commun.

In the present work, ionoluminescence by highly-charged ion-beams is investigated with a thin erbium oxide (Er_2O_3) film. Previously, Tona et al. [1] observed strongly enhanced ionoluminescence of a thin organic-dye film by bombardment of highly-charged iodine ions with *L*-shell vacancies. This enhanced luminescence appears caused by energetic *L* Auger electrons emitted from the iodine ions above the target surface; the luminescence due to bombardment of the Auger electrons is added to that due to an electronic stopping power of the projectile ion in the organic-dye film. It is one of unique phenomena observed with highly-charge ions of interacting with optical materials.

Optical transitions of trivalent Er^{3+} ions in oxides have been exploited for applications in optoelectronics [2]. Recently, optical transitions useful to evaluate radiation damages in Er_2O_3 oxide coatings are also being searched for advanced nuclear fusion materials research [3]. In a visible range, a strong luminescence band due to $4f^{11} \ ^4F_{9/2} - \ ^4I_{15/2}$ transition of the Er^{3+} ions has been observed at 640-690 nm by electron and singly-charged ion bombardments [3, 4]. We will investigate the luminescence at 640-690 nm by using slow highly-charged ions, putting an emphasis on distinct excitation mechanisms of the luminescence from those by using singly-charged ion-beams. Target samples are thin polycrystalline Er_2O_3 oxide films of about 500-600 nm thickness coated on stainless steel substrates by using Metal Organic Chemical Vapor Deposition (MOCVD) [5]. Kobe Electron Beam Ion Source (Kobe-EBIS) [6] is used to produce intense highly-charged ion-beams (e.g. Ar^{12+} ion-beams of a few nA in current for acceleration voltages of 1.5 – 3 kV). We will be studying intensity variation of the luminescence with respect to charge states and kinetic energies of the projectile ions. Since degradation of the intensity is anticipated due to ion-induced damages created on target surfaces [3, 4], ion-dose dependences of the luminescence are also measured at respective charge states and kinetic energies of the incident ions.

References

- [1] M. Tona et al., Phys. Rev. A 77 (2008) 052902.
- [2] A. Polman, J. Appl. Phys. 82 (1997) 1.
- [3] T. Tanaka et al., J. Nucl. Mater. 417 (2011) 794.
- [4] D. Kato et al., Plasma Fusion Res. 7 (2012) 2405043.
- [5] Y. Hishinuma et al., J. Nucl. Mater. 417 (2011) 1214.
- [6] M. Sakurai et al., J. Vac. Soc. Jpn. 48 (2005) 317; 50 (2007) 390; 55 (2012) 180.

* kato.daiji@nifs.ac.jp

High-resolution Elastic Recoil Detection for Boron Depth Profiling

Kaoru Sasakawa^{(1),(2)*}, Kaoru Nakajima⁽²⁾, Motofumi Suzuki⁽²⁾ and Kenji Kimura⁽²⁾

⁽¹⁾*Kobelco Res. Inst. Inc.*, ⁽²⁾*Kyoto University*

High-resolution Rutherford backscattering spectroscopy (HRBS) is a powerful surface analysis technique, which has better depth resolution compared to the conventional RBS. It allows quantitative and non-destructive depth profiling of constituent elements with sub-nm depth resolution within a reasonably short measurement time (typically 10 - 20 min.) without any special pre-treatment of the sample. However, the typical sensitivity of HRBS for light elements, such as boron, is ~ 1 at.%, which is not good enough for some applications, such as for microelectronics [1].

Elastic recoil detection analysis (ERDA) is more suitable to analyze the light elements than RBS. Dollinger et al demonstrated that depth profiling of boron in silicon can be performed with sub nanometer depth resolution and high sensitivity of ~100 ppm by using their high-resolution ERDA (HERDA) setup [2]. Although the performance of their HERDA is excellent, they need a large facility including a high energy accelerator and a large magnetic spectrometer. If much smaller equipment can be used for the analysis of light elements with depth resolution and sensitivity comparable to their system, it should be useful. It was already demonstrated that our compact HRBS system can be used for high-resolution ERDA. Hydrogen depth profiling was performed with sub-nm depth resolution and a sensitivity of 0.1 at.% [3]. However, there are several issues to be solved to analyze other light elements heavier than hydrogen, such as boron.

In our hydrogen analysis, we used an electrostatic deflector to reject the scattered probe ions. Unfortunately, the electrostatic deflector cannot separate recoiled boron ions from the scattered probe ions unless very heavy ions are used. Another issue is charge state distributions of recoiled ions. Because the magnetic spectrometer cannot measure recoiled ions of all charge states simultaneously, the information of charge state distribution of the recoiled ions is necessary for quantitative analysis. However, there is almost no measurement on the charge state distribution of light elements in the relevant energy region.

In this paper, we employed two different methods to reject probe ions in boron depth profiling using HERDA. One is the use of He⁺ ions as a probe. The magnetic spectrometer itself can reject the scattered He ions when the magnetic field is adjusted for the recoiled boron ions. The other is the use of a mylar foil in front of the focal plane detector as is in the conventional ERDA. Feasibility of these methods is examined and the pros and cons of these methods are discussed. The charge state distribution of the recoiled boron ions is also measured and the result is compared with an available semi-empirical formula to check the accuracy of the formula.

References

- [1] K. Kimura, Y. Oota, K. Nakajima, and Tamel H. Buyuklimanli, *Curr. Appl. Phys.* 3 (2003) 9.
- [2] G. Dollinger, A. Bergmaier, L. Goergens, P. Neumaier, W. Vandervorst, and S. Jakschik, *Nucl. Instr. and Meth. B* 219-220 (2004) 333.
- [3] K. Kimura, K. Nakajima, S. Yamanaka, M. Hasegawa, and H. Okushi, *Appl. Phys. Lett.* 78 (2001) 1679.

* sasakawa.kaoru@kki.kobelco.com

Temperature dependence of low-energy electron irradiation induced nanocrystal in GaSb

N. Nitta^{(1)*}, T. Nishiuchi⁽²⁾, M. Taniwaki⁽²⁾, A. Hatta⁽¹⁾⁽³⁾, and H. Yasuda⁽⁴⁾

⁽¹⁾ Nanotechnology Research Institute, Kochi University of Technology, ⁽²⁾ School of Environmental Science and Engineering, Kochi University of Technology, ⁽³⁾ School of Systems Engineering, Kochi University of Technology, ⁽⁴⁾ Research Center for Ultra-High Voltage Electron Microscopy, Osaka University

We recently found that the nanocrystal which has same orientation, are observed in GaSb low-energy electron irradiated at 373 K over [1]. There are two types variants in the matrix. The domains are pseudo-{110} planes in the matrix formed by irradiation-induced Shockley partial dislocations. The low-energy electron irradiation induces electronic excitation. It is well known that bond breaking and displacement of atoms can be induced by electron irradiation [2]. In this study, we investigate the temperature dependence of low-energy electron irradiation induced nanocrystal in GaSb.

Single crystals of GaSb were supplied in the form of 450-mm-thick wafers with the (001) plane normal. Discs of about 3 mm diameter were cut from the wafer, and the disks were thinned by a polisher until the thickness was below 100 μm . A dimple was formed at the center of the discs by a dimple grinder. Then the disks were thinned by ion milling with argon ions for TEM observation. Low-energy electron irradiation experiments and observations were performed using the same microscope (Hitachi H-7000) operating at an accelerating voltage of 125 kV. The electron flux used for the irradiations was 2×10^{21} electrons/ m^2s . The temperatures of the thin films were kept at 293 K, 373 K, and 473 K during the experiments. The column vacuum was 5×10^{-5} Pa. Structural changes associated with electron irradiation were observed in situ by bright-field image (BFI), dark-field image (DFI), and selected-area electron diffraction pattern (SAED).

Structural changes were not observed in GaSb kept at 293 K during electron irradiation. The nanocrystals formed over the entire sample kept at 373 K after irradiation for 1.2 ks and 2.4 ks, respectively. The average diameter of the atomic region was approximately 3 nm (1.2 ks) and 6 nm (2.4 ks). With increasing electron fluence, the size of the crystal domains and the density increased. The size of the crystal domains was 10 nm (1.2 ks) and 18 nm (2.4 ks) in the sample kept at 473 K. The large size nanocrystals were formed in the higher irradiation temperature. The migration of dislocation in high temperature is faster than that in low temperature [3]. It is considered that the large deformation occurs in the high temperature irradiation.

References

- [1] N. Nitta, Y. Aizawa, T. Hasegawa and H. Yasuda, *Philos. Mag. Lett.* **91** (2011) 676.
- [2] J. Singh, N. Itoh, Y. Nakai, J. Kanasaki and A. Okano, *Phys. Rev. B* **50** (1994) 11370.
- [3] D. N. Nasledov and B. V. Sokolov, *Zh. Tekh Fiz.* **28** (1958) 704.

* nitta.noriko@kochi-tech.ac.jp

Surface and Interface Roughness Estimations by X-ray Reflectivity and RBS Measurements

Y. Fujii^{(1)*}, K. Nakajima⁽²⁾, M. Suzuki⁽²⁾, K. Namura⁽²⁾, H. Minamitake⁽²⁾,
and K. Kimura⁽²⁾

⁽¹⁾ *Kobe University*, ⁽²⁾ *Kyoto University*

In the conventional x-ray reflectivity analysis, the reflectivity is calculated based on the Parratt formalism[1], incorporating the effect of the interface roughness according to Nevot and Croce [2]. However, estimation results of surface and interfacial roughness by x-ray reflectivity measurements did not correspond to those from TEM and AFM observations. We have also found that the calculated x-ray reflectivity show a strange behavior, i.e. the amplitude of the oscillation increases with interfacial roughness in the case of rough surfaces. The origin of the strange behavior was attributed to the fact that the diffuse scattering at the rough interface was not correctly taken into account by Nevot and Croce [3]. This might be also responsible for the disagreement between the x-ray reflectivity measurement and TEM/AFM observation. We have developed a new formalism in which the effects of the surface and interface roughness are included correctly. Using accurate formulae for $R_{j-1,j}$ and $R_{j,j+1}$, the x-ray reflectivity R of a multilayer consisting of N layers is given by

$$R = |R_{0,1}|^2, \quad R_{j-1,j} = \frac{\Psi_{j-1,j} + (\Phi_{j-1,j} \Phi_{jj-1} - \Psi_{j-1,j} \Psi_{jj-1}) R_{jj+1}}{1 - \Psi_{jj-1} R_{jj+1}} \exp(2ik_{j-1,z} h_{j-1}), \quad R_{N,N+1} = 0$$

where h_j is the thickness of j -th layer, $k_{j,z}$ is the z component of the wave vector in the j -th layer, and $\Psi_{j-1,j}$ and $\Phi_{j-1,j}$ are the Fresnel coefficients for reflection and refraction, respectively, at the interface between $(j-1)$ th and j -th layers. Although formula for $\Psi_{j-1,j}$ is well known

$$\Psi_{j-1,j} = \frac{k_{j-1,z} - k_{j,z}}{k_{j-1,z} + k_{j,z}} \exp(-2k_{j-1,z} k_{j,z} \sigma_{j-1,j}^2), \quad \Psi_{j,j-1} = -\Psi_{j-1,j},$$

where $\sigma_{j-1,j}$ is the interface roughness between $(j-1)$ -th and j -th layers, an accurate analytical formula for $\Phi_{j-1,j}$ including the effect of the interface roughness is not available. There are several approximations proposed so far and all these results can be written as

$$\Phi_{j-1,j} = \frac{2k_{j-1,z}}{k_{j-1,z} + k_{j,z}} \exp\{-[C_1(k_{j-1,z} - k_{j,z})^2 + C_2 k_{j-1,z} k_{j,z}] \sigma_{0,1}^2\}, \quad \Phi_{j,j-1} = \Phi_{j-1,j} \frac{k_{j,z}}{k_{j-1,z}},$$

where parameters C_1 , C_2 depend on the proposed approximations. In the present work, we try to determine these parameters experimentally by comparing the measurements of high-resolution RBS and x-ray reflectivity. We will present the detailed results and discuss the improvement of the x-ray reflectivity analysis using this new formalism.

References

- [1] Parratt L G, *Phys. Rev.* **95** 359 (1954).
- [2] Nevot L and Croce P, *Rev. Phys. Appl.* **15** 761 (1980).
- [3] Y. Fujii: *Mater. Sci. Eng.* **24**, 012009 (21pp) (2011).

* e-mail: fujiiyos@kobe-u.ac.jp

Structural changes induced by low-energy electron irradiation in III-V compound semiconductors

T. Nishiuchi^{(1)*}, N. Nitta⁽²⁾, M. Taniwaki⁽¹⁾, A. Hatta⁽²⁾⁽³⁾, and H. Yasuda⁽⁴⁾

⁽¹⁾ School of Environmental Science and Engineering, Kochi University of Technology ⁽²⁾ Nanotechnology Research Institute, Kochi University of Technology ⁽³⁾ School of Systems Engineering, Kochi University of Technology, ⁽⁴⁾ Research Center for Ultra-High Voltage Electron Microscopy, Osaka University

Effect of structural changes on high-energy electron irradiation in bulk III-V compound semiconductors reported by some articles [1-3]. Electron irradiation induces chemical disordering, crystalline-amorphous transition, and dislocation loop in irradiated samples with 2 MeV electrons. On the other hand, low-energy electron irradiation in the sample kept at 373 K over induces the formation of nanocrystal in GaSb and InSb [4]. This phenomenon shows only GaSb and InSb. In this study, structure changes induced by low-energy electron (125 keV) irradiation in III-V compound semiconductors are investigated by transmission electron microscopy.

Single crystals of GaSb, InSb, GaP, and InP were supplied in the form of 450 mm thick wafers with the (001) and (111) plane normal. Discs of about 3mm diameter were cut from the wafer, and these were thinned by a polisher until their thickness was below 100 μm . A dimple was formed at the center of the discs by a dimple grinder. Then the discs were thinned by ion milling with argon ions for TEM observation. The electron irradiation experiments and the observations were performed using the same microscope (Hitachi H-7000, JEOL JEM-2010F, and 2100F) operating at an accelerating voltage of 125 kV. The electron flux used for the irradiations was 5×10^{24} electrons/ m^2s . The temperatures of the thin films were kept at 473 K during the experiments. The column vacuum was 2×10^{-4} Pa.

The nanocrystal of In_2O_3 variant were formed in InSb kept at 474 K during 125 keV electron irradiation. The average diameter of the nanocrystal was approximately 42 nm in the sample irradiated to a fluence of 9×10^{26} electrons/ m^2 . However, no structural changes were observed in GaP and InP before or after irradiations. The single-crystal structure of zinc-blende remained in after irradiation.

References

- [1] M. Hirata, Bull. Kobe C. Col. of Nursing **9** (1990) 121.
- [2] H. Yasuda and K. Furuya, Philo. Mag. A **80** (2000) 2355.
- [3] H. Yasuda and H. Mori, Materials Transactions **45** (2004) 1.
- [4] N. Nitta, Y. Aizawa, T. Hasegawa and H. Yasuda, Philos. Mag. Lett. **91** (2011) 676.

* 165012z@gs.kochi-tech.ac.jp

Fabrication of Ordered Nano-Cell Structure on Ge Surface by FIB

Kenji Morita^{(1)*}, Noriko Nitta⁽²⁾, Masafumi Taniwaki⁽¹⁾

⁽¹⁾*Department of Environmental Systems Engineering, Kochi University of Technology, Tosayamada-cho, Kami-shi, Kochi-prefecture, 782-8502, Japan* ⁽²⁾*Nanotechnology Research Institute, Kochi University of Technology, Tosayamada-cho, Kami-shi, Kochi-prefecture, 782-8502, Japan*

Anomalous behaviors such as the surface elevation and the cellular structure formation have been observed in ion irradiated GaSb, InSb and Ge. Nitta *et al.* proposed the formation mechanism of the cellular structure on the basis of movement of the point defect and proved it experimentally [1]. The cellular structure is very fine, which inspire us to apply it for nano-devices. However it is lack in regularity. Then, some of the authors proposed a novel nano-technique in order to fabricate the ordered nano-cell structure, and developed the technique mainly for InSb and GaSb [2,3]. The cellular structure formation process in Ge is somewhat different from that in GaSb and InSb. In the case of Ge, the irradiated layer is amorphized prior to cell formation while the irradiated layer is amorphized after the cell formation in GaSb and InSb by ion irradiation. On the basis of this fact, in this work, two kinds of nano-cell fabrication were performed and compared. One is the method used in nano-cell fabrication of GaSb and InSb, in which two-processes, formation of initial ordered void lattice and development of the void lattice to the cell lattice. In the other method, initially the surface layer of Ge wafer was amorphized by ordinary ion irradiation and then, nano-cell structure was formed on it by the same process. These processes were performed using 30 keV Ga⁺ in a focused ion beam apparatus (FIB) at room temperature. The results showed that the secondary void formation was remarkable in the initially amorphized Ge. Probably the vacancy mobility in amorphous Ge is large, which might have accelerated the formation of secondary voids between the initial voids.

References

- [1] N. Nitta, M. Taniwaki, Y. Hayashi, T. Yoshiie, J. Appl. Phys. **92** (2002) 1799.
- [2] N. Nitta, M. Taniwaki, Nucl. Instrum. Methods. B **206** (2003) 482.
- [3] S. Morita, N. Nitta, M. Taniwaki, Surf. Coat. Technol. **206** (2011) 792.

*165017k@gs.kochi-tech.ac.jp

Production of C₆₀ Microbeams by Single-Microcapillary Methods

H. Tsuchida^{(1),(2)*}, T. Majima^{(1),(2)}, S. Tomita⁽³⁾, K. Sasa⁽⁴⁾, K. Narumi⁽⁵⁾, Y. Saitoh⁽⁵⁾,
A. Chiba⁽⁵⁾, K. Yamada⁽⁵⁾, K. Hirata⁽⁶⁾, H. Shibata⁽²⁾, and A. Itoh^{(1),(2)}

⁽¹⁾ *Quantum Science and Engineering Center, Kyoto University, Kyoto 611-0011, Japan*

⁽²⁾ *Department of Nuclear Engineering, Kyoto University, Kyoto 606-8501, Japan*

⁽³⁾ *Institute of Applied Physics, University of Tsukuba, Ibaraki 305-8573, Japan*

⁽⁴⁾ *Tandem Accelerator Complex, University of Tsukuba, Ibaraki 305-8577, Japan*

⁽⁵⁾ *Takasaki Advanced Radiation Research Institute, Japan Atomic Energy Agency, Gumma 370-1292, Japan*

⁽⁶⁾ *National Institute of Advanced Industrial Science and Technology (AIST), Ibaraki 305-8565, Japan*

A single tapered capillary with micron-sized outlet diameter is used as a new tool of producing charged particle microbeams. This capillary-microbeam method is capable of easily producing focused beams for various types of charged particles in a wide energy range from keV to MeV. In this work, we applied this method to production of fast C₆₀ microbeams. By using capillaries with two different outlet diameters of 5.5 and 14 μm, transmission properties of 360 keV C₆₀⁺ and 720 keV C₆₀²⁺ through a capillary were investigated. In order to evaluate beam qualities of the produced microbeams, we performed systematic studies on a composition of the transmitted particles.

The experiment was performed at Japan Atomic Energy Agency (JAEA)/Takasaki. A C₆₀ primary ion beam obtained from a 400 kV ion implanter was introduced into a single capillary mounted on a goniometer. To obtain information about a composition of the transmitted particles, particles emerging from a capillary were deflected with electrostatic parallel plates and detected by a microchannel plate with a phosphor screen (two-dimensional imaging measurement). From the measurement, we obtained some interesting results: (1) a main component of transmitted particles is due to direct transmission of incident C₆₀ beams, (2) the other component is due to transmission of neutral particles and large-sized fragments of C₅₈ or C₅₆ ions produced via C₂-emission from C₆₀, (3) small-sized carbon fragments of C₁ or C₂ ions resulting from C₆₀-multifragmentation are not detected.

* tsuchida@nucleng.kyoto-u.ac.jp

Auger electron emission from Si(111) surface during 11 keV Ar⁺ ion sputtering

K. Kawai^{*}, Y. Sakuma, M. Kato and K. Soda

*Department of Quantum engineering, Graduate School of Engineering, Nagoya University,
Furo-cho, Chikusa-ku, Nagoya 464-8603, Japan*

Secondary ion mass spectroscopy is known as a useful tool for compositional analysis of material surfaces. However, for the quantitative analysis, the understanding of ion production mechanism is indispensable. We have paid an attention to the production mechanism of Si²⁺ ions during ion sputtering and have realized the importance of Si^{0*} or Si⁺ as precursors of the Si²⁺ ion. In order to obtain the deeper insight about Si²⁺ production, we have planned a new experiment, in which the ion induced Auger electrons and the sputtered Si species are measured coincidentally. Although, at this moment, we are unable to offer the detailed information obtained from such measurements, we report here a strong correlation between the penetration depth of Ar ion and the Auger electron yield.

In our experiments, a Si(111) wafer was irradiated by the 11 keV Ar⁺ beam. The Auger electron yield was measured at a fixed angle of 45° with respect to the primary Ar⁺ beam. We changed the incident angle of Ar⁺ to the surface. Fig.1 shows the energy spectra of Auger electron for different incident angles, θ , measured from the surface normal. The positions marked by the arrows correspond to the atomic LMM-Auger or the broad spectrum of the bulk LVV-Auger (ref.[1]). Although the individual Auger peaks are not clearly distinguishable, the Auger yield significantly increases for the larger θ . This can be explained in terms of the electron escape depth (1 nm for 90 eV) and the ion range of 11 keV Ar (10 nm). For the larger θ , the collision cascades are created in the shallower place, and the more Auger electrons can escape from the surface, and the atomic Auger is also increased with the increase of sputter yield.

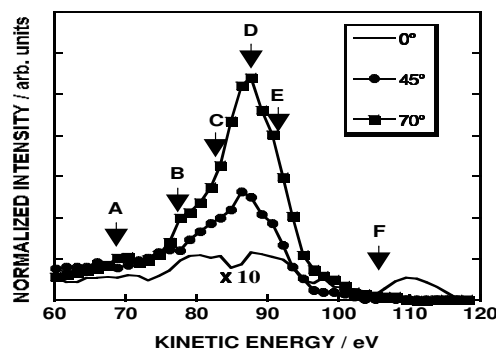


Figure 1. the Auger spectra for different incident angles. The yield for $\theta=0^\circ$ has been multiplied by 10.

References

- [1] R. Whaley and E.W. Thomas, J. Appl. Phys. **56**, 1505 (1984).

* kawai.kengo@h.mbox.nagoya-u.ac.jp

Temperature dependent damage production in SIMP steel under 196 MeV Kr-ions irradiation

Y.F. Li^{(1),(2)(3)}, T.L. Shen^{(1),(2)}, Z.G. Wang^{(1)*}, J.R. Sun⁽¹⁾, P. Zhang⁽⁴⁾,
X.Z. Cao⁽⁴⁾, K.F. Wei⁽¹⁾, C.F. Yao⁽¹⁾, B.S. Li⁽¹⁾, H.L. Chang⁽¹⁾, Y.B. Zhu^{(1),(2)},
L.L. Pang^{(1),(2)}, M.H. Cui^{(1),(2)}, J. Wang^{(1),(2)}, H.P. Zhu^{(1),(2)}

(1) Institute of Modern Physics, Chinese Academy of Sciences, Lanzhou 730000, PR China

(2) Graduate University of Chinese Academy of Sciences, Beijing 100049, PR China

(3) The School of Nuclear Science and Technology, Lanzhou University, Lanzhou 730000, PR China

(4) Key Laboratory of Nuclear Analysis Techniques, Institute of High Energy Physics, Chinese Academic of Sciences, Beijing 100039, PR China

Energetic heavy-ions have been widely used to assess the irradiation response of materials and to study some basic aspects of irradiation damage. Atom displacements caused by energy deposition process will produce a large amount of the point defects. Although a small fraction of the point defects will survive after the collision stage, interactions between these defects can substantially lead to irradiation induced microstructure changes. Different mechanisms control the defects motion at different temperature regimes. In the present work, we focused on the temperature dependent of defect evolution in Ferritic/Martensitic (F/M) steel under high energy heavy ion irradiation.

A F/M steel named SIMP steel was employed in this work. Specimens were irradiated with 196MeV Kr-ions at room temperature, 723 and 823 K, respectively. After irradiation, the samples were investigated using positron annihilation spectroscopy (PAS) and Conversion Electron Mössbauer Spectroscopy (CEMS). From the obtained Doppler broadening PAS spectra under the condition of positrons with different energies, vacancy-type defects and their distribution at different irradiation temperatures varying with the positrons penetrating depths are analyzed. More, the changes of the environment of iron atoms linked to irradiation damage are analyzed based on the recorded CEMS spectra. Then, the irradiation damage produced in the near-surface region of the SIMP steel were deduced, and the damage process was discussed.

E-mail address: zhgwang@impcas.ac.cn

Charge State Evolution for 2 MeV/u Carbon Ions Passing through Carbon Foils

M. Imai^{(1)*}, M. Sataka⁽²⁾, K. Kawatsura⁽³⁾, K. Takahiro⁽⁴⁾,
K. Komaki⁽⁵⁾, H. Shibata⁽¹⁾ and K. Nishio⁽²⁾

⁽¹⁾ Department of Nuclear Engineering, Kyoto University, ⁽²⁾ Japan Atomic Energy Agency (JAEA),
⁽³⁾ Kansai Gaidai University, ⁽⁴⁾ Kyoto Institute of Technology, ⁽⁵⁾ RIKEN

Non-equilibrium and equilibrium charge state distributions for 2.0 MeV/u carbon ions after penetrating carbon foil have been studied experimentally, following experimental [1,2,3] and theoretical [4] studies for 2.0 MeV/u sulfur ions. The initial charge states for the carbon projectile were between 2 and 6, whereas the target foil thickness was between 0.9 and 200 $\mu\text{g}/\text{cm}^2$. The measured equilibrium mean charge state and distribution width were 5.57 and 0.58, respectively. For the projectiles with charge states lower than the equilibrium charge state, i.e., for C^{2-5+} projectile ions, all the measured charge fractions except for C^{6+} showed similar dependence on target thickness that the fractions increase to show maxima in the non-equilibrium region and turn to decrease to the equilibrium values. This trend can be explained by a difference of collision cross sections or collision rates for consecutive single-charge transfers as for the sulfur projectile ions [3] and has been reproduced by ETACHA [5] code, although ETACHA predicts a bit higher equilibrium mean charge state 5.71 and a bit narrow distribution width 0.51.

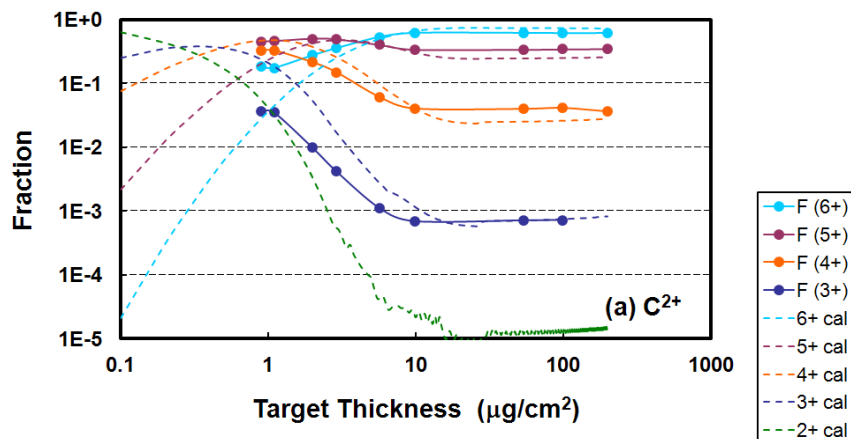


Figure 1. Charge state evolution for 2.0 MeV/u C^{2+} ion after penetrating C-foil targets. Full and dashed lines show experimental data and ETACHA calculation, respectively.

References

- [1] M. Imai *et al.*, *Nucl. Instr. and Meth.* **B230** (2005) 63.
- [2] M. Imai *et al.*, *Nucl. Instr. and Meth.* **B256** (2007) 11.
- [3] M. Imai *et al.*, *Nucl. Instr. and Meth.* **B267** (2009) 2675.
- [4] O. Osmani and P. Sigmund, *Nucl. Instr. and Meth.* **B269** (2011) 813.
- [5] J.P. Rozet *et al.*, *J. Phys.* **B22** (1989) 33.

* imai@nucleng.kyoto-u.ac.jp

Transmission of Fast Carbon Cluster Ions through an Al₂O₃ Nano-Capillary Foil

S. Tomita^{(1)*}, H. Tsuchida⁽²⁾, Y. Shiina⁽¹⁾, R. Kinoshita⁽¹⁾, J. Yokoe⁽²⁾, K. Yamazaki⁽¹⁾, S. Ishii⁽³⁾, and K. Sasa⁽³⁾

⁽¹⁾ *Institute of Applied Physics, University of Tsukuba, Tsukuba, Ibaraki 305-8573, Japan*

⁽²⁾ *Department of Nuclear Engineering, Kyoto University, Kyoto 606-8501, Japan*

⁽³⁾ *Tandem Accelerator Complex, University of Tsukuba, Tsukuba, Ibaraki 305-8577, Japan*

The transmission of fast carbon cluster ions C_n^+ ($n=1$ to 4) through Al₂O₃ nano-capillary foil was studied. The experiments were conducted at the University of Tsukuba, using 1 MV Tandem accelerator. Nano-capillary foils were purchased from SmartMembaranes GmbH. The capillaries are highly ordered and have high aspect ratio; the pore size was 75 nm in diameter and the thickness was 50 μ m. Front surface of the film was coated with platinum avoiding charging-up of the surfaces during ion beam exposure. The transmitted ions are detected by solid state detector (SSD).

Fig. 1 shows typical spectra for 0.98 MeV C_2^+ . Main peak corresponds to the transmitted C_2^+ through the nano-capillaries. At the half energy of the peak, there can be seen a peak of C. The peak has low energy tail, which is considered to be due to the fragmentation of C_2^+ scattered on the inner wall of the capillary. Comparing the intensity of these two peaks, survival ratio of C_2^+ is obtained to be nearly 90%. This high survival ratio is considered to be result of high aspect ratio which lowered the transmission of scattered particles.

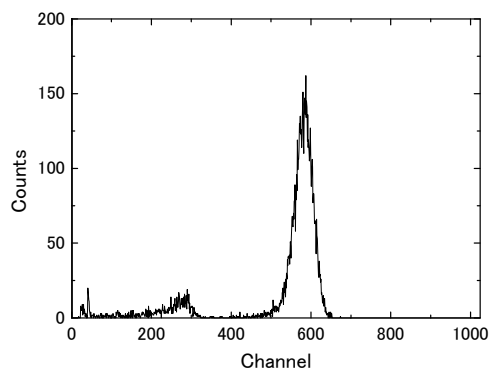


Figure 1. Typical energy spectrum of 0.98MeV C_2^+ transmitted through nano-capillary foil. The pore size was 75 nm in diameter, and the thickness is 50 μ m.

* tomita@bk.tsukuba.ac.jp

Isotope Dependence of the Equilibrium Charge State of Cl Ions

Passing through Carbon Foils

K. Sasa^{(1)*}, T. Takahashi⁽¹⁾, N. Nagashima⁽¹⁾, and K. Shima⁽¹⁾

⁽¹⁾*Tandem Accelerator Complex, University of Tsukuba, Ibaraki 305-8577, Japan*

The information on the charge state distribution of different isotope ions is important for accelerator mass spectrometry (AMS), meanwhile systematic measurements of the charge state distribution of isotope ions are limited^[1, 2]. The purpose of this research is that there is any isotope effect or not in the charge state distribution of Cl isotope ions at higher energy regions for ³⁶Cl AMS. Since the charge state distribution of ions passing through a foil is caused by a distant collision, an observation of the isotope effect would be a little expected even if the ion energy becomes higher. In order to confirm this query, equilibrium charge distributions of 0.607 – 2.51 MeV/u for ³⁵Cl and ³⁷Cl ions after the passage through carbon foils have been measured by a high resolution magnetic spectrograph ESP-90 with the 12UD Pelletron tandem accelerator at the University of Tsukuba.

When the equilibrium charge state distributions of ³⁵Cl and ³⁷Cl ions after the passage through carbon foils are compared at equal exit energy from carbon foils in units of MeV/u, quite a good agreement has been observed between ³⁵Cl and ³⁷Cl ions. Equilibrium mean charge of 2.51 MeV/u for ³⁵Cl and ³⁷Cl ions, for instance, is 14.04. In this work, the isotope effect of charge state distributions between ³⁵Cl and ³⁷Cl ions has not been observed at the higher energy region.

References

- [1] C. Stoller et al., *IEEE Trans. Nucl. Sci.* NS-30 (1983) 1074.
- [2] H. J. Hofmann et al., *Nucl. Instr. Meth. B*, 29 (1987) 100.

* ksasa@tac.tsukuba.ac.jp

The effects of Oxygen on Hydrogen retention in Tungsten: a first-principles investigation

Alkhamees Abdullah[#] . Guang-Hong Lu^{*}

Department of Physics, Beihang University, Beijing 100191, China

Abstract

We investigate the physical origin of hydrogen-oxygen (H–O) interaction in Tungsten (W) in terms of total energy and charge density by calculating the energetics and diffusion properties using a first-principles method. The interaction between H and O in bulk W show a strong attractive interaction with solution energy $\sim 0.61\text{eV}$ and correspond binding energy $\sim 0.341\text{ eV}$ along the $\langle 031 \rangle$ directions with the H–O distance of $\sim 2.38\text{ \AA}$. Energetically, both a single H atom and O atom are prefer to occupy tetrahedral interstitial site (TIS). Two interstitial H atoms are attractive and tend to be paired up at two neighboring TIS with a H-H distance of 1.74 \AA and O-H distance of 2.43 \AA for both two H atoms with $\text{H}-\overset{\wedge}{\text{O}}-\text{H}$ angle $\sim 42^\circ$ and solution energy $\sim 1.26\text{eV}$ with corresponding binding energy $\sim 0.5\text{eV}$. According to the distances between O-H, H-H and H-O-H complexes and the H-O-H angle, the possibilities of format the OH, H₂ and H₂O molecules are excluded.

PACS: 21.10.Dr, 21.10.Ft, 71.15.Mb, 81.05.Bx, 61.72.-y

Keywords: Tungsten, Oxygen, Hydrogen, First principles

**Corresponding author.* Tel.: (86)10-82339917; fax: (86)10-82339917

E-mail address: [#] akhamis11@gmail.com, ^{*} lgh@buaa.edu.cn

Stark effect in Resonant Coherent Excitation of 2s electron of Li-like Fe²³⁺ ions Channeling in a Si crystal

Y. Nakai^{(1, 2) *}, Y. Nakano^(3, 4), T. Ikeda⁽¹⁾, Y. Kanai⁽¹⁾, T. Kambara^(1, 2),
N. Fukunishi⁽²⁾, C. Kondo⁽⁵⁾, T. Azuma^(3, 4), K. Komaki^(1, 5), Y. Yamazaki^(1, 5)

⁽¹⁾ Atomic Physics Laboratory, RIKEN

⁽²⁾ RIKEN Nishina Center

⁽³⁾ Atomic, Molecular and Optical Physics Laboratory, RIKEN

⁽⁴⁾ Department of Physics, Tokyo Metropolitan University

⁽⁵⁾ Graduate School of Arts and Sciences, University of Tokyo

In resonant coherent excitation (RCE) of the 2s electron to the n=3 states for Li-like Fe²³⁺ ions channeling in a silicon crystal at 83.5MeV/u, it was found that the RCE corresponding to optically forbidden transitions could be seen as intense as optically allowed transitions.[1] We considered that the Stark mixing of the n=3 states due to the electric field of the static planar potential was the most possible reason for the observation of the optically forbidden transitions. This effect is very small close to the channel center and becomes more important with increasing distance from the channel center because the electric field of a planar potential increases with distance from the channel center.

We performed RCE measurement of 83MeV/u Fe²³⁺ ions using a silicon surface barrier detector (SSD) as a crystal target in order to obtain information on the ion trajectory in the channel. The energy deposit (ΔE) to the SSD increases with the amplitude of oscillating ion trajectory. Therefore, RCE measurement coincident with ΔE gives information on the amplitude of ion trajectory where the optically forbidden transitions occur. This method was used by Azuma et al. for 390 MeV/u H-like Ar ions and the transition energies of RCE to the n=2 states were found to strongly depend on the ion trajectory due to Stark mixing by the planar potential.[2]

In the low ΔE , i.e., near the channel center, optically allowed 2s-3p transitions were intense compared with other transitions. Increasing ΔE , i.e., increasing the amplitude of ion trajectory, the optically forbidden 2s-3s transition rapidly became intense. On the other hand, the optically forbidden 2s-3d transitions did not become intense as rapidly as 2s-3s transition. Furthermore, it was found that the excitation energies to the n=3 states changed with ΔE , which was at least qualitatively consistent with the estimation for the energy levels of the Stark-mixed n=3 states depending on the distance from the channel center.

References

[1] Y. Nakai *et al.*, Nucl. Instrum. Methods Phys. Res. B **230**, 784 (2005).

[2] T. Azuma *et al.*, Phys Rev. Lett. **83**, 528 (1999).

* nakaiy@riken.jp

Modification of Optical Band-gap of Silicon Films Induced by Ion Irradiation

Yabin Zhu⁽¹⁾, Cunfeng Yao⁽¹⁾, Zhiguang Wang^{(1)*}, Jianrong Sun⁽¹⁾, Kongfang Wei⁽¹⁾, Tielong Shen^{(1),(2)}, Lilong Pang⁽¹⁾, Minghuan Cui^{(1),(2)}, Yuanfei Li^{(1),(2)}, Ji Wang^{(1),(2)}, Huiping Zhu^{(1),(2)}

⁽¹⁾ *Institute of Modern Physics, Chinese Academy of Sciences, Lanzhou 730000, China*

⁽²⁾ *Graduate University of Chinese Academy of Sciences, Beijing 100049, China*

The researches about the effects of ion irradiation on the mono-crystalline silicon (c-Si) have been progressed for several decades. However, the studies about the modification of the structures and optical properties of silicon films induced by the ion irradiation are limited. In the present work, the effects of ion irradiation on the optical band-gaps of silicon films have been studied.

Hydrogenated amorphous silicon (a-Si:H), nano-crystalline silicon (nc-Si), hydrogenated nano-crystalline silicon (nc-Si:H) films and c-Si samples have been irradiated at room temperature (RT) by 2.0, 3.0, 4.0, 30, 196 MeV Kr-ions and 5.0, 6.0, 9.0, 94 MeV Xe-ions. The fluence of Kr-ions is in the range from 1.0×10^{13} to 2.0×10^{14} ions/cm², and the fluence of Xe-ions is in the range from 1.0×10^{11} to 1.0×10^{14} ions/cm². The samples were investigated by the means of X-ray diffraction (XRD), Raman spectroscopy, transmission electron microscopy (TEM) and UV-Vis-NIR spectroscope. The obtained results show that the optical band-gaps of the silicon films decrease with the increasing fluence. For a-Si:H, nc-Si and nc-Si:H films, the optical band-gaps decrease from 1.78 to 1.54 eV, from 1.76 to 1.14 eV and from 2.1 to 1.37 eV, respectively. While the optical band-gaps of c-Si samples remain identical at 1.12 eV before and after the irradiation. Possible mechanisms on the irradiation-induced modification of the optical band-gaps of silicon films with different structures are discussed.

Keywords: Ion irradiation, Silicon films, Optical band-gap

* E-mail address for correspondence: zhgwang@impcas.ac.cn.

Emission Rates of Selected L Sub-Shell Proton Induced X-Rays as a Function of Projectile Energy

O. G. de Lucio*, C. E. Canto

*Instituto de Física, Universidad Nacional Autónoma de México,
Apartado Postal 20-364, México D.F., México 01000*

Characteristic X-Ray spectra of Gd, induced by proton impact were recorded in order to generate information on the dependence of the L-Shell X-Ray emission rates as a function of the projectile energy. For the present study, samples were prepared in the form of thin films by deposition of GdF₃ on pyrolytic carbon substrates. Proton beams were produced by means of a Van de Graaff accelerator, and the range of bombardment energies covered from 200 keV up to 750 keV.

Experimental results will be presented as relative intensities of the X-Ray lines, corresponding to some of the different L-subshell transitions on the target. By comparing these results with theoretical predictions, some disagreement can be found in the case of the L₁ and L₃ subshells, particularly for bombardment energies below 400 keV. Also, by considering relative intensities of selected individual X-Ray emission lines instead of only sub-shell multiplets, it has been possible to show with more detail the origin of such disagreement with the calculations.

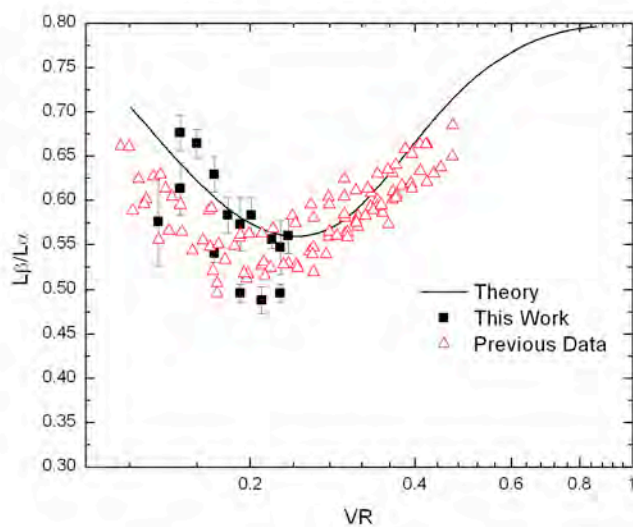


Figure 1. Relative intensity of L_{β} / L_{α} X-Ray lines, as a function of a scaling parameter defined as the *reduced velocity*. Results from this work are compared with previous measurements and theoretical calculations.

* dododrillo@yahoo.com

Dynamic features of slow highly charge ion beam guiding with glass surface

T. Ikeda^{*}, T. M. Kojima, Y. Kanai, and Y. Yamazaki

Atomic Physics Laboratory, RIKEN, Wako, Saitama 351-0198, Japan

We have developed a scheme to produce microbeams of slow highly charged ions with single tapered glass capillaries based on the guiding by a self-organized charge up [1, 2]. A similar transmission experiment with thin gaps of paired glass plates has been performed as one of different types of guiding optics, where we found a peculiar oscillation feature in the beam transmission [3]. We have proposed a periodic resistive switching of the glass plates which causes drastic discharges of the accumulated charge on the glass surface when the strength of the electric field by the charge becomes strong enough. The field becomes weak after the discharge and then the charging starts again. When the switching occurs decreasing of guided transmission is observed. In order to examine the switching can occur even with a single plate, we have started an experiment of grazing incidence to a glass surface with the incidence angles of 1-10° or less as shown in Fig.1. A position sensitive detector was installed not only to count the reflected ions but also to measure the deflection angles of the ions. Increasing of the number of reflected ions was observed as reported in [4], while inhomogeneous distribution within the beam spot was obtained. And some islands within the spot appeared and disappeared depending on time. According to the appearances of the islands, the counts of reflected ions fluctuated. This dynamic inhomogeneous distribution corresponds possibly to the localized discharge-positions in the irradiated area. We will report on the details of the reflected beam profile and compare the results of the experiments employing paired glass plates and single glass plate.

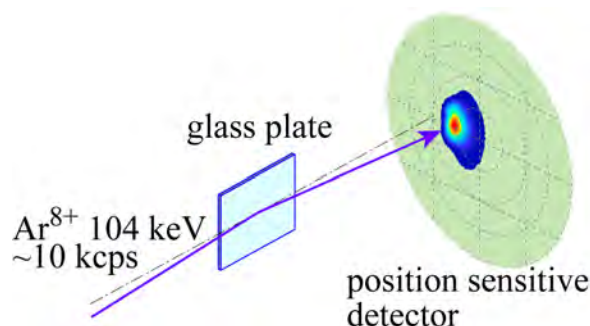


Figure 1. Setup of the experiment. The soda lime glass plates had a metal plate on the rear side connected to the ground.

References

- [1] T. Ikeda *et al.*, Appl. Phys. Lett. 89, 163502 (2006).
- [2] T. Ikeda *et al.*, Surf. Coat. Technol. 206, 859 (2011).
- [3] T. Ikeda *et al.*, Nucl. Instrum. Methods Phys. Res. B, in press (doi:10.1016/j.nimb.2012.06.001).
- [4] N. Bundaleski *et al.*, J.Phys.: Conf. Ser. 133, 012016 (2008).

^{*} tokihiro@riken.jp

High-resolution EUV/X-ray Spectroscopy for Investigations of Ion-Surface Interactions at EBIS

D. Banaś⁽¹⁾, Ł. Jabłoński⁽¹⁾, P. Jagodziński⁽²⁾, D. Sobota⁽¹⁾, and M. Pajek^{(1)*}

⁽¹⁾*Institute of Physics, Jan Kochanowski University, 25-406 Kielce, Poland,* ⁽²⁾*Department of Physics, Kielce Univeristy of Technology, 25-314 Kielce, Poland*

The electron beam ion traps and sources (EBIT/S) offer unique experimental conditions for the studies of interaction of highly charged ions (HCI) with plasma and solids [1]. In particular, the neutralization of slow HCI at surfaces leads to formation of exotic hollow which relaxation is accompanied by the emission of x-rays carrying information on the dynamics of this process as well as the structure and deexcitation channels of hollow atoms. Additionally, in such collisions the surface can be locally strongly modified leading to formation of nanostructures such as hillocks or craters. This process is of great fundamental and technological interest [1].

Here we report on the development of EUV/X-ray spectroscopy program at the EBIS-A facility [2] (Dreebit GmbH Dresden) which was installed recently [3] at the Institute of Physics of Jan Kochanowski University. The x-rays emitted from the recombination processes will be measured by the IncaWave diffraction x-ray spectrometer manufactured by Oxford Instruments. This spectrometer covers a wide range of photon energies from 70 eV to 15 keV including thus both the extended ultraviolet (EUV) and x-ray regions, which is important feature for the studies of ion-surface interaction. The IncaWave is a compact ($R = 21$ cm) x-ray spectrometer having six diffraction crystals, including two multilayers, which are installed in Johann or Johansson geometry. In order to optimize the use of this spectrometer at EBIs the simulations of its characteristics have been initiated using the ray tracing Monte Carlo approach (see Ref. [4]). The simulations covers both the geometries of the spectrometer calibration using the electron beam excited x-rays as well as the measurements of x-ray emission from HCI colliding with surfaces. In particular, the influence of the x-ray source size on the energy resolution of the spectrometer for various geometries, including grazing angle emission [5], will be studied in details. In this simulations a modeling of the crystal rocking curve will be also investigated. Finally, the results of optimization of the installation of the IncaWave x-ray diffraction spectrometer for the observation of x-rays emitted from collision of slow HCI with surfaces will be presented.

This work is supported by the Polish Ministry of Science and Higher Education under Grant No. N N202 463539.

References

- [1] F. Aumayr, H.P. Winter, E-J Surf. Sci. Nonotech. 1, 171 (2003).
- [2] G. Zschornack et al., Rev. Sci. Instrum. **79** (2008) 02A703.
- [3] D. Banaś et al. J. Instrum. 5, C09005 (2010).
- [4] D. Banaś et al., J. Phys. Conf. Ser. 58, 415 (2007).
- [5] A. Kubala-Kukuś et al., Phys. Rev. B80, 113305 (2009).

* pajek@ujk.edu.pl

Ion beam Guiding with Curved Glass Tubes

Takao M. Kojima^{*}, Tokihiro Ikeda, Yasuyuki Kanai, and Yasunori Yamazaki

Atomic Physics Laboratory, RIKEN, Wako, Saitama 351-0198, Japan

The ion beam guiding phenomena with macroscopic-size (a few cm long and some tens to hundreds μm inner diameter) single glass capillaries and tubes were reported by several groups [1,2]. In those studies, the transmission became smaller as the tilt angle became larger. The observed guiding limit in tilt angles was about 5 degrees or less. In our previous work, we have observed that curved Teflon tubes can guide ion beams to the angles larger than the guiding limit of straight Teflon tubes [3]. Recently, we have tested the guiding capability of straight and curved glass tubes. The experiment and some typical results are shown in Fig.1. The injected beam current was estimated from the current I_h+I_t and the diameter ratio of inlet to shield aperture. The inner and outer diameters ID/OD, the radii of curvature R, and the bending angle ϕ of the tubes are given in the figures. Very stable transmission was observed for bending angles much larger than the guiding limit of the straight tube. It continued for more than 40 minutes until the measurement was stopped. However, the transmission oscillated (see Fig.1d) when the entrance of the tube was slightly (0.5-1 degrees) tilted in the direction of the bottom in Fig.1a. The oscillation continued stably more than 15 minutes until the tilt angle was changed. This phenomena might be caused by 'resistive switching' of the glass as reported in Ref. [4].

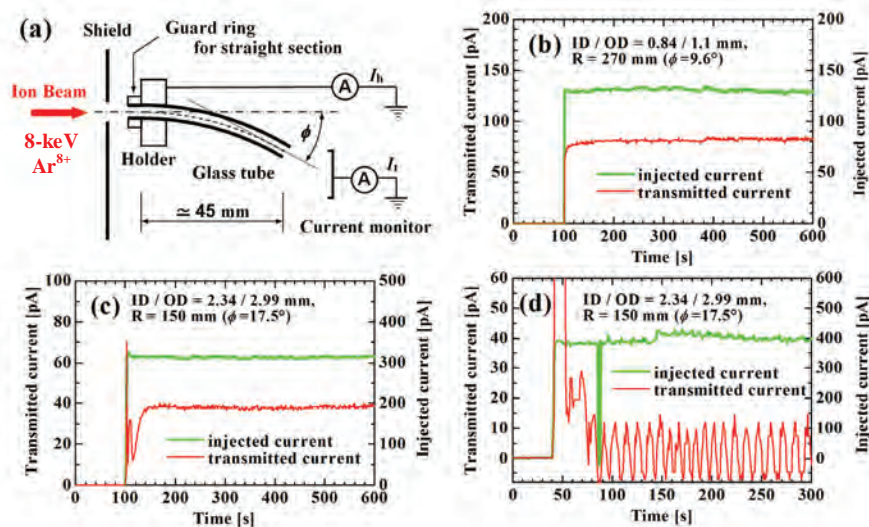


Figure 1. (a) Experimental setup. (b)-(d) Time dependence of ion beam transmission with curved glass tubes. The primary beam was turned on at around 100 s in b and c, and 40 s in d.

References

- [1] T. Ikeda, Y. Kanai, T. M. Kojima, et al., *Appl. Phys. Lett.* **89** (2006) 163502.
- [2] R. J. Berezky, G. Kowarik, F. Aumayr and K. Tokesi, *Nucl. Instrum. Methods B* **267** (2009) 317.
- [3] T. M. Kojima, T. Ikeda, Y. Kanai, et al., *J. Phys. D: Appl. Phys.* **44** (2011) 355201.
- [4] T. Ikeda, Y. Iwai, T. M. Kojima, S. Onoda, Y. Kanai, Y. Yamazaki, *Nucl. Instrum. Methods B*, in press.

^{*} kojima@riken.jp.

Medium-Energy Helium Ion-Stimulated Desorption

T. Kobayashi^{(1)*}, S. Toda^(1,2), R. Andrzejewski⁽¹⁾, H. Baba⁽¹⁾, S. Shimoda⁽¹⁾,
K. Ueda⁽³⁾, and Y. Kuwahara⁽²⁾
⁽¹⁾RIKEN, ⁽²⁾Osaka University, ⁽³⁾Nara Institute of Science and Technology

We have investigated an interaction between medium-energy helium ion beam and lithium-containing materials. Lithium-containing materials used in this investigation have been a MgLi alloy and a LiCoO₂ of a positive-electrode material for lithium-ion battery. The investigation has been performed using a three-dimensional medium-energy ion scattering (3D-MEIS) spectrometer[1-4]. 3D-MEIS is that a pulsed He ion beam with a pulse width of 2 ns at a medium energy of 100 keV is used as an incident beam, and emissions coinciding with the incident beam are detected using a two-dimensional position sensitive and time-resolving micro-channel plate detector. We have found for the first time that hydrogen and Li ions are emitted from sample surfaces by the He ion beam impact with a medium energy. It is considered that the mechanism of the phenomenon which has been drawn from evidences of emission energy and emission efficiency of hydrogen and Li ions is desorption induced by electronic transition. The phenomenon may be a novel method for analyzing light elements, especial Li.

References

- [1] S. Shimoda, T. Kobayashi, Nucl. Instr. and Meth. B 219–220, 573 (2004).
- [2] S. Shimoda, T. Kobayashi, J. Appl. Phys. 96, 3550 (2004).
- [3] T. Kobayashi, Nucl. Instr. and Meth. B 249, 266 (2006).
- [4] T. Kobayashi, Phys. Rev. B 75, 125401 (2007).

* tkoba@riken.jp

Sputtering and Erosion of Carbon and Tungsten Surfaces Exposed to Fusion-relevant Plasma

A. Deslandes^{(1)*}, Guenette MC⁽²⁾, Batty SW⁽²⁾, Karatchevtseva I⁽²⁾, Samuell C⁽³⁾, Cohen DC⁽¹⁾, Blackwell B⁽³⁾, Corr C⁽³⁾, and Riley DP⁽²⁾

⁽¹⁾ *Institute of Environmental Research, ANSTO, Locked Bag 2001, Kirrawee DC, New South Wales 2232, Australia,* ⁽²⁾ *Institute of Materials Engineering, ANSTO, Locked Bag 2001, Kirrawee DC, New South Wales 2232, Australia,* ⁽³⁾ *Plasma Research Laboratory, Research School of Physics and Engineering, Australian National University, Canberra 0200, Australia*

Plasma facing materials for nuclear fusion devices encounter plasma-surface interaction processes such as chemical and physical erosion, re-deposition and implantation. Understanding and overcoming the detrimental effects that these phenomena can have upon component integrity, plasma stability, and the associated device performance, is key to the development of materials and components for fusion devices.

The MAGnetised Plasma Interaction Experiment (MAGPIE) at the Australian National University (ANU) is a high density ($n_e = 10^{17} - 10^{19} \text{ m}^{-3}$), low temperature ($T_e \sim 5 \text{ eV}$), and high flux ($\sim 10^{17} \text{ ions cm}^{-2} \text{ s}^{-1}$) linear plasma device for plasma surface interaction studies. This prototype device uses an external RF helicon antenna capable of delivering plasma power of up to $\sim 2.5 \text{ kW}$ in continuous operation or up to $\sim 5 \text{ kW}$ pulsed. A series of external coils are used to magnetically confine the plasma and create conditions similar to that of the divertor region of a fusion device.

We report on the sputtering and erosion processes of carbon and tungsten materials from some of the first materials-exposure experiments in MAGPIE. Surface morphologies of the samples have been characterised using scanning electron microscopy, revealing erosion and blistering. Changes to the nature of chemical bonding are observed via Raman spectroscopy. Ion beam analysis is used to measure the elemental composition of the exposed surfaces.

* acd@ansto.gov.au

Muon Acceleration in Cosmic-ray Sources

J. B. Tjus⁽¹⁾, S. R. Klein^{(2), (3)}, and R. Mikkelsen^{(2), (4)*}

⁽¹⁾ *Fak. f. Phys. & Astron., Ruhr-Universität Bochum, Germany,* ⁽²⁾ *Lawrence Berkeley National Laboratory, Berkeley CA 94720 USA,* ⁽³⁾ *Physics Dept. University of California, Berkeley, USA* ⁽⁴⁾ *Dept. of Physics and Astronomy, Aarhus University, DK-8000 Aarhus C, Denmark*

The sites of cosmic-ray acceleration seem to require extreme conditions involving turbulent plasmas. Protons, pions and muons may interact with the matter and fields in these sites, and be accelerated to high energies, up to 10^{20} eV. Several mechanisms are proposed for accelerating cosmic-rays with gradients up to 10^{13} keV/cm. At gradients above 1.6 keV/cm, the muons produced by hadronic interactions undergo significant acceleration before decay. We study the effect of muon acceleration on neutrino production. The resulting constraints preclude models of linear acceleration and by this set strong constraints on plasma wakefield accelerators and on specific sources for linear accelerators like Gamma Ray Bursts and magnetars.

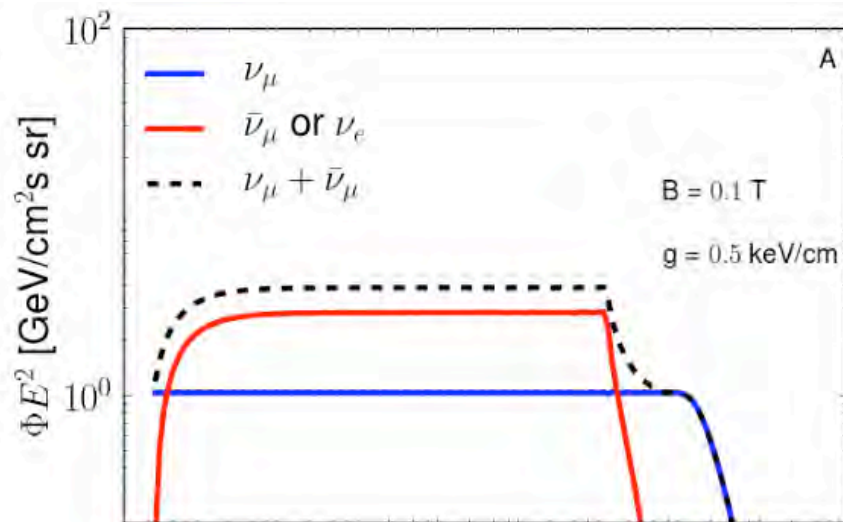


Figure 1. Enhancement factors for different neutrino flavors.

* runemikkelsen@phys.au.dk.

Anomalous Deep Ion-induced Modification of HOPG

N.N. Andrianova⁽¹⁾, A.M. Borisov⁽¹⁾, E.S. Mashkova⁽¹⁾, V.S. Sevostyanova⁽¹⁾,
Yu.S. Virgiliev⁽²⁾

⁽¹⁾ Skobeltsyn Institute of Nuclear Physics, Lomonosov Moscow State University, Moscow, Russia,

⁽²⁾ NIIGraphite, Moscow, Russia

The ion-induced structure and morphology changes of highly oriented pyrolytic graphite (HOPG) are different from ones for less ordered carbon-based materials and these changes manifest inherent differences in the temperature range from RT to ~ 400 °C. This displays the temperature dependences of ion-induced electron emission yield $\gamma(T)$ which are essentially different from each other during heating and following cooling [1]. The purpose of the presented work is to study the regularities of high-fluence (10^{18} – 10^{19} ion/cm²) 10 - 30 keV Ar⁺ ion modification of HOPG (grade UPV-1T) basal plane. The Rutherford Backscattering (RBS) has been applied to estimate the modified layer depth h . The morphology changes have been studied by scanning electron microscopy (SEM). It has been found that at sufficiently high ion energy h can be ten times more than the ion projectile range R_p . The different effects of deep modification with $h > 1000$ nm are observed in two temperature intervals. Firstly, at the temperatures smaller than the temperature of ion-induced texture transition $T < T_t \approx 150$ °C and the topography is not significantly changed from initial one and modified layer becomes in polycrystalline state according to RBS in channelling regime. Secondly, at $T_t < T < 400$ °C when the SEM shows the development of needle and ridge-like elements and deep argon incorporation takes place. The ion irradiation at temperature of texture transition T_t , as the irradiation at sufficiently high $T \geq 400$ °C, does not lead to deep modification effect and the depth h of disordered layer is about R_p . The influence of ion energy on the deep modification effect is seen from Figure 1. There are the energy thresholds of deep modification which correspond to threshold values of stationary level of radiation damage – about 45 and 65 displacements per atom accordingly for deep modification at RT and at $T \sim 250$ °C.

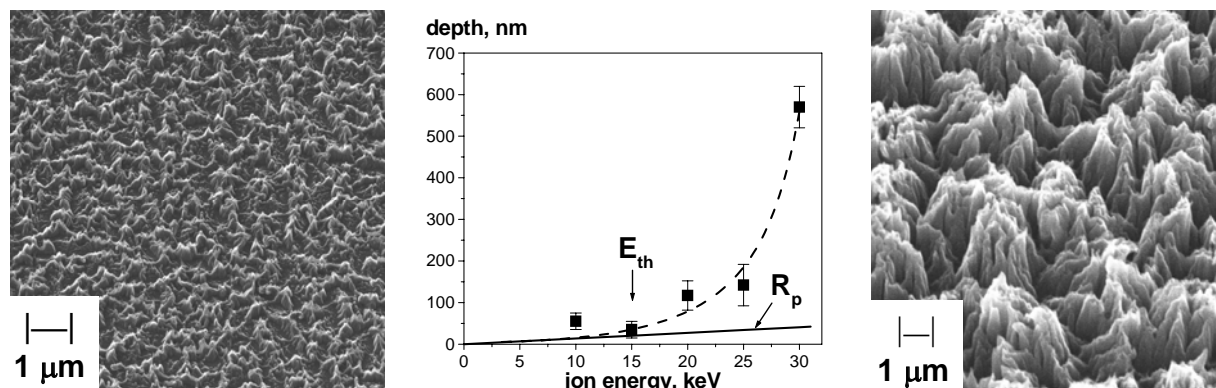


Figure 1. FWHM of argon concentration profile in HOPG versus Ar⁺ ion energy E at $T = 250$ °C. SEM-micrographs of HOPG surface after irradiation at $E = 10$ keV (left) and $E = 30$ keV (right)

References

- [1] Andrianova N.N., Avilkina V.S., Borisov A.M., Mashkova E.S. Nucl. Instrum. Methods in Phys. Res. B. 2012. V. 273. P. 58-60.

anatoly_borisov@mail.ru

Electrical Resistivity Change due to High-Energy X-ray Irradiation of Oxide Ceramics

N. Ishikawa^{(1)*}, Y. Chimi⁽¹⁾, A. Iwase⁽²⁾

⁽¹⁾ Japan Atomic Energy Agency, Japan, ⁽²⁾ Osaka Prefecture University, Japan

Electrical properties of $\text{YBa}_2\text{Cu}_3\text{O}_{6+x}$ can be easily changed over a wide range, from dielectric to metallic, by varying the oxygen concentration within the limits of $0 \leq x \leq 1$. In addition to variation of chemical composition, its conductivity can be influenced by visible light [1,2]. The excess conductivity persists for a long time even after switching off the light, and this phenomenon is called persistent photoconductivity (PPC). The importance of this finding is that light irradiation can be an alternative method of carrier doping. Although there are many literatures concerning visible light irradiation effect, there has been a few literature concerning X-ray irradiation effect of $\text{YBa}_2\text{Cu}_3\text{O}_{6+x}$ in the energy range of more than keV. The objective of this study is to investigate whether or not the high-energy X-ray (5-9keV) irradiation makes any difference compared with the visible light irradiation.

Distinguished feature of high-energy X-ray in the order of keV is its ability to excite inner shell electrons. Another important aspect of the present study is to elucidate whether or not the excitation of inner shell electrons generates a specific influence on the irradiation effect.

In this study $\text{EuBa}_2\text{Cu}_3\text{O}_7$, which has a same crystallographic structure as $\text{YBa}_2\text{Cu}_3\text{O}_7$, was irradiated with high-energy (5-9keV) X-ray at low temperature (100K), and the electrical resistivity was measured in situ. The low temperature irradiation is to minimize the thermal annihilation of defects created by X-ray. In fact, the irradiation-induced change in the resistivity observed at 100K is completely recovered after thermal annealing at 300K. The result of the in-situ measurement shows that electrical resistivity increases as increasing photon dose, suggesting that the atomic displacements are taken place due to the electron excitations. The effect has quite the opposite trend compared with that observed for the visible light irradiation. It is found also that the resistivity increase scales with the absorbed energy whether the energy level is near Cu K-edge (9.0 keV), Eu L3-edge (7.0 keV) and Ba L3-edge (5.2 keV). These results suggest that, irrespective of whether the high-energy X-ray causes inner shell electron excitation or not, the atomic displacements are caused as the relaxation process of the energy absorbed by the electron system of $\text{EuBa}_2\text{Cu}_3\text{O}_7$ sample.

References

- [1] V. I. Kudinov et al., Phys. Rev. B **47** (1993) 9017.
- [2] A. I. Kirilyuk et al., Pis'ma Zh. Eksp. Teor. Fiz. 52, 696 (1990) [JETP Lett. 52, 49 (1990)].

* ishikawa.norito@jaea.go.jp

Low Energy Metal Ion Beam Injection to SiO₂ Thin Films for Development of Novel Catalysts

S. Yoshimura^{(1)*}, K. Ikuse⁽¹⁾, M. Kiuchi^{(1),(2)}, Y. Nishimoto⁽¹⁾, M. Yasuda⁽¹⁾,
A. Baba⁽¹⁾, and S. Hamaguchi⁽¹⁾

⁽¹⁾ Osaka University, ⁽²⁾ National Institute of Advanced Industrial Science and Technology (AIST)

It has been pointed out that interaction of different metal atoms such as Indium (In) and Silicon (Si) located in close proximity shows high catalytic abilities for certain organic chemical reactions [1-3]. Recently, we have proposed a “physical” approach, i.e., metal ion implantation into target materials, as a technique to prepare materials that contain different metal atoms in close proximity as potential candidates for catalysts [4]. In this study, we have developed a metal ion beam production system with a low energy mass-selected ion beam machine. The obtained mass-selected ion beam is identified to be that of pure metal with no impurity in the range of 0-500 eV. The full width at half maximum of the energy distribution is about 5 eV. We currently attempt to develop novel catalysts by injecting metal ions such as Indium (In) and Gallium (Ga) into SiO₂ thin films. In conventional experiments of metal ion beam injection, a solid-state metal is heated to produce liquid or gaseous metal atoms and then metal ions are produced. On the contrary, we modified a Freeman-type ion source so that a solid-state material can be set inside the ion source chamber as a sputter target. In the ion source, metal ions can be obtained from sputtering of the target by Ar ions generated from an Ar plasma [5]. We have measured the sticking probabilities or the self-sputtering yields of metal ions with energies in the range of 50-500 eV using a quartz crystal microbalance. For example, in the In ion beam experiment, we used In₂O₃ as the target in the ion source because the melting temperature of metal solid In is too low. Interaction of In and Si atoms are known to catalyze certain organic chemical reactions [1-3]. In an attempt of creating a material that manifests the interaction, In implanted SiO₂ films were prepared. It has been found that In implanted SiO₂ film can catalyze an organic chemical reaction. It has been also shown that there are optimal ion energies and optimal ion doses for the highest catalytic ability in the film preparation process [6]. Furthermore, we have found that catalytic ability of In implanted SiO₂ thin film is strongly dependent on the substrate temperature.

References

- [1] Y. Onishi, T. Ito, M. Yasuda, A. Baba, *Eur. J. Org. Chem.* (2002) 1578.
- [2] T. Saito, M. Yasuda, A. Baba, *Synlett* (2005) 1737.
- [3] U. Schneider, S. Kobayashi, *Angew. Chem. Int. Ed.* 46 (2007) 5909.
- [4] S. Yoshimura, K. Hine, M. Kiuchi, Y. Nishimoto, M. Yasuda, A. Baba, S. Hamaguchi, *Appl. Surf. Sci.* 257 (2010) 192.
- [5] S. Yoshimura, M. Kiuchi, Y. Nishimoto, M. Yasuda, A. Baba, S. Hamaguchi, *e-J. Surf. Sci. Nanotech.* 10 (2012) 139.
- [6] S. Yoshimura, M. Kiuchi, Y. Nishimoto, M. Yasuda, A. Baba, S. Hamaguchi, *Thin Solid Films* 520 (2012) 4894.

* yosimura@ppl.eng.osaka-u.ac.jp

Slow HCI Nanobeam Produced through an Insulating Tapered Glass Capillary

C. L. Zhou^a, T. Ikeda^b, S. Guillous^a, J. Rangama^a, A. Méry^a, W. Iskander^a, E. Sezestre^a, S. Wickramarachchi^c, A. Ayyad^c, C. Grygiel^a, H. Lebius^a, J. A. Tanis^{a,c}, A. Cassimi^a

^aCIMAP CEA/CNRS/ENSICAEN/UCBN, BP5133, F-14070 Caen cedex 5, France

^bAtomic Physics Laboratory, Riken, 2-1 Hirosawa, Wako, Saitama 351-0198, Japan

^cDepartment of Physics, Western Michigan University, Kalamazoo, Michigan 49008, USA

In the last decade microbeam fabrication for biological cell radiation and ion surface interaction has attracted considerable attention [1-3]. Low priced and unconventional insulating glass capillaries have been developed to produce slow HCI microbeams for ion beam analysis (IBA) [2,3]. Very recently we have performed measurements at the GANIL facility (Caen, France) with 27 keV Ar⁹⁺ ions transmitted through a tapered glass capillary for the purpose of producing nanometer sized beams. The capillary had an inlet diameter of ~800 μm, an outlet diameter of ~500 nm and overall length of ~8 cm, with a region near its center where the taper goes from the larger radius (800 μm) to the smaller radius (500 nm) in a relatively short distance (~4 mm). Using a well aligned primary ion beam, a transmitted beam of intensity $1.5 \times 10^8 \text{ ions}\cdot\text{cm}^{-2}\cdot\text{s}^{-1}$ and having a diameter of several hundred nanometers was obtained at the capillary exit. Transmission was measured for tilt angles over a range up to 1.2° with a 2-dimensional position sensitive detector (2-D PSD). Further results will be presented at the conference.

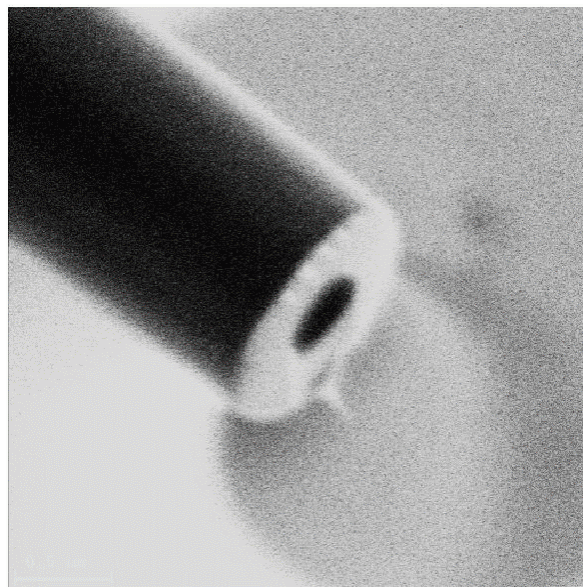


Figure 1: Exit of glass capillary with a diameter of 500nm.

References

- [1] T. Nebiki, *et al.*, J. Vac. Sci. Technol. A **21** 1671(2003).
- [2] A. Cassimi *et al.*, Nucl. Instr. and Meth. B **267**, 674 (2009).
- [3] T. Ikeda *et al.*, Appl. Phys. Lett. **89**, 163502 (2006).

Raman Spectroscopic Study of Rutile TiO₂ Irradiated by Swift Heavy Ions

Jie Luo^{(1)*}, Youmei Sun⁽¹⁾, Jinglai Duan⁽¹⁾, Huijun Yao⁽¹⁾, and Jie Liu⁽¹⁾

⁽¹⁾*Institute of Modern Physics, Chinese Academy of Science*

Titanium dioxide has drawn much research attention for its various applications in photocatalysis, photovoltaics, photochromics,^[1] etc. Many fabrication techniques aiming at material property modification have been proposed. Here we present a method by irradiating single crystal rutile TiO₂ with swift heavy ions. The irradiated rutile samples with (100) face orientation were tested by raman spectroscopy. Figure 1 shows spectrum peak broadening of the irradiated samples which indicates the rutile crystal lattice damage by ion irradiation. An other significant phenomenon is that the spectrum expands greatly at the site of anatase E_{g(1)} mode which implies that the rutile crystal transits to the anatase phase while irradiating.^[2] The expansion grows bigger as the irradiating fluence becomes higher at the same irradiating ion energy. The samples with (001) and (110) face have also been tested and there appears the same tendency in the spectrum profile. Other testing method is now being taken to establish the conclusion and deeper insight into the material damage mechanism of irradiation needs to be analyzed.

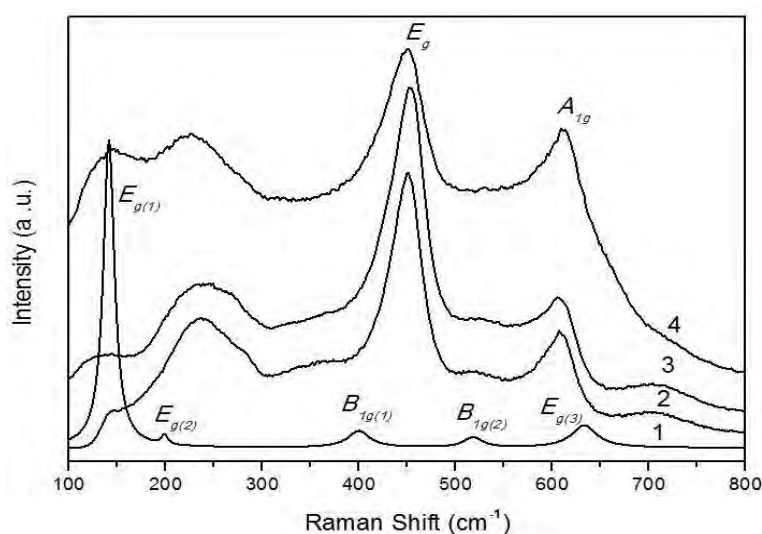


Figure 1. Raman spectrum of TiO₂ samples. 1. anatase pristine 2. rutile pristine with (100) face orientation 3. rutile TiO₂ with (100) face irradiated by 370 MeV U ions at 5×10^{12} ions/cm² 4. rutile TiO₂ with (100) face irradiated by 370 MeV U ions at 1×10^{12} ions/cm²

References

- [1] X. Chen and S. S. Mao, Chem. Rev. 107, 2891, 2007.
 [2] V. Swamy, Phys. Rev. B 77, 195414, 2008.

* E-mail: luojie@impcas.ac.cn

Low Energy Ar⁸⁺ Scattering on ZnO (0001) and (000 $\bar{1}$) Surfaces

K. Motohashi^{(1)*}, T. Ikeda⁽²⁾, T. Kojima⁽²⁾, T. Koyama⁽¹⁾, and Y. Suzuki⁽¹⁾

⁽¹⁾Toyo University, ⁽²⁾RIKEN

Lattice-polarized compound-semiconductors with two atomic elements, for example GaN, ZnO, AlN, and so on, have been available recently. They are attracting attention because of the wide band gap and some excellent optical properties. The two elements of the crystals align along with a specific axis of the surface. A lattice-polarized ZnO crystal has the (0001) and (000 $\bar{1}$) surfaces which are at right angle to the *c*-axis. The former is terminated by heavier Zn atoms, and the latter is terminated by lighter O atoms [1]. It is natural to consider that the scattering mechanisms between multicharged ions and the two surfaces are different because the surface dipoles or the electron affinities are different. We carried out an ion scattering experiment of ZnO(0001) and (000 $\bar{1}$) surfaces in order to study the influence of the first atomic layer on the collision processes [2]. The goal of this study is to develop a particle-beam-transportation technique by utilizing the surfaces of paired semiconducting plates [3].

The experiment was performed at an ion-beam line (BL3) of RIKEN. Ar⁸⁺ (≤ 32 keV) ion beam with a rectangular cross-sectional shape (0.16mm in horizontal width and 0.6mm in vertical height) entered onto the single crystalline ZnO(0001) and (000 $\bar{1}$) surfaces. The number of scattered particles was measured with a channel electron multiplier. Figs. 1(a) and (b) show the numbers of detected particles as a function of the scattering angle in three different angles of incidence. The vertical axes of these figures were normalized by a constant dose of Ar⁸⁺ ions. The angle at the maximum intensity, which is very close to the specular reflection angle, increases with an increase of the angle of incidence for both surfaces. Every maximum intensity of the (000 $\bar{1}$) surface is larger than that of the (0001) surface in the specific angle of incidence.

Reference

- [1] S.H. Overbury et al., Surf. Sci. **410** (1998) 106.
- [2] K. Motohashi et al., Surf. Sci. **601** (2007) 5304.
- [3] T. Ikeda et. al., Nucl. Instrum. Meth. Phys. Res. B in printing.

* motohashi@toyo.jp

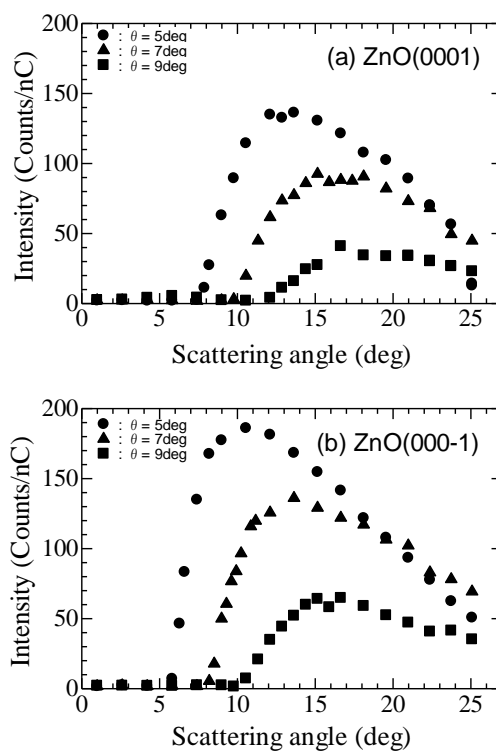


Fig. 1 Intensity of scattered particles in incidence of Ar⁸⁺ (32keV) on ZnO (0001) and (000 $\bar{1}$) surfaces.

Fragmentation of protein using collision with Xe^{q+} multicharged ions.

S. Martin⁽¹⁾, L. Chen⁽¹⁾, R. Brédy⁽¹⁾, A. Vernier⁽¹⁾, P. Dugourd⁽¹⁾, R. Antoine⁽¹⁾, J. Bernard⁽¹⁾, T. Schlathölter⁽²⁾, O. Gonzalez Maganad⁽²⁾ and G. Reitsma⁽²⁾

⁽¹⁾ *Université de Lyon, F-69622, Lyon, France Université Lyon 1, Villeurbanne CNRS, UMR 5579, LASIM*

⁽²⁾ *KVI Atomic and Molecular Physics, University of Groningen, Zernikelaan 25, NL-9747 AA Groningen, The Netherlands*

Fragmentations of protein have been investigated using a new set-up developed to the KVI laboratory [1]. We have studied electron multicapture processes and dissociation of a trapped protonated Cytochrome C (Cyt-C) as induced by keV Xenon multicharged ions ($q = 5$ to 12). Collisions between selected charge state of Cyt-C (from 15+ to 18+) and Xe^{q+} present a very simple fragmentation patterns. An example is shown on figure 1 for Xe^{12+} on Cyt-C^{18+} . As expected, Cyt-C^{19+} and Cyt-C^{20+} peaks are mainly attributed to the single and double capture processes, while the Cyt-C^{17+} is attributed tentatively to a large deprotonation of the highest charge states of Cyt-C produced in the collision. This new and no expected fragmentation channel has never been observed for the other smaller biological molecule. Higher mass resolution spectra will be necessary to confirm this mechanism.

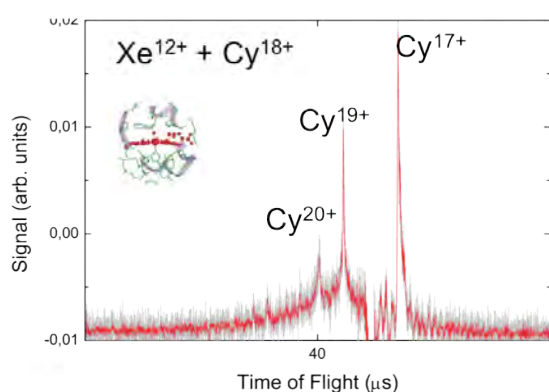


Figure 1. Fragmentation Spectrum of $\text{Xe}^{12+} + \text{Cyt-C}^{18+}$

Corresponding author: smartin@univ-lyon1.fr

Reference

[1] S. Bari et al, Phys. Chem. Chem. Phys. 2010, 12, 3376

Theoretical Study for DNA Damage Due to Radiation: Are Plasmas Produced from Heavy Ion Irradiation useful for the Understanding of RBE ?

Kengo Moribayashi^(1,2)

⁽¹⁾ Japan Atomic Energy Agency, ⁽²⁾ Doshisha University

Cancer therapy using carbon ions has a powerful therapeutic effect.. This is based on the fact that relative biological effectiveness (RBE) of carbon ions is higher than that of protons and X-rays. A hypothesis has been proposed that clustered DNA damage, which is refractory to repair, is highly relevant to RBE values. Although evidence on the biological significance of clustered DNA damage has been accumulated, it remains largely unknown how clustered DNA damage is generated after irradiation [1]. We proposed and quantified that the electric field traps the emitted electrons near a radiation track, which, in turn, may lead to a clustering of DNA lesions [2].

Our model on the production of clustered DNA damage due to the composite electric fields is as follows. (i) The mean path between ionization events becomes shorter as the cross sections increase. (ii) A shorter mean paths between ionization events form the stronger electric field. (iii) This electric field traps electrons near the track of the incident ion, which form plasma. According to our calculations based on this model in the case of the irradiations of a carbon ion with an energy of 3 MeV/u, plasma with the electronic temperature of about 10 eV and the density of $10^{21}/\text{cm}^3$ appears within the diameter of 2 nm from this track. The electrons in this plasma may more often interact with DNA which is located near the track and may produced the larger number of clustered DNA damages than the case where electric field is not considered and plasma is not formed [comparison of Fig.1(a) with Fig.1(b)].

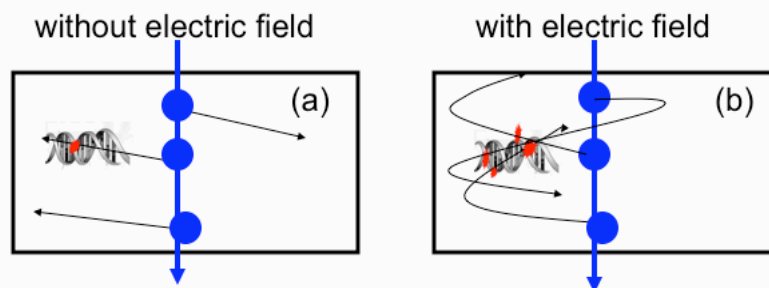


Figure 1. Images for the places of water molecule ions produced from the incident ion impact ionization, the tracks of electrons, and the DNA damage produced from the electron impact. The tracks of electrons are treated (a) without and (b) with the electric field. \rightarrow : Track of an incident ion, \rightarrow : track of an electron, \bullet : water molecular ions, \star :DNA damage.

References

- [1] N. Shikazono *et al.*, J. Radiat. Res. **50**, 27 (2009).
 [2] K. Moribayashi, Phys. Rev.A, **84**, 012702(2011).

Ion Beam Surface Nanostructuring of Ag–Au Bilayers Deposited on SiO₂ Glass

Xuan Meng⁽¹⁾, Tamaki Shibayama^{(2)*}, Ruixuan Yu⁽¹⁾, Shinya Takayanagi⁽¹⁾, and Seiichi Watanabe⁽²⁾

⁽¹⁾ Graduate School of Engineering, Hokkaido University, Sapporo, Hokkaido 060–8628, Japan, ⁽²⁾ Center for Advanced Research of Energy Conversion Materials, Faculty of Engineering, Hokkaido University, Sapporo, Hokkaido 060–8628, Japan

Metallic nanoparticles either sustained on the surfaces or dispersed in dielectric matrices have been extensively studied because of their pronounced optical and electrical properties. Most of the studies have focused on surface plasmon excitation, which dominates the photoabsorbance spectra in the UV/visible range. In recent years, there are many interests in synthesizing silica glass based bimetallic–silica nanocomposites for their considerable applications in nano–optical devices [1]. However, from the viewpoint of practical applications, controlling in the size, shape, and volume fraction of the bimetallic nanoparticles embedded in the silica substrate still remains a challenge.

Recently, we successfully fabricated a layer of photosensitive Ag–Au compound nanoballs embedded in a SiO₂ glass substrate by 100 keV Ar ion irradiation and consequent annealing of Au film (20nm) and Ag (25nm) film consecutively thermal deposited on SiO₂ glass. Thermal annealing was carried out in high vacuum at 1073 K for one hour. The effects of the irradiation dose on the nanoballs formation was studied by increase the dose from $1.0 \times 10^{16}/\text{cm}^2$ to $10.0 \times 10^{16}/\text{cm}^2$. A scanning electron microscope (SEM) was used to study the ion–beam–induced surface nanostructuring. The microstructural evolution and the chemical concentration of Ag–Au nanoballs were investigated using a transmission electron microscope (TEM) equipped with an energy dispersive X–ray spectrum (EDS). With the increase of the irradiation dose, the dewetting of the Ag–Au films on the SiO₂ glass substrate was occurred and finally a layer of Ag–Au compound nanoballs with highly spherical shape embedded in the substrate was obtained. High resolution TEM (HRTEM) image of Ag–Au nanoballs before and after the thermal annealing were obtained, and the annealing effects was studied. Also, irradiation induced interface ion–mixing was observed, and a numerical estimation of the interface ion–mixing was carried out by the SRIM 2011 codes.

In addition, photo absorbance spectra were obtained to characterize the optical properties. Surface plasmon resonance (SPR) peaks were observed after the irradiation and the peaks became narrowing after the thermal annealing. In summary, ion irradiation has been considered as an effective approach in surface nanostructuring and also in fabrication of metal–silica nanocomposites, and the potential implications of these nanocomposites in optical device is expected.

References

[1] L. M. Liz–Marzán, *Langmuir*, **22** (2006) 32.

* shiba@qe.eng.hokudai.ac.jp

Interaction of Deuterium with Vacancies induced by Ion Irradiation in W

Q. Xu^{(1)*}, K. Sato⁽¹⁾, X.Z. Cao⁽²⁾, P. Zhang⁽²⁾, B.Y. Wang⁽²⁾, T. Yoshiie⁽¹⁾,
H. Watanabe⁽³⁾ and N. Yoshida⁽³⁾

⁽¹⁾ *Research Reactor Institute, Kyoto University, Osaka 590-0494, Japan*

⁽²⁾ *Institute of High Energy Physics, Chinese Academy of Sciences, Beijing 100049, China*

⁽³⁾ *Research Institute for Applied Mechanics, Kyushu University, Fukuoka 816-8580, Japan*

Plasma-facing materials (PFMs) in a fusion reactor suffer two types of damage: displacement damage caused by high energy neutrons, and surface damage, such as erosion, sputtering and blistering, caused by hydrogen and helium from plasma. Important criteria for choosing PFMs are high melting point, high thermal conductivity and low sputtering erosion. Metallic materials, such as tungsten and molybdenum, are potential candidates for PFMs according to the results of recent studies. The damage induced by intense fluxes of energetic deuterium and tritium particles, as well as 14 MeV neutrons, will influence tritium retention in PFMs. In the present study, deuterium retention instead of tritium retention in ion-irradiated W was investigated.

The samples were prepared from polycrystalline W (99.95 wt.% purity) delivered by Allied Material Corporation. A 0.2 mm thick W plate was cut into 10 x 10 mm² size samples, and mechanically polished to mirror-like finish. The samples were then annealed at 1773 K for 1 h in vacuum with a background pressure of 1x10⁻⁴ Pa. After electropolishing in 4% NaOH water solution with 15 V, the samples were irradiated with 2.4 MeV Cu²⁺ ions using a Tandem type accelerator in Kyushu University. The damage induced by the ions in the matrix was not uniform, and the damage peak was about 400 nm from the irradiation surface. The damage rate was 2.5x10⁻⁴ dpa/s and the total damage was 0.3 dpa at the peak position. Deuterium implantation was subsequently carried out in samples using a mono-energetic D₂⁺ ion beam at room temperature. To avoid displacement damage, implantation was performed at 1 keV. The nominal deuterium dose was 1x10²¹ D/m². In order to investigate the irradiation depth dependence of microstructural evolution, the Doppler broadening of annihilation radiation measurements were performed using a mono-energetic positron beam apparatus.

In the present study, we introduced a parameter, namely S , defined as the ratio of the low-momentum ($|P_L| < 1.5 \times 10^{-3} mc$) region in the Doppler broadening spectrum to the total region, where m is the electron rest mass and c is the velocity of light. S represents the smaller Doppler shift resulting from the annihilation of valence electrons. The increase in S in the same materials compared with that in a well-annealed sample is due to the annihilation at vacancy-type defects. The S parameter increased in Cu ion irradiated W compared with well-annealed one. However, it decreased after deuterium implantation. The results indicated that deuterium implanted in W was trapped by vacancies induced by Cu ion irradiation. The stability of deuterium in vacancies was also investigated.

* Corresponding author, Q. Xu; Email: xu@rri.kyoto-u.ac.jp.

In-Situ Analysis System to Detect Vacancy-Type Defects during Ion Beam Irradiation

A. Kinomura^{(1)*}, R. Suzuki⁽¹⁾, T. Ohdaira⁽¹⁾, N. Oshima⁽¹⁾, B. E. O'Rourke⁽¹⁾,
and T. Nishijima⁽¹⁾

⁽¹⁾ *National Institute of Advanced Industrial Science and Technology (AIST),*

1-1-1 Umezono, Tsukuba, Ibaraki 305-8568, Japan.

Defects induced by ion irradiation are initially formed as point defects (i.e., monovacancies and interstitial atoms). Concentrations and depth distributions of such point defects can be calculated by Monte-Carlo simulations. However, except for the low-temperature irradiations, point defects annihilate or grow to secondary defects through migration, recombination and clustering. It is difficult to experimentally characterize such defect behaviors during irradiation. To date, various in-situ analysis techniques, such as transmission electron microscopy combined with ion irradiation, have been developed. In this study, we employed a positron annihilation lifetime spectroscopy (PALS) as a probe of vacancy-type defects for in-situ analysis during ion beam irradiation.

An electron linear accelerator was used to generate a thermalized positron beam. Positrons were magnetically guided to a target chamber connected to an ion accelerator, followed by chopping and bunching to obtain pulsed positrons necessary for PALS measurements. Positrons can be accelerated up to 30 keV after the pulsing electrodes. Ar ions at energies up to 150 keV were used to introduce defects near the surface of samples. The ion beam is pulsed by chopper electrodes and its irradiation can be synchronized with positron irradiation. The incident directions of positron and ion beams were 0 and 45° to the surface normal, respectively [1].

As a preliminary experiment, PALS spectra of a thermal oxide layer on Si (SiO₂) were collected during 150 keV Ar⁺ irradiation. The irradiation-induced change of PALS spectra was observed with increasing ion fluence, indicating that the in-situ measurement during ion irradiation was successfully achieved. Similar experiments were also performed for metal samples. The spectrum change associated with positron diffusion length was observed in this case.

Acknowledgement: This work was supported by a Grand-in-Aid for Scientific Research (24310080) from Japan Society for the Promotion of Science.

References

[1] A. Kinomura, R. Suzuki, T. Ohdaira, N. Oshima, B. E. O'Rourke and T. Nishijima, *Physics Procedia* (accepted for publication).

*a.kinomura@aist.go.jp

Measurement of electronic sputtering yield of amorphous ^{13}C thin film

Saif A. Khan^{(1)*}, A. Tripathi⁽¹⁾, M. Toulemonde⁽²⁾, C. Trautmann⁽³⁾, and W. Assmann⁽⁴⁾

⁽¹⁾Inter-University Accelerator Centre, Aruna Asaf Ali Marg, New Delhi, 110067, India, ⁽²⁾ Centre de Recherche sur les Ions, les Matériaux et la photonique, CIMAP-GANIL, CEA-CNRS-ENSICAEN-Univ. Caen, BP 5133, Bd H. Becquerel, 14070 Caen, France, ⁽³⁾ GSI Helmholtzzentrum für Schwerionenforschung, Planckstr. 1, 64291 Darmstadt, Germany, ⁽⁴⁾ Fakultät für Physik, Ludwig-Maximilians-Universität, München, 85748 Garching, Germany

Electronic sputtering yield measurements of carbon films are uncertain because of various factors which makes it challenging. The problem which affects the yield is the presence of hydrocarbon contamination on the surface of the materials either on the irradiated material or on the catcher on which the sputtered atoms are collected. In order to avoid this complication, the carbon sputtering yield was quantified by measuring the thickness decrease of a 80 nm ^{13}C thin film (with 16% ^{12}C content) using high resolution online ERDA. The measurements showed that 194 MeV Au ions produce a sputtering yield of 33 ± 8 of ^{13}C /ion along with a deposition rate of 5 ± 2 ^{12}C /ion, which is caused by beam induced beak-up of hydrocarbons. Moreover, inelastic thermal spike simulations fit to the sputtering yield from the present measurement and other published measurements [1], by using a sublimation energy of ^{13}C film of 2.5 ± 0.5 eV/at. Extrapolation of the inelastic thermal spike model will be done for several values of electronic energy losses with different beam energies.

References

[1] G. Dollinger, M. Boulouednine, A. Bergmaier, T. Faestermann, C.M. Frey Nucl. Instr. Meth. B 118 (1996) 291.

* khansaifahmad@gmail.com

Advanced SiC fiber strain behaviour during ion beam irradiation in the electronic slowing down regime

A. Jankowiak^{1*}, C. Grygiel², I. Monnet², Y. Serruys³, C. Colin¹, S. Miro³, L. Gelebart¹, L. Gosmain⁵, J.-M. Costantini⁴

1. CEA, DEN, DANS, DMN, SRMA, LC2M, F-91191 Gif-sur-Yvette, France
2. CIMAP, CEA, CNRS, ENSICAEN, UCBN, BP5133-14070 Caen cedex 5, France
3. CEA, DEN, DANS, DMN, SRMP, Laboratoire JANNUS, F-91191 Gif-sur-Yvette, France
4. CEA, DEN, DANS, DMN, SRMA, LA2M, F-91191 Gif-sur-Yvette, France
5. CEA, DEN, DANS, DMN, SEMI, LPCMI, F-91191 Gif-sur-Yvette, France

*corresponding author: jean-marc.costantini@cea.fr

Tel: (+33) 1 69 08 43 88

Fax: (+33) 1 69 08 71 67

Abstract

Third generation SiC fibers have significantly improved the thermo-mechanical properties of SiC_f/SiC_m ceramic matrix composite which are considered as advanced materials for fission reactor applications. These materials exhibit interesting features such as a low activation level and a higher operating temperature in comparison to ferritic steels and V alloys. However, their thermo-mechanical performances strongly depend on their complex microstructure which undergoes significant changes when they are irradiated. Thus, the possible use of SiC_f/SiC_m composites points out the need to carefully study their properties to determine if they can fully comply with the aimed application requirements. Consequently, a multi-scale approach is currently ongoing and aims to provide a satisfying predictive modeling of the SiC_f/SiC_m composite behaviour in a reactor. The different components of the composite, i.e. the fibers, the matrix and the interphase, are then characterized separately.

As a first step, the *in-situ* strain behaviour under irradiation in the electronic slowing down regime of a Tyranno SA3 SiC fiber (UBE Industries Ltd Japan) was investigated in real time. For this purpose, a tensile test device suitable for micrometrical samples was developed with the JANNUS Saclay irradiation platform where the first *in-situ* test was successfully performed. The second experiment, which is the subject of this work, was achieved at the GANIL facility in Caen. A 7.44μm diameter SiC fiber was submitted to both low mechanical loading level at 300MPa and 92MeV Xe²³⁺ ion beam irradiation at room temperature. The fiber has exhibited a gradual increase of its longitudinal strain reaching a maximum value of 0.50% for an average damage level of 0.1dpa. Raman spectroscopy analyses performed on fibers submitted to the same irradiation conditions have shown significant local structure modification but no total amorphisation could be evidenced. The irradiated fiber was then submitted to cyclic isochronal annealing treatments up to 1800°C leading to a partial strain recovery of 0.45%.

This work will be taking further using complementary range of ions and energies in order to study various material damaging processes and their impact on the fiber properties. The next step will consist in coupling fiber heating and ion irradiation since creep tests can be performed with the above mentioned equipment. Consequently, these conditions will be as close as possible to the extreme conditions which could be found in nuclear reactor core. They will provide the opportunity to determine damage mechanisms involved in this material during an irradiation at high temperature.

Compositional Effects on Track Formation in A_2TiO_5 (A = La, Nd, Sm, Gd) Irradiated With Swift Heavy Ions

C.L. Tracy⁽¹⁾, M. Lang⁽²⁾, J. Zhang⁽²⁾, F. Zhang⁽²⁾, Z. Wang⁽³⁾, and R.C. Ewing^{(1), (2)*}

⁽¹⁾ Department of Materials Science & Engineering, University of Michigan, Ann Arbor, MI 48109, USA ⁽²⁾

Department of Earth and Environmental Sciences, University of Michigan, Ann Arbor, MI 48109, USA ⁽³⁾

Cornell High Energy Synchrotron Source, Cornell University, Ithaca, NY 14853

Different compositions of orthorhombic A_2TiO_5 (A = La, Nd, Sm, Gd) were irradiated with swift Xe ions (1.47 GeV) to fluences from 5×10^{10} to 1×10^{13} ions/cm². Cylindrical tracks consisting in part of an amorphous phase were formed in all compositions. Systematic analysis of the structural modifications induced by ion track formation was completed using transmission electron microscopy, synchrotron x-ray diffraction, and Raman spectroscopy. Significant radiation-induced amorphization occurred for all compounds, but the size of the amorphous regions within the tracks, along with the degree of amorphization achieved in the bulk material for a given ion fluence, decreased as smaller cations (higher Z) occupied the A-site. This decrease in the amorphous domain size is attributed primarily to epitaxial recrystallization of a disordered defect fluorite phase at the outer edge of the initially liquid-like tracks, the stability of which is related to the ratio of the ionic radii of the A- and B-site (B = Ti) cations. While similar ion track recrystallization phenomena have been observed in pyrochlores ($A_2B_2O_7$) of varying composition [1], A_2TiO_5 is unique in that the disordered phase is not a high-temperature polymorph, suggesting kinetic control of the radiation-induced transformation.

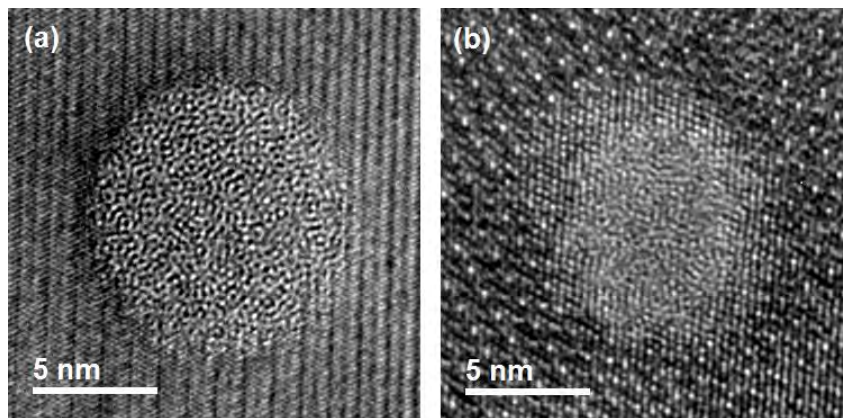


Figure 1. HRTEM images of ion track cross sections in (a) La_2TiO_5 and (b) Sm_2TiO_5 irradiated with 1.47 GeV Xe. The former shows only amorphous material within the track, while the latter features a defect fluorite track shell.

References

[1] Sattonnay G, Moll S, Thome L, Legros C, Calvo A, Herbst-Gysel M, Decorse C, Monnet I. Nucl Instrum Methods Phys Res Sect B 2012 ;272 :261.

* rodewing@umich.edu

Latent ion tracks in amorphous Ge

M.C. Ridgway^{(1),*}, T. Bierschenk⁽¹⁾, R. Giulian⁽¹⁾, B. Afra⁽¹⁾, M.D. Rodriguez⁽¹⁾,
L.L. Araujo⁽¹⁾, A.P. Byrne⁽¹⁾, N. Kirby⁽²⁾, O.H. Pakarinen⁽³⁾, F. Djurabekova⁽³⁾,
K. Nordlund⁽³⁾, M. Schleberger⁽⁴⁾, M. Toulemonde⁽⁵⁾, W. Wesch⁽⁶⁾ and P. Kluth⁽¹⁾

⁽¹⁾ Australian National University, Canberra, Australia, ⁽²⁾ Australian Synchrotron, Clayton, Australia, ⁽³⁾ University of Helsinki, Finland, ⁽⁴⁾ University of Duisburg-Essen, Duisburg, Germany, ⁽⁵⁾ CIMAP-GANIL, Caen, France, ⁽⁶⁾ Friedrich-Schiller University, Jena, Germany

We identify and characterise latent ion tracks formed in Ge by swift heavy-ion irradiation with 185 MeV Au⁺¹³ ions, correlating experimental results with first-principle calculations and Molecular Dynamics simulations. For our irradiation conditions, tracks were formed only in amorphous material, as attributed to much weaker electron-phonon coupling in crystalline material. Simulations indicate rapid heating following deposition of the ion energy yields a solid-to-liquid transformation within the track. The ensuing volume contraction necessary to accommodate the high-density liquid produces open volume in the form of voids interspersed along the ion path. Indeed, voids of bow-tie-like shape aligned with the incident ion direction are apparent with transmission electron microscopy and we suggest these voids are the precursor to the widely-reported swift heavy-ion irradiation-induced porosity in amorphous Ge. Experiment and simulation both indicate the latent ion track does not recrystallise but remains amorphous upon solidification. Using small-angle x-ray scattering, we show the ion track is of radius ~11 nm and comprised of an under-dense core and over-dense shell relative to unirradiated amorphous material, as consistent with a frozen-in pressure wave. Similarly, experiment and simulation can accurately fit and predict, respectively, the intriguing shape of the voids.

Thresholds of Etchable Track Formation and Chemical Damage Parameters in PI, PET, PC, and PADC Films at the Stopping Powers Ranging from 10 to 12,000 keV/ μm

T. Yamauchi^{(1)*}, Y. Mori⁽¹⁾, M. Kanasaki⁽¹⁾, A. Hattori⁽¹⁾, Y. Matai⁽¹⁾,

K. Matsukawa⁽¹⁾, K. Oda⁽¹⁾, S. Kodaira⁽²⁾, H. Kitamura⁽²⁾, T. Konishi⁽²⁾, N. Yasuda⁽³⁾,
S. Tojo⁽⁴⁾, Y. Honda⁽⁴⁾, and R. Barillon⁽⁵⁾

⁽¹⁾ Kobe University, ⁽²⁾ National Institute of Radiological Sciences, ⁽³⁾ Fukui University, ⁽⁴⁾ Osaka University,
⁽⁵⁾ Institute Pluridisciplinaire Hubert Curien

The damage structure of latent tracks in Polyimide (PI) films, KAPTON and UPILEX, has been examined by Fourier transform infrared (FT-IR) measurements. Results are compared with those from previous studies on poly(ethylene terephthalate) (PET), bisphenol A polycarbonate (PC), and poly(allyl diglycol carbonate) (PADC). These polymers are exposed to protons and heavy ions (He, C, Ne, Si, Ar, Fe, Kr, and Xe) in air with energies less than 6 MeV/n, as well as gamma rays from an intense Co-60 source [1-5]. Chemical damage parameters, namely, damage density, which is the number of losses of considered functional groups per unit length of tracks, radial size of the track core, in which the considered chemical groups are lost, and radiation chemical yields (G values) for each group are evaluated as a function of the stopping power. It has been confirmed that latent tracks will be etchable when the radial track core size is larger than the distance between two adjacent breaking points of polymer chains. The predominant breaking points are the C-O bonds in diphenyl ether, ester, carbonate ester, and ether bonds.

References

- [1] T. Yamauchi, Y. Mori, A. Morimoto, M. Kanasaki, K. Oda, S. Kodaira, T. Konishi, N. Yasuda, S. Tojo, Y. Honda, and R. Barillon: *Jpn. J. Appl. Phys.* **51** (2012) 056301.
- [2] Y. Mori, T. Yamauchi, M. Kanasaki, Y. Maeada, K. Oda, S. Kodaira, T. Konishi, N. Yasuda, and R. Barillon: *Radiat. Meas.* **46** (2011) 1147.
- [3] T. Yamauchi, Y. Mori, K. Oda, S. Kodaira, N. Yasuda, and R. Barillon: *KEK Proc. Radiation Detectors and Their Uses*, 2010, p. 1.
- [4] Y. Mori, T. Ikeda, T. Yamauchi, A. Sakamoto, H. Chikada, Y. Honda, and K. Oda: *Radiat. Meas.* **44** (2009) 211.
- [5] T. Yamauchi, Y. Mori, K. Oda, N. Yasuda, H. Kitamura, and R. Barillon: *Jpn. J. Appl. Phys.* **45** (2008) 3606.

E-mail:yamauchi@maritime.kobe-u.ac.jp

Optical properties in the wavelength of visible and near-infrared for chalcogenide glass waveguides formed by swift Kr ion irradiation

Tao Liu⁽¹⁾, Chun-Xiao Liu⁽²⁾, Hai-Tao Guo⁽²⁾, Qing Huang⁽¹⁾, Peng Liu⁽¹⁾, Sha-Sha Guo⁽¹⁾, Lian Zhang⁽¹⁾, Yu-Fan Zhou⁽¹⁾, and Xue-Lin Wang⁽¹⁾*

⁽¹⁾*School of Physics, State Key Laboratory of Crystal Materials and Key Laboratory of Particle Physics and Particle Irradiation (MOE), Shandong University, Jinan 250100, P.R.China*

⁽²⁾*State Key Laboratory of Transient Optics and Photonics, Xi'an Institute of Optics precision Mechanics, Chinese Academy of Science (CAS), Xi'an, Shanxi 710119, P.R. China*

Planar waveguide structures in chalcogenide glass were fabricated by 17MeV or 150MeV swift Kr ion irradiation. Photograph of the polished end facet of the Kr-irradiated chalcogenide glass was measured by metallographic microscope using reflected polarized light. SRIM 2006 was used to simulate the electronic and nuclear stopping powers for swift Kr ion irradiation, which were in agreement with the measured results. The micro-Raman spectrum were measured at atmosphere. The near-field intensity distributions were investigated at the wavelength of visible (633nm) and near-infrared (1300nm, 1500nm, 1539nm and 1620nm) band, which makes them candidates for infrared laser devices.

References

- [1] Q. Huang, P. Liu, T. Liu, L. Zhang, and X. L. Wang, "Waveguide structures for the visible and near-infrared wavelength regions in near-stoichiometric lithium niobate formed by swift argon-ion irradiation," *Opt. Express* 20, 4213-4218 (2012).
- [2] H.T. Guo, L. Liu, Y.Q. Wang, C.Q. Hou, W.N. Li, M. Lu, K.S. Zou, and B. Peng, "Host dependence of spectroscopic properties of Dy³⁺-doped and Dy³⁺, Tm³⁺- doped Ge-Ga-S-CdI₂ chalcogenide glasses," *Opt. Express* 17, 15350-15358 (2009).

* xuelinwang@sdu.edu.cn

Thickness Dependence of Secondary-electron Yield from Carbon Foils Bombarded with 62.5-300-keV/u H₂⁺ and C₂⁺ Ions

K. Narumi^{(1), (2)*}, Y. Takahashi⁽²⁾, A. Chiba⁽¹⁾, Y. Saitoh⁽¹⁾, K. Yamada⁽¹⁾,
N. Ishikawa⁽³⁾, H. Sugai⁽²⁾, Y. Maeda^{(2), (4)}

⁽¹⁾ *Takasaki Advanced Radiation Research Institute, Japan Atomic Energy Agency*

⁽²⁾ *Advanced Science Research Center, Japan Atomic Energy Agency*

⁽³⁾ *Nuclear Science and Engineering Directorate, Japan Atomic Energy Agency*

⁽⁴⁾ *Department of Energy Science and Technology, Kyoto University*

Secondary-electron (SE) emission from a solid surface bombarded with fast charged particles has been studied extensively for a long time and extended to various kinds of applications. Although it is a very fundamental phenomenon, it is not still understood completely. Vicinage effect on the SE emission induced by swift molecular/cluster ions is one of the unresolved problems [1, 2]. We have investigated the vicinage effect on the SE emission by measuring the SE yield emitted from an amorphous carbon foil bombarded with swift C₂⁺ ions. It has been observed for the first time that the vicinage effect on the SE yield in the forward direction induced by 62.5-keV/u C₂⁺ ions disappears for thicker foils than 60 μg/cm² [3]. This result means that a *transport* or *transmission* process of scattered electrons is very important for the appearance of the vicinage effect. In order to study the previous result further, we have investigated the vicinage effect on the SE emission induced by bombardment with H₂⁺ and C₂⁺ ions in the same velocity region.

62.5-300-keV/u H₂⁺ and C₂⁺ ions were incident on self-supporting amorphous carbon foils of 2-100 μg/cm² thickness, which was tilted by 45° to the beam axis. SE's emitted in the forward and backward directions from a carbon foil were detected with two microchannel-plate (MCP) detectors placed at the both sides of the target holder in parallel with the target. Particles transmitted through the foil were detected with a solid-state detector (SSD) placed at the backside of the target on the beam axis, which made it possible to measure the energy and the number of the transmitted particles. The forward and backward SE yields per incident projectile $\gamma_{F,B}$ were determined from the pulse-height distributions of the forward and backward MCP signals, respectively, which were proportional to the number of detected SE's. The vicinage effect was evaluated with the ratios of the forward and backward SE yields $R_{F,B} = \gamma_{F,B}(2)/2\gamma_{F,B}(1)$, where $\gamma_{F,B}(2)$ and $\gamma_{F,B}(1)$ are SE yields induced by bombardment with diatomic and monatomic ions with the same velocity, respectively. The origin of the vicinage effect on the SE yield will be discussed based on the observed foil-thickness and velocity dependence of the vicinage effect.

References

- [1] A. Billebaud *et al.*, Nucl. Instrum. Methods B **112** (1996) 79.
- [2] H. Kudo *et al.*, Jpn. J. Appl. Phys. **45** (2006) L565.
- [3] Y. Takahashi *et al.*, EPL **88** (2009) 63001.

* narumi.kazumasa@jaea.go.jp

Morphological Modification of Teflon Surface by Proton Microbeam and Nitrogen Ion Beam

A. Kitamura(Ogawa)^{(1)*}, T. Satoh⁽¹⁾, M. Koka⁽¹⁾, T. Kamiya⁽¹⁾, and T. Kobayashi⁽²⁾

⁽¹⁾ Department of Advanced Radiation Technology, Takasaki Advanced Radiation Research Institute, Japan Atomic Energy Agency (JAEA), ⁽²⁾ RIKEN

Polytetrafluoroethylene (PTFE) and fluorinated ethylene propylene (FEP) are well known as Teflon®. They have many unique properties, which make it valuable in micro electro mechanical system (MEMS), bio-chemical and medical tools. In fabricating microstructures on their surfaces, synchrotron radiation (SR) and focused ion beam (FIB) are effective [1]. Their irradiated surfaces are generally flat, but using keV order ion beam irradiation, needle-like protrusions can be created at high density [2]. This spiky surface can be fabricated only with this technique. Recently, we could uplift the PTFE surface locally by proton microbeam irradiation [3]. The morphological change occurred only at the irradiated area, and it was quite opposite to the case of using the former processes. In this study, we fabricated microstructures on Teflon surface using proton microbeam and nitrogen ion beam irradiation.

PTFE and FEP sheets (100 μm , 250 μm and 500 μm in thickness) were used. A 3 MeV proton beam 1 μm in diameter was scanned along the square pattern, 50 μm on a side, at various rates. Subsequently, these surfaces were evenly irradiated with 250 keV N_2^+ ion beam at the fluence from 1×10^{15} ions/ cm^2 to 1×10^{17} ions/ cm^2 . Both the irradiations were performed at TIARA (JAEA). The surface morphology of the samples was observed with scanning electron microscopy (SEM) and optical microscope.

When the proton microbeam scan rate was 500 $\mu\text{m}/\text{s}$, the morphological change of FEP surface was not observed by SEM. After the surface irradiated by N_2^+ ion beam at 2.5×10^{15} ions/ cm^2 , the surface changed as shown in Fig. 1. The protrusions were not formed at the square areas irradiated by proton beam (Fig. 1(b)). These areas were quite flat because they were selectively melted by the temperature elevation due to N_2^+ ion beam irradiation after the pattern irradiation of the proton microbeam. The result indicated the surface morphology could control using MeV proton microbeam and keV N_2^+ ion beam. The details of the mechanism will be discussed.

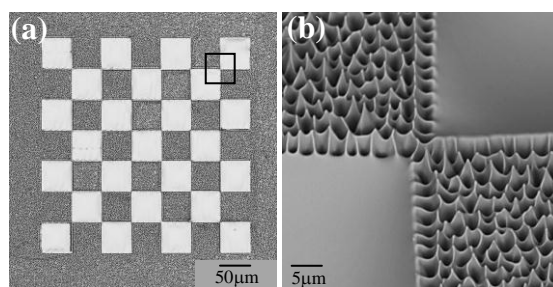


Fig. 1 SEM images of FEP surface scanned with proton microbeam followed by N_2^+ ion beam irradiation. (b) SEM image of the enlargement of the square shown in Fig. 1(a). The FEP thickness was 100 μm .

References

- [1] N. Miyoshi, A. Oshima, et. al., Radiat. Phys. Chem., 80, 230-235 (2011).
- [2] A. Kitamura, T. Kobayashi, T. Meguro, A. Suzuki, T. Terai, Trans. Mater. Res. Soc. Jpn., 33, 4, 1035-1038 (2008).
- [3] A. Kitamura, T. Satoh, M. Koka, T. Kamiya, T. Kobayashi, Trans. Mater. Res. Soc. Jpn., (2012), in press.

* ogawa.akane@jaea.go.jp

Structural Modification of ZnO Materials induced by Xe-ion Bombardments

Z.G. Wang^{(1)*}, H. Zang^{(1),(2)}, L.L. Pang⁽¹⁾, C.F. Yao⁽¹⁾, K.F. Wei⁽¹⁾, J.R. Sun⁽¹⁾, Y. B. Zhu⁽¹⁾

⁽¹⁾ Institute of Modern Physics, CAS, P. R. China, ⁽²⁾ Xi'an Jiaotong University, Xi'an, P. R. China

Zinc oxide (ZnO) is a typical generation III semiconductor material with attractive potential applications in the fields of optical devices (LED, solar cells), piezoelectric & surface acoustic wave devices, chemical sensors and so on. It is also suggested that ZnO should be an excellent detector used in intense radiation environment. However, a series of questions such as the formation and evolution of radiation damage, the chemical effects of incident ion species, the effect of crystal structures are still open in ZnO for answer. In the present work, we pay more attention on the experimental study of the structural modification of ZnO materials induced energetic ion bombardment.

In the experiments, ZnO films and single crystal samples were bombarded at room temperature (RT) with 400keV, 3.0, 3.64 or 308 MeV Xe-ions, respectively. The Xe-ion fluences are in the range from 1.0×10^{12} to 2.0×10^{16} Xe-ions/cm². After Xe-ions bombardments, the ZnO samples were investigated using X-Ray diffraction (XRD), Raman spectroscopy, atomic force microscope (AFM), transmission electron microscope (TEM). From the analyses of the obtained results we found that (1) ZnO thin film is of high resistance to Xe-ion implantation/ irradiation (stable bulk structure), but its c-axis lattice constant changes depending on implantation (swelling)/irradiation (compress); (2) Intense electronic excitations could induce significant surface modification of ZnO (thin film — amorphisation; single crystal — surface swelling); (3) Φ_{Se} plays a dominant role in bulk damage process of ZnO films under Xe-ion irradiation.

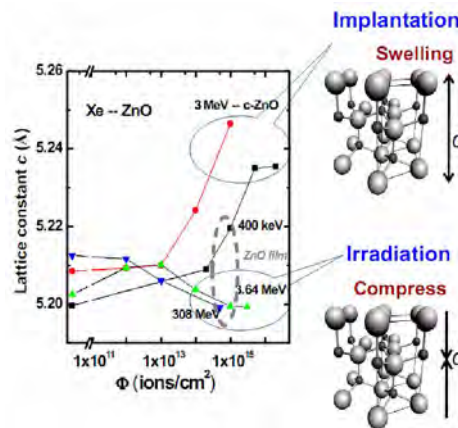


Fig.1 The c-axis lattice constant of ZnO materials varying with Xe-ion fluence.

Keywords: ZnO, Xe-ion bombardment, Structural modification

* E-mail address for correspondence: zhgwang@impcas.ac.cn

Deuterium Diffusion in Zr Oxide Irradiated with Zr Ions

I. Takagi^{(1)*}, H. Watanabe⁽¹⁾, K. Sawada⁽¹⁾, K. Une⁽²⁾, and K. Sakamoto⁽²⁾

⁽¹⁾ *Graduate School of Engineering, Kyoto University, Kyoto 606-8501, Japan*

⁽²⁾ *Nippon Nuclear Fuel Development, Co. Ltd., Narita-cho, Oarai, Ibaraki 311-1313, Japan*

Hydrogen diffusion in metals is generally affected by irradiation of energetic particles such as ions and neutrons. Meanwhile, irradiation effects on hydrogen diffusion in ceramics are not exactly known due to some difficulties in measuring low diffusion coefficients, typically $10^{-17} \text{ m}^2\text{s}^{-1}$ or less. In the present work, deuterium diffusion in oxide layers of zirconium alloy irradiated with a self ion of Zr has been examined by using a nuclear reaction analysis (NRA) of the $\text{D}(^3\text{He}, \text{p})^4\text{He}$ reaction. Sample materials were Zr-based alloys of Zircaloy-2 and GNF-Ziron.

Two types of experiment were conducted. One was that a sample was corroded with steam at 673 K to be covered with a 1.7- μm thick oxide layer and subsequently irradiated with 8.3-MeV Zr ions at room temperature. An average damage in the oxide was 1.3 dpa. After that the sample was continuously exposed to deuterium RF plasma at 573 K and evolution in a deuterium depth profile was in-situ observed by the NRA. In the other experiment, oxidation and irradiation of a sample were similar to the first one but the sample was charged with deuterium from deuterium water steam. While keeping the sample temperature 623 K, decrease in the deuterium concentration was observed.

The results of the two experiments showed that the ion irradiation significantly affected deuterium diffusion, that is, deuterium migration into the oxide layer was restricted in the first experiment and deuterium desorption from the oxide layer became much lowered in the second experiment. In metals, ion irradiation newly produces deep potential sites which trap hydrogen atoms to retard hydrogen migration. Trapping was, however, not significant in the present work because the deuterium concentration was not increased by the irradiation. A plausible reason for decrease in the diffusion coefficient is compressive stress [1] introduced by the irradiation

Reference

[1] K. Une et al., J. Nucl. Mater. 420 (2012) 445.

* Takagi@nucleng.kyoto-u.ac.jp

We-093

WITHDRAWN

Damage Cross Section Measurements on Irradiated Polyethylene with Swift Heavy Ion Beams

M.F. del Grosso^{(1),(2)}, G. García Bermúdez^{(1),(2),(3)}¹, C.R. Arbeitman^{(1),(2)}, and V.C. Chappa^{(1),(2)}

⁽¹⁾ *G. Investigación y Aplicaciones, CNEA, Bs. As., Argentina,* ⁽²⁾ *CONICET, Argentina.*

⁽³⁾ *Escuela de Ciencia y Tecnología, Universidad Nacional de San Martín, Argentina.*

When ions suddenly pass through a polymeric material, they induce a very complex path of excited and ionized molecules. The large amount of deposited energy near their trajectory creates a very inhomogeneous distribution of physico-chemical effects and damage. It can lead to polymer bond breaking, free radicals, excited species and secondary chemical processes that modified the polymer structure. These effects will depend on ion parameters such as ion mass, energy, stopping power and fluence as well as polymer structure. Most of the existing works observed qualitative effects induced by the ion irradiation of polymers, only a few analyzed the chemical damage and its correlation with the energy transfer process. The works of Papaléo et al. [1] measured the damage cross section in poly(phenylene sulphide) as a function of stopping power (dE/dx). They keep the fast ion velocities constant, so the track dimensions are fixed. Following this idea we extended the study to other polymer and ion velocities. For this purpose we irradiated High Density Polyethylene (HDPE) films with swift heavy ions provided by the Tandem accelerator (Buenos Aires, Argentina): ⁷Li, ¹²C, ¹⁶O, ³²S at a selected velocity of 1 and 2 MeV/amu. The analysis of the structural change produced by the irradiation was measured by means of infrared spectroscopy in the transmission and reflectance mode. Finally we will discuss the damage cross section measurements at this new range of ion velocities.

References

[1] R.M. Papaléo, A. Hallén, B.U.R. Sundqvist, L. Farenzena, R.P. Livi, M.A. de Araujo, R.E. Johnson. Phys. Rev. B 53, 2303 (1996).

¹ e-mail address: ggb@tandar.cnea.gov.ar

Computer Simulation of High-Energy-Beam Irradiation of Uranium Dioxide

Y. Sasajima^{(1)*}, T. Osada⁽¹⁾, N. Ishikawa⁽²⁾, and A. Iwase⁽³⁾

⁽¹⁾ Ibaraki University, ⁽²⁾ Japan Atomic Energy Agency, ⁽³⁾ Osaka Prefecture University

The structural relaxation caused by the high-energy-beam irradiation of single-crystalline uranium dioxide was simulated by the molecular dynamics method. As the initial condition, high thermal energy was supplied to the individual atoms within a cylindrical region of nanometer-order radius located in the center of the specimen. The potential proposed by Basak[1] was utilized to calculate interaction between atoms. The supplied thermal energy was first spent to change the crystal structure into an amorphous one within a short period of about 0.3ps, then it dissipated in the specimen. The amorphous track radius R_a was determined as a function of the energy density of the thermalized region. As shown in Fig.1, it was found that the relationship between R_a and the effective stopping power gS_e follows the relation $R_a^2 = a \log(gS_e) + b$. Compared to the case of Si and SiO₂ (β -cristobalite) single crystals, it was harder to produce amorphous track because of the long range interaction between U atoms.

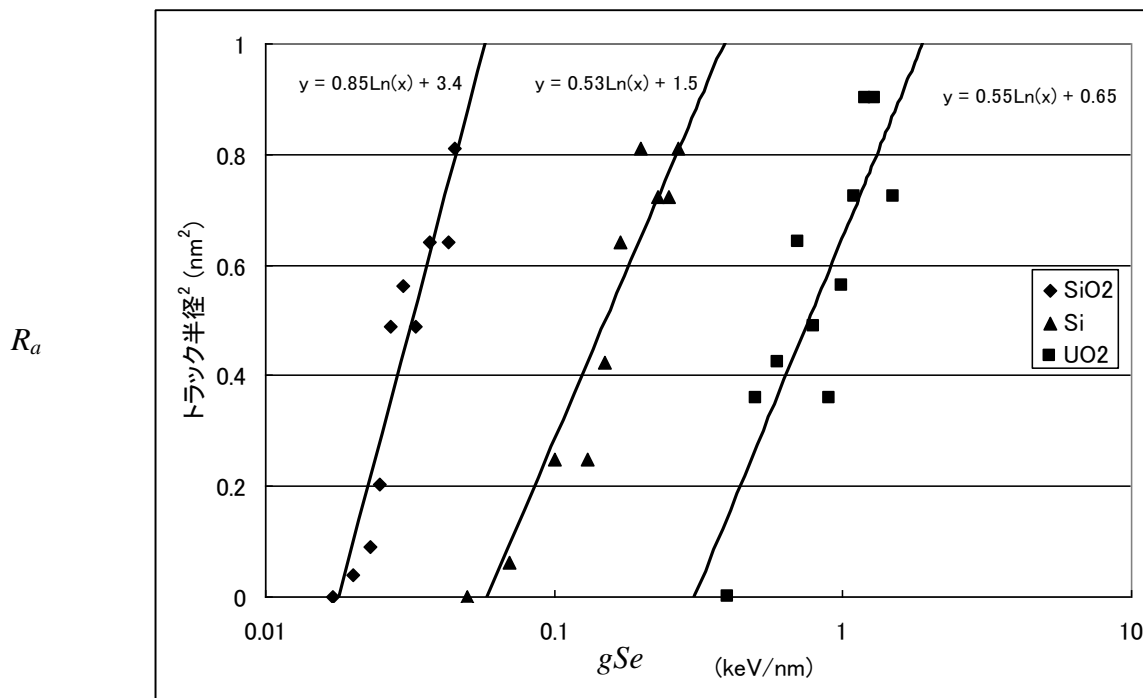


Figure 1. Relationship between square of track radius R_a and effective stopping power gS_e .

Reference

[1] C.B.Basak : Journal of Alloys and Compounds 360(2003)210-216.

* sasajima@mx.ibaraki.ac.jp

Strain buildup and saturation in GaAs due to 100 MeV Ag Irradiation

Shramana Mishra¹, Sudipta Bhaumik¹, Jaya Kumar Panda¹, Sunil Ojha²,
Achintya Dhar¹, Anushree Roy¹ and D. Kabiraj²

¹*Department of Physics and Meteorology, Indian Institute of Technology, Kharagpur 721302*

²*Inter-university Accelerator Center, Aruna Asaf Ali Marg, New Delhi 110067*

Structural evolution in high energy (100 MeV) silver ion irradiated undoped semi-insulating GaAs has been investigated by Raman spectroscopy, high resolution x-ray diffraction (HRXRD) and Rutherford back-scattering ion channeling (RBS) measurements. HRXRD measurements reveal the formation of compressively strained layer at the low fluence of irradiation. With further increase in fluence, both compressive and tensile strain appears in GaAs. Similar modulation of strain in the system with increase in ion fluence is observed from Raman measurements. The evolution of compressive strain in GaAs with increase in Ag ion fluence, as obtained from Raman and HRXRD measurements shows that the compressive strain in the material increases non-monotonously with fluence. The rate of evolution of the strain with increase in ion fluence reduces by an order of magnitude beyond a certain fluence of irradiation (1×10^{13} ions/cm²). We define this as the critical fluence. Due to the increase in defect concentration, ion-irradiation induces a positive perpendicular lattice strain with an increase in ion-fluence. However, beyond the critical fluence of irradiation the rate of increase in strain with ion fluence decreases followed by an onset of a near dynamical equilibrium (NDE) between generation and annihilation of defect states in the system. At this point, some of the new vacancy type defects, generated by irradiated ions, are annihilated by the process of recombination. In the case of MeV ion irradiated GaAs, from the model of single ion-lattice collisions, it has been concluded that a combination of collision damage and electronic ionization can set in an equilibrium of defect population in the system; hence, a saturation of the surface lattice strain at a certain fluence of irradiation. Damage fraction in the crystal due to ion irradiation was estimated from Raman line-shape analysis and has been correlated with the same observed from RBS for higher fluences.

Cratering on ultra-thin polymer films: Ion tracks under confinement

R. S. Thomaz⁽¹⁾, M. R. da Silva⁽¹⁾, L. G. Barbosa⁽¹⁾, V. M. de Menezes⁽¹⁾,
P. L. Grande⁽²⁾, C. T. Trautmann⁽³⁾, and R. M. Papaléo^{(1)*}

⁽¹⁾ Faculty of Physics, Catholic University of Rio Grande do Sul, Porto Alegre, Brazil, ⁽²⁾ Instituto de Física, Universidade Federal do Rio Grande do Sul, ⁽³⁾ Gesellschaft für Schwerionenforschung, Darmstadt, Germany

Individual fast heavy ions impacting polymer surfaces, produce nanometer-size craters and raised regions due to massive particle ejection and transport from the impact site. In this contribution, we present results on cratering produced by individual MeV heavy ions on thin (30-100 nm) and ultra-thin (2-30 nm) polymer films. We have focused on the effect of the layer thickness t , on the size and shape of the impact features produced by 0.1 MeV/u Au ions (Tandetron accelerator, Porto Alegre, Brazil) and 4.8 MeV/u Pb ions (GSI, Darmstadt, Germany). The samples were irradiated both at normal (0°) and grazing (79°) incidence and analyzed by scanning force microscopy. We have found that the size of the impact features remain basically unchanged until a thickness $t \sim 40$ nm is reached. Below this thickness, holes start to become slightly smaller and rims quickly diminish in size. For $t < 10$ nm holes are still observed but rims and tails are suppressed. Our data clearly show that excited layers as deep as ~ 30 -40 nm below the surface contribute to the formation of the hillocks, but material excitation leading to the crater is much more restricted to the near surface. We show that the effects produced by swift heavy ions on a polymer film are *weakened* when the length of the ion track is confined to layers of few nanometers, because cooperative effects, that are of importance for mass transport induced by the swift heavy ions, are severely reduced. This behaviour is confirmed by calculations of the total outward impulse produced at the surface as a function of the layer thickness, obtained using the pressure pulse analytic model. We also compare our experimental findings to simple molecular dynamic simulations applied to a polymer-like Lennard-Jones solid.

* papaleo@pucri.br

Study of the Single Ion Track Form by Microprobe Loss Energy Spectroscopy

J. Vacik^{(1)*}, V. Havranek⁽¹⁾, V. Hnatowicz⁽¹⁾, D. Fink⁽¹⁾, and P. Apel⁽²⁾

⁽¹⁾ *Nuclear Physics Institute ASCR, Husinec - Rez, 250 68, Czech Republic*

⁽²⁾ *Joint Institute for Nuclear Research, Joliot-Curie 6, 141 980 Dubna, Russia*

Ion energy loss spectroscopy is suggested to determine the shape of the (latent, etched and filled) ion tracks in polymers using ion probes of a various beam size. For a milli -probe, it can be considered as a one-dimensional tomography of many identical (rotationally symmetric) objects. For a micro-probe, the technique can be understood as a micro-tomography of the single ion track. In both cases, the ion energy loss spectrometry requires mono-energetic ions with a relatively low intensity (with a counting rate $<10^4 \text{ s}^{-1}$) and a well defined angular beam (parallel or divergent) set-up. Here, a possible use of the ion milli- and micro-probes in a tomographic study of the ion track 3D geometry is presented and discussed.

* E-mail address of the corresponding author: vacik@ujf.cas.cz

Structural and Optical properties of Porous Silicon prepared by anodic etching of Swift Heavy Ions Irradiated Silicon

V.S. Vendamani¹, S.V.S. Nageswara Rao², N. Manikanthababu², V. Saikiran², N. Srinivasa Rao²,
G. Devaraju² and A.P. Pathak²

¹*Department of Physics, Pondicherry University, Pondicherry 605014, India*

²*School of Physics, University of Hyderabad, Hyderabad 500046 India.*

Porous silicon is considered to be a potential material in the field of electronics and optoelectronics because of its strong luminescence in visible region. Ion beam irradiation shows versatile effects on physical and optical properties of porous silicon. However there are only few reports on the structural and optical properties of porous silicon prepared from irradiated silicon. Here we present a study on the influence of swift heavy ion irradiation on the surface roughness of silicon and consequent effects on the formation of porous silicon. The p-type (100) Si was irradiated with 80 MeV Ni ions at various fluences ranging from 1×10^{11} to 5×10^{13} ions/cm². The irradiated samples were anodically etched to get porous Si. These ion induced effects are being investigated by Photoluminescence (PL), Raman Spectroscopy, Fourier Transform Infrared Spectroscopy (FTIR), AFM and FESEM and will be discussed in detail during the conference.

*Corresponding and presenting author E-mail: appsp@uohyd.ernet.in & anandp5@yahoo.com

Tel: +91-40-23010181 / 23134316, Fax: +91-40-23010227 / 23010181

